Graph-based Random Access Protocols for Massive Multiple Access Networks

Shun Ogata

Department of Computer and Network Engineering
The University of Electro-Communications

This dissertation is submitted in partial fulfillment of the requirements for the degree of *Doctor of Philosophy*

March 2019

Supervisory Committee

Chairperson: Associate Professor Koji Ishibashi

1. Member: Professor Yasushi Yamao

2. Member: Professor Takeo Fujii

3. Member: Professor Giuseppe T. F. de Abreu

4. Member: Associate Professor Hideki Yagi

Day of the Predefense: November 9, 2018.
Day of the Defense: January 29, 2019.

Acknowledgements

I firstly would like to thank my supervisor, Associate Professor Koji Ishibashi, for his kind and ardent support. His thoughtful discussions and ideas have largely motivated me to focus on our research. Thanks to his support, I could have a lot of interesting and exciting experiences throughout the time in our laboratory. My special thanks go to Professor Giuseppe Abreu, as he has triggered me to go for PhD course, through my visiting his working group. I am also indebted to Professor Yasushi Yamao, Professor Takeo Fujii, Associate Professor Hideki Yagi, and Associate Professor Koichi Adachi, for their insightful comments and discussion.

Moreover, I am grateful to my colleagues in Advanced Wireless Communication Research Center, Ritsumeikan University, and Jacobs University Bremen. I have to express my gratitude to Dr. Koya Sato, for his help both in my public and private life.

Last but not least, I would like to add a personal note of heartfelt gratitude for my family, for their continuous help and support for me.

Shun Ogata
Bremen, Germany
October 26, 2018

Abstract

Following the advance of wireless communication technologies, in future, many more users than today will simultaneously communicate. However, in grant-based access scheme, where each user is assigned its own wireless resource such as time slots or frequency band, a massive number of users leads to large overhead, and consequently, large delays would cause a serious problem. To this end, a possible solution is to use grant-free access, based on random access, where each user autonomously transmits, such that prior resource allocation is no longer required. Although random access schemes achieve less overhead than grant-based access, packet collision due to the autonomous transmission becomes the problem, resulting in degradation of throughput.

In this dissertation, focusing on frameless ALOHA, we propose novel random access schemes that can achieve higher throughput performance than conventional schemes. Firstly, we propose ZigZag decodable frameless ALOHA, by introducing ZigZag decoding into frameless ALOHA. ZigZag decoding is a technique to resolve collisions of two packets, utilizing the retransmission of collided packets. It is shown that the combination of ZigZag decoding and frameless ALOHA achieves higher throughput performance than the original frameless ALOHA, with some modification in the transmission protocol. The drawback of introducing ZigZag decoding is the increase of complexity at the base station. To this end, we focus on multiple base station environments and propose frameless ALOHA with multiple base station cooperation, where base stations are connected via a backhaul network and share retrieved packets with each other. Deriving the exact packet loss rate performance of the proposed system, we show that our proposed scheme achieves higher throughput than original frameless ALOHA and conventional multiple base station cooperation. Finally, these proposals are jointed, where ZigZag decoding and multiple base station cooperation are performed together. The combinated scheme is revealed to achieve higher throughput performance than conventional schemes, even in a practical environment where the traffic is fluctuating and BSs cannot track the load.

Through these proposals, we address the possibility to realize wireless networks with massive number of users.

Table of Contents

List of Figures

List of Tables

Nomenclature

Roman Symbols

d_i	Degree of the user node i
G	Target degree
g	A realization of walk graph
I	Number of user groups
$L(x)$	Node-perspective degree distribution of variable nodes
L_k	Probability that a user transmits k times during a frame
$L_i(x)$	Node-perspective degree distribution of variable nodes of the i-th user group
$L_{i,k}$	Probability that the variable node of the i-th user group has degree-k
M	Number of base stations
N	Number of users
p	Transmission probability
$p_{\mathrm{e}}(T)$	Packet loss rate at the T-th time slot
$p_{\mathrm{e},i}(T)$	Packet loss rate of the i-th user group at the T-th slot
$\Pr(g)$	Occurrence probability of the realization of walk graph g
$R(x)$	Node-perspective degree distribution of observation nodes
R_k	Probability that k users simultaneously transmit in the same slot

$R_i(x)$	Node-perspective degree distribution of observation nodes with respect to the i-th user group
$R_{i,k}$	Probability that the observation node is connected with k edges from variable nodes of the i-th user group
$\mathcal{R}$	A set of walk graphs
$S(T)$	Throughput at the T–th slot
S_1	Maximized throughput performance of frameless ALOHA with a single BS
S^{c}	Throughput performance of frameless ALOHA with multiple base station cooperation
S^{nc}	Throughput performance of frameless ALOHA without multiple base station cooperation
s_j	The j-th base station
T	Number of time slots
u_i	The i-th user group

Greek Symbols

α	Threshold on the fraction of retrieved users
δ	Spatial degree in spatio-temporal cooperation
Γ	Multi-access diversity gain
$\lambda(x)$	Node-perspective degree distribution of variable nodes
Λ	Degree distribution for spatio-temporal cooperation
$\lambda_i(x)$	Edge-perspective degree distribution of variable nodes of the i-th user group
λ_k	Probability that an edge is connected with a degree-k variable node
$\lambda_{i,k}$	Probability that an edge is connected with a degree-k variable node of the i-th user group

$\rho(x)$	Node-perspective degree distribution of observation nodes
$\rho_i(x)$	Edge-perspective degree distribution of observation nodes with respect to the i-th user group
ρ_k	Probability that an edge is connected with a degree-k observation node
$\rho_{i,k}$	Probability that an edge is connected with an observation node with k edges connected from variable nodes of the i-th user group

Acronyms / Abbreviations

5G	5th generation
BEC	Binary erasure channel
BER	Bit error rate
BP	Belief propagation
bpcu	Bits per channel use
BS	Base station
CRC	Cyclic redundancy check
CRDSA	Contention resolution diversity slotted ALOHA
CTS	Clear-to-send
DSA	Diversity slotted ALOHA
ETC	Electronic toll collection system
E-ZDFA	Enhanced ZigZag decodable frameless ALOHA
IoT	Internet of Things
IRSA	Irregular repetition slotted ALOHA
LDPC	Low-density parity check
LTE	Long term evolution
M2M	Machine-to-machine

MAC	Medium access control
MAP	Maximum *a posteriori* probability
MIMO	Multiple-input multiple-output
ML	Maximum likelihood
NOMA	Non-orthogonal multiple-access
OFDMA	Orthogonal frequency division multiple access
PEG	Progressive edge-growth
PLR	Packet loss rate
PPP	Poisson point process
PSK	Phase shift keying
QAM	Quadrature amplitude modulation
R-ALOHA	Reservation ALOHA
RFID	Radio frequency identification
RS	Reed-Solomon
RTS	Ready-to-send
SIC	Successive interference cancellation
SINR	Signal-to-interference-plus-noise ratio
STBC	Space-time block codes
TDMA	Time division multiple access
WLANs	Wireless local area networks
WSNs	Wireless sensor networks
ZDFA-coop	ZigZag decodable frameless ALOHA with multiple base station cooperation
ZDFA	ZigZag decodable frameless ALOHA
ZD	ZigZag decoding

Chapter 1

Introduction

This chapter reviews the development of wireless communications, showing the motivation to discuss multiple access techniques. The organization of this dissertation is then presented.

1.1 Advances in Physical Layer Techniques

Wireless communication technology is advancing daily so as to achieve higher data rates, higher reliability, or higher connectivity. The upcoming standard for wireless local area networks (WLANs), namely IEEE 802.11ax, realizes the transmission rate of 1.2 Gigabits per second for each downlink spatial stream [1]. One of the underlying mechanism is a dense constellation such as 1024 quadrature amplitude modulation (QAM). Although it is obvious that higher order modulation allows higher data rate, robustness to internal noise degrades as the number of constellation points increases [2].

To deal with erroneous symbols, error correcting codes have been used. A popular class of error correcting codes is the class of Algebraic codes [3]. One of the simplest, well-known algebraic codes is Hamming code [4]. Hamming codes use parity checks, which can be represented by a parity check matrix. For instance, supposing that the size of a parity check matrix is given by $(k \times n)$, where k and n denote the number of parity checks and the length of the codeword, respectively, the parity check matrix $\mathbf{H}$ of the Hamming code with $(n, k) = (7, 3)$ is given by

$$\mathbf{H} = \begin{pmatrix} 1 & 0 & 1 & 0 & 1 & 0 & 1 \\ 0 & 1 & 1 & 0 & 0 & 1 & 1 \\ 0 & 0 & 0 & 1 & 1 & 1 & 1 \end{pmatrix}. \tag{1.1}$$

Let $\mathbf{x}$ denote the codeword vector, the dimension of which is $(n \times 1)$, so that $\mathbf{x}^{\mathrm{T}} \in \{0,1\}^n$, where T denotes the transposition. Then, arbitrary codeword $\mathbf{x}$ satisfies following:

$$\mathbf{H}\mathbf{x}^{\mathrm{T}} = \mathbf{0}, \tag{1.2}$$

where $\mathbf{0}$ corresponds to $(k \times 1)$ all-zero vector.

The Hamming code with $(n, k) = (7, 3)$ can correct one bit flipping error. When the codeword includes error, the product $\mathbf{H}\mathbf{x}^{\mathrm{T}}$ has non-zero element, which is checked against columns of $\mathbf{H}$. If the error is one bit, the position of the error is same as the position where the checked column locates. In addition to Hamming codes, Reed-Solomon (RS) codes [5] are also popular, which is defined in Galois field. RS codes are widely used, and the first example of its application is the compact disc system [6].

Another class of error correcting codes is the class of *convolutional codes* [7]. Conventional WLAN standards [8] use convolutional codes, where information bits are sequentially encoded using a shift register so as to calculate the convolution of the bits. Convolutional codes can be decoded by the Viterbi algorithm [9], which can efficiently (in linear time with the codeword length) achieve the maximum likelihood (ML) solution. Based on the convolutional code, Ungerboeck has proposed trellis coded modulation (TCM), where codeword bits of convolutional codes are mapped into constellation of phase shift keying (PSK) [10–12]. Forney has proposed *concatenated codes* [13], where data bits are first encoded by an error correcting code, and then further encoded by the different error correcting code. The concatenation of multiple error correcting codes enables to achieve robustness against bursty errors, while the decoder of convolutional codes would stack when bursty errors occur. Because of this feature, Japanese digital terrestrial broadcasting system employs a concatenated code, where the convolutional code is used as the inner code, and the RS code is used as the outer code [14]. Moreover, the concatenated RS/convolutional code was used in the communication of the Voyager 2 spacecraft [15]. Berrou *et al*. have then proposed *turbo codes* [16] by concatenating two convolutional encoders *in parallel* with an interleaver. Using iterative decoding over two decoders, turbo codes achieve bit error rate (BER) performance that is close to Shannon's limit. Turbo codes are currently used in long term evolution (LTE) [17].

More powerful error correcting codes are *low-density parity check (LDPC)* codes, which was originally proposed by Gallager [18] in 1962, and was shed light by MacKay *et al*. in 1996 [19]. An LDPC code is a type of linear code, in which the parity check matrix has a *sparse* structure, *i.e*. only a small number of elements in the matrix have non-zero values. Various decoders for LDPC codes have been proposed, and the

notable one is *belief propagation (BP)* (or message-passing) decoder [20]. In the BP decoder, the parity check matrix is treated as a bipartite graph [21] with *variable nodes* and *check nodes*, where variable (check) nodes correspond to codeword bits (parity checks). Especially, the graph is called *Tanner graph* [22]. Thanks to the sparsity of the parity check matrix, BP decoder can be performed with low complexity. Moreover, if the bipartite graph does not contain any cycles, *i.e.* the graph is a tree, BP decoder achieves the exact maximum *a posteriori* probability (MAP) decoding [23]. Hu *et al.* has proposed a scheme to obtain cycle-free Tanner graph, called progressive edge-growth (PEG) [24]. PEG provides lower error rate than codes constructed by random graphs, especially when the length of the codeword is small. However, cycle-free Tanner graphs yield large number of low-weight codewords, which are connected to small number of parity checks, and hence, such codes generally exhibit high error probability [23].

The decoding performance of an LDPC code is determined by its *degree distribution*, which is the probability mass function of the number of non-zero values in the parity check matrix. Using degree distributions, the BER performance can be calculated via *density evolution* [25]. In density evolution, message-passing over the bipartite graph can be theoretically tracked, supposing that the graph is typical and the number of nodes is infinite. Theoretical analysis based on density evolution is then used to optimize degree distributions so that the threshold of the code is maximized, where the threshold is the channel parameter (*e.g.* signal-to-noise power ratio (SNR) or channel erasure probability) such that the resulting BER converges to zero. By optimizing degree distributions, in [25], LDPC codes are shown to approach less than 0.13 dB away from Shannon's limit with asymptotically long codeword.

Although turbo codes and LDPC codes exhibit excellent decoding performance, they are not proved to achieve the channel capacity. More recently, Arikan has first shown a method to construct *capacity-achieving* error correcting codes, namely *channel polarization* or *polar codes* [26]. In the encoder of polar codes, virtual binary memoryless channels are copied and jointed, resulting in a vector channel. Within the vector channel, the capacity of each channel is not identical, but distributed between 0 and 1 bit/channel use (bpcu), because the channel is assumed to be binary input. Furthermore, when the number of channels contained in the vector channel is infinitely large, the capacity is *polarized*; approaches to either 0 or 1, and the fraction of channels with capacity of 1 bpcu is equal to the actual channel capacity. Then, by assigning information bits to the capacity-1 channel inputs while assigning dummy bits (called frozen bits) to capacity-0 channel inputs, information bits can be decoded at the receiver. Since polar codes utilizes channel polarization, the length of the codeword

should be sufficiently long so that channels are polarized; in [26], it is shown that a polar code with 2^{20}-bit codewords achieves a transmission rate of about 0.45 bits/symbol in a binary erasure channel (BEC) with erasure probability of 0.5. To improve the decoding performance of polar codes, the application of cyclic redundancy check (CRC)-aided decoding for polar codes has been investigated in [27], where information bits are encoded by CRC codes in advance. Thanks to the aid of CRC, polar codes outperform turbo codes even when the length of the codeword is 2^{10} bits.

In addition to the progress of error correcting codes, techniques of signal processing have been also advanced in recent years. The idea of multiple-input multiple-output (MIMO), where the transmitter and the receiver employs multiple antennas, is definitely one of the most important innovation. Keya *et al.* first discussed the problem of transmission over multiple channels in [28]. The use of multiple antennas, especially multiple transmit antennas, enables to obtain robustness against fading, *i.e.*, *diversity*. Alamouti [29] proposed a technique to obtain diversity gain via two transmit antennas with arbitrary number of receive antennas. Alamouti's scheme, which is referred to as *space-time block codes* (STBC), is then generalized into more than two transmit antennas by Tarokh *et al.* in [30]. It has been shown that the achievable diversity gain is the product of the number of transmit and receive antennas. On the other hand, multiple antennas can also be used to increase data rate by transmitting independent data via different antennas, such that each channel is stochastically independent to each other, namely *spatial multiplexing* [31], [32]. It has been shown that the capacity increases with the minimum of the number of transmit and receive antennas. There exists a tradeoff between the diversity gain and multiplexing gain, which has been analyzed by Zheng *et al.* [33]. MIMO is essential for today's wireless communication platform, *e.g.*, 802.11n supports the use of MIMO [8]. With all of the above in mind, we can conclude that reliable data transmission with high data rate (*e.g.* higher than 1 Gigabits/second) can be established in point-to-point wireless channel.

1.2 Medium Access Control for Future Wireless Communications

1.2.1 Grant-Based Access Protocols and their Problems

It is also a natural demand to efficiently accommodate multiple users. In the next standard of cellular communications, namely 5th generation (5G), *densification* is a key feature to achieve higher spectral efficiency, where date rate is defined as the amount

of deliverable bits/second per unit area [34]. Moreover, as represented by the idea of Internet of Things (IoT), the number of users in the network would be increased in the near future. Thanks to the advance in error correcting codes, as described in the previous section, we can concentrate on the design of medium access control (MAC) layer without considering physical layer issues, *i.e.*, demodulation error caused by noise or fading [35]. Under this assumption, a received packet would be erroneous when the packet is *collided* with other packets, since the received power of colliding packets is in general much higher than noise power. Hence, in order to achieve higher spectral efficiency, the design of multiple access protocol is crucial.

The most intuitive solution is to allocate wireless resources *e.g.* time slots or frequency band, to active users, *i.e.*, time division multiple access (TDMA) [36]. Current cellular system, namely LTE, employs orthogonal frequency division multiple access (OFDMA) [37], where each user transmits with the given subcarrier. Although such resource-assignment protocols guarantee interference-free communications for all users, it is required to allocate resources to all the users in advance, which leads to large overhead when the number of users becomes massive [38].

To this end, random access approaches are attractive to accommodate massive number of users. In the current WLAN standard, random access protocol so called *carrier sense multiple access with collision avoidance (CSMA/CA)* [39] is used, where users randomly transmit their packets upon confirming that there are no transmitting users. Although carrier sense can prevent the interference from other users, there is a well known *hidden terminal problem* [40]. When two users and a receiver exist and the users are not visible to each other, they cannot detect the other, leading to packet collision. In order to mitigate this problem, in the 802.11 standard for WLANs, CSMA/CA protocol is utilized with ready-to-send (RTS) and clear-to-send (CTS) acknowledge signals. RTS is used to inform the receiver that a user is going to transmit. If the receiver successfully receives the RTS, then the receiver broadcasts CTS to reserve the following time frame for the user. It can be said that CSMA/CA with RTS/CTS is a kind of *grant-based* random access protocol, and the grant causes large overhead with large number of users.

1.2.2 Classical ALOHA Protocols

There is a growing interest in *grant-free* random access [41], which does not utilize any permission for users, so that users can autonomously and independently transmit their packets. The simplest grant-free random access is *pure ALOHA* proposed in [42], where users immediately transmit their packets as soon as they are generated.

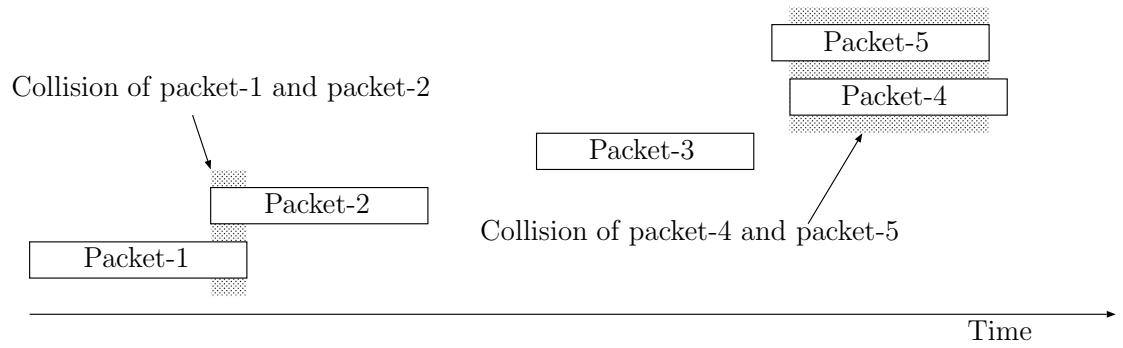

Fig. 1.1 Illustration of pure ALOHA transmission. Because of collision, only packet-3 can be recovered at the receiver.

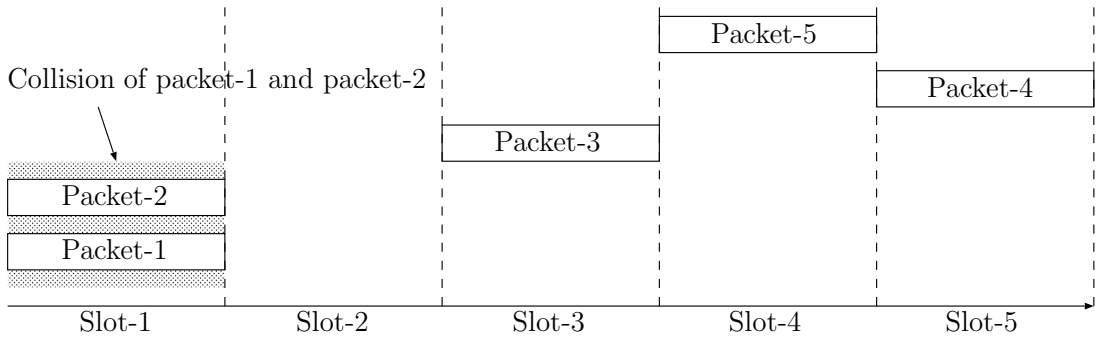

Fig. 1.2 Illustration of slotted ALOHA transmission. Collision occurs in slot-1, and other slots are free of collision.

Figure 1.1 illustrates the transmission of pure ALOHA. As collided packets cannot be demodulated at the receiver, packet-1, 2, 4, and 5 fail to be demodulated in the figure. It is well known that pure ALOHA achieves the throughput of at most $1/2e \approx 0.18$, *i.e.*, only 18% of transmitted packets can be retrieved at the receiver, because of frequent collision. On the other hand, pure ALOHA still has advantage of not requiring strict synchronization of time among users, and a number of works on pure ALOHA have been recently published [43–45].

To suppress collision of pure ALOHA, *slotted ALOHA* [46] has been proposed, where time domain is divided into time slots, and each user transmits its packet within a time slot. Transmission of slotted ALOHA is depicted in Fig. 1.2. Thanks to the slotted structure, packets are received without collision or with fully collided; in other words, partial collisions can be suppressed, and slotted ALOHA attains the throughput of $1/e$, which is twice as high as pure ALOHA. As the introduction of

time slots doubles the throughput of pure ALOHA, slotted ALOHA is widely used in several applications today (*e.g.*, Japanese electronic toll collection system (ETC) [47] and radio frequency identification (RFID) tagging [48]), and its variations have been studied nowadays [49–52]. Since there is no coordination among users, slotted ALOHA suffers from the high probability of collisions which results in the loss of stability and throughput of system. Framed ALOHA was then proposed to overcome this issue [53]. In framed ALOHA, a user is permitted to transmit a packet at most once per frame where the frame length is composed of the fixed number of time slots. The use of frame structure imposes a constraint on re-transmission probability which leads to the stability of the system. However, the average throughput performance of framed ALOHA is still the same as slotted ALOHA. Reservation ALOHA (R-ALOHA) [54] was further proposed based on the structure of framed ALOHA in order to increase the average throughput. In this scheme, the time slot in the frame is considered *reserved* by the user who successfully transmitted in the previous frame until it completes its own transmission. Although R-ALOHA achieves higher average throughput than framed ALOHA, large overhead is obviously needed to reserve slots. More recently, diversity slotted ALOHA (DSA) has been proposed to avoid packet collisions and to improve the average throughput performance without such an overhead [55]. The idea of DSA is also based on the framed ALOHA. In DSA, each user transmits some replicas of its packet in the frame. This multiple transmission increases the probability of the successful reception without interference and thus achieves higher throughput than framed ALOHA. Yet still, collisions are considered as a problem to be avoided, while collisions are inevitable due to random transmission of users.

1.2.3 Coded ALOHA Schemes: Exploiting Collisions

A paradigm shift in random access has arisen in the 2000's, following by the proposal of contention resolution DSA (CRDSA) [56]. The key idea of CRDSA is to resolve the collisions of DSA using inter-slot *successive interference cancellation* (SIC). Inter-slot SIC (hereafter designated as SIC) proceeds as follows.

1. From collision-free slots, transmitted packets are demodulated.
2. Replica signals of demodulated packets are subtracted from all the received signals, resolving collisions.
3. Other packets can be further retrieved when new slots become collision-free after subtracting replica signals.

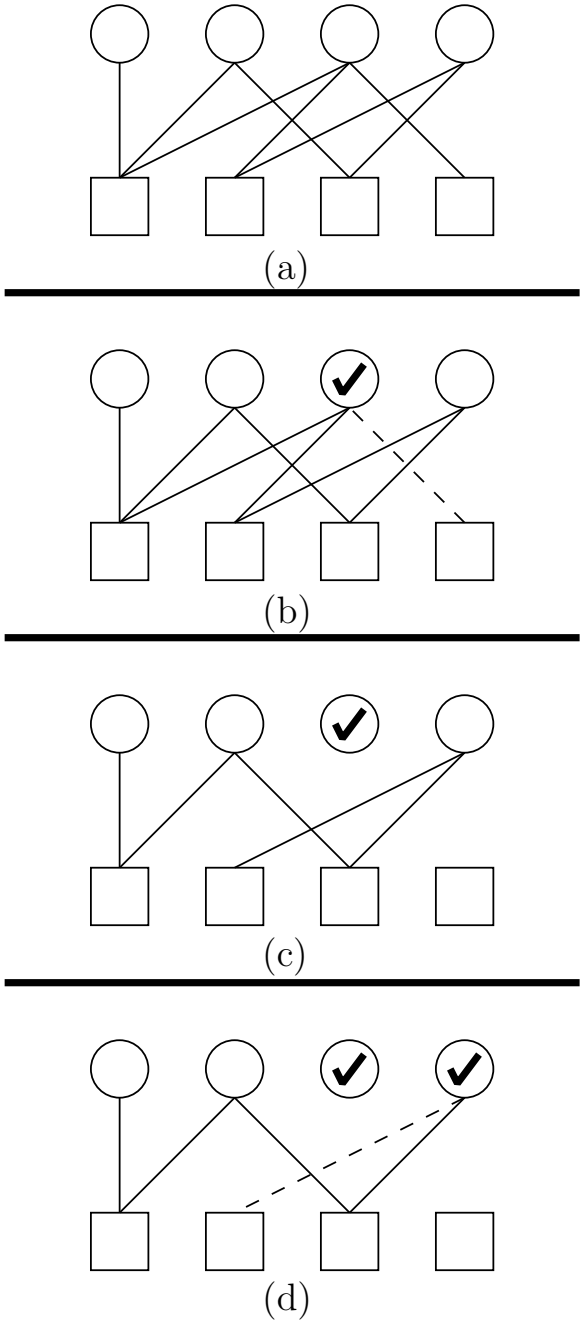

Fig. 1.3 Illustration of SIC. Circles and squares correspond to transmitted packets and received packets (time slots), respectively. (a) Four packets are colliding during four slots. (b) The third packet can be retrieved from the fourth slot. (c) The retrieved packet is canceled from all the corresponding slots. (d) The fourth packet can be retrieved from the second slot.

Figure 1.3 depicts the procedure of SIC with four colliding packets. The resolution process of SIC can be represented by a bipartite graph which is regularly utilized in coding theory, and actually, the process of SIC is equivalent to peeling decoder of LDPC codes [23]. This feature allows us to theoretically analyze the packet loss rate (PLR) performance of SIC by *density evolution* [25], originally developed for graph-based codes. In CRDSA, all users transmit the same number of replicas in the frame; in other words, the resulting graph corresponding to the transmission is *regular*. Generally, for graph-based codes, those based on *irregular* graphs exhibit superior performance to regular graph codes in terms of the decoding threshold [23]. Irregular repetition slotted ALOHA (IRSA), hence, has been proposed to exploit the irregularity [57]. The throughput and PLR performance of IRSA is characterized by degree distribution, which determines the number of retransmission of users. Given degree distribution, density evolution analyzes the PLR performance, and the analysis has been used to optimize the degree distribution so as to maximize the achievable throughput performance. In [57], allowing 16 retransmissions at most, IRSA has been revealed to achieve throughput as high as 0.965. While density evolution analyzes the asymptotic PLR performance assuming infinitely large number of users and time slots, finite-length analysis of PLR performance for IRSA has been studied in [58], where finite-length analysis for LDPC codes [59] is exploited. The PLR performance of IRSA has two visible features: waterfall region and error floor. In [58], waterfall region of IRSA with finite users is approximated using well-known Q-function[1], and it is revealed that the PLR performance of IRSA in waterfall region scales with the number of users. Moreover, assuming different importance of users, a prioritized version of IRSA has been proposed in [62]. The prioritization can be realized by using multiple degree distributions, so that more important users can transmit more frequently than less important ones. IRSA has been generalized into *coded slotted ALOHA* in [63], where each user encodes the data via erasure correcting codes beforehand, and the encoded sequence is divided into multiple segments to be transmitted. The erasure correcting code is selected from a set of codes with different coding rate, and each code is selected with a given probability distribution. Then, IRSA can be seen as a special case of coded slotted ALOHA, where the set of codes consists of multiple repetition codes. The degree distribution of IRSA is further optimized allowing 30 retransmissions at most in [63], so as to maximize the achievable throughput, and the reported maximum throughput is 0.977.

[1]It is noteworthy that bounds and approximations for Q-function have been discussed, see *e.g.*, [60], [61].

More recently, a new graph-based random access scheme, *frameless ALOHA*, has been proposed by applying the idea of rateless codes [64–66] to the slotted ALOHA framework [67, 68]. In rateless codes, the coding rate is not fixed *apriori* but instead defined by the erasure probability of the channel. Specifically, the encoder sends newly encoded symbols until the message is correctly decoded, thus the name *frameless*. The initial practical realization of rateless codes is Luby-transform (LT) codes [64], whose encoding process is as follows: d out of K information symbols are randomly chosen and bit-wise XORed to produce each coded symbol where d is called *degree* and is sampled from the degree distribution. Similar to rateless codes, the frame of frameless ALOHA is not a priori fixed but defined on the fly; users keep retransmitting with the given transmission probability, and the receiver tries to retrieve transmitted packets using SIC, upon receiving any packets. The frameless structure enables to adapt to channel traffic load automatically so that the frame length is fixed optimally for the instantaneous channel traffic. While frameless ALOHA is inferior to IRSA from the viewpoint of achievable throughput, the frameless structure is suitable for practical situations, where the number of active users is not constant, but fluctuating. As IRSA utilizes a framed structure, the frame length should be appropriately chosen in advance of transmission. Hence, at the beginning of every transmission frame, the receiver has to determine the frame length and broadcast it to all users, while each user should decide in which time slots the user transmits. In contrast, as frameless ALOHA automatically determines the frame length on the fly, prior arrangement of frame length and transmission scheduling of users is not required.

In recent years, several studies on frameless ALOHA and its derivations have been reported. In [69], frameless ALOHA is discussed in the presence of capture effect, where collision can be resolved if each colliding packet is received with different power level. As capture effect can resolve collision without performing SIC, the throughput performance increases than the original frameless ALOHA, where capture effect has not been considered. Moreover, it has been revealed that transmission probability that is higher than that used in the original frameless ALOHA should be used so as to increase the throughput. Similarly with the case of IRSA, finite-length analysis for frameless ALOHA has been studied in [70], where the analysis is based on a dynamic programming. Then, the analysis is expanded to the case of multiple user detection in [71], where the receiver is capable of retrieving multiple packets from single slot. Focusing on the tradeoff between reliability and latency, the design of frameless ALOHA considering reliability-latency guarantees has been discussed in [72], showing that very high probability of user resolution (*e.g.*, 5 nines) can be achieved via suitable design

of the transmission probability. There are a few derivations of frameless ALOHA. In [73], a technique to increase energy efficiency of users with frameless ALOHA has been proposed, where each user updates the transmission probability whether or not the user has transmitted the packet in the previous slot. Such updating of parameters cannot be adopted by framed schemes, *e.g.*, IRSA. Improved frameless ALOHA [74] is another derivation, where users are required to transmit at least once during the pre-defined frame. After that, users perform probabilistic transmission according to the original frameless ALOHA. The introduce of the pre-defined frame eliminates the error floor of the PLR performance of frameless ALOHA.

1.2.4 Requirements for Multiple Access of Next-Generation Wireless Communications

As discussed in section 1.2.1, massive number of wireless devises would be connected to the network, and in order to accommodate these devises, the use of grant-free access techniques is inevitable. Especially, communications without interactions from human, namely machine-to-machine (M2M) communications [75], would be deployed in, *e.g.*, factory automation [76], smart home [77], and connected cars [78].

In such applications, *not every* wireless devises (users) connected to the network will communicate simultaneously, but *only a fraction* of users actually communicates. This nature can be regarded that the channel has *sparsity*, which leads to the use of compressed sensing techniques [79–81]. In these approaches, the receiver estimates transmitted signals which are received simultaneously, *i.e.*, multiplexed, where it is assumed that the number of active users are sufficiently smaller than the number of all users. The use of compressed sensing is especially useful for activity-detection [82, 41]. On the other hand, the estimation performance of compressed sensing degrades as the number of active users increases, *i.e.*, the network becomes dense. Moreover, communications of users would be sporadic, and hence, the traffic is supposed to be fluctuating, as transmission of each user would be event-driven [83]. Besides the sporadic nature, high throughput performance is required, so as to efficiently accommodate large number of users with limited wireless resources [84]. Furthermore, communications should be sufficiently reliable, especially in particular applications such as control in industrial plant [85].

Let us summarize requirements for multiple access schemes for next generation as follows:

- Massive number of users should be accommodated.

- High throughput should be achieved even with fluctuating demand.
- Communications should be reliable, *i.e.*, sufficiently high fraction of packets should be retrieved at the receiver.

1.3 Focus and Aim of This Dissertation

To meet the requirements listed above, we focus on the use of coded ALOHA schemes. However, framed ALOHA schemes such as IRSA would not be suitable in terms of supporting fluctuating traffic, as the frame length should be appropriately determined according to the number of transmitting users. In other words, at the beginning of each frame, the receiver has to estimate the appropriate frame length. Although IRSA is known to attain high throughput performance, as shown in [57], [63], the base station (BS) is required to suitably select the number of time slots, *i.e.*, frame length prior to the transmission of users to achieve the designed throughput performance. If the frame length is not appropriate, the throughput performance would be degraded than the designed value; a shorter frame results in an overloaded situation where transmitted packets frequently collide, whereas a longer frame leads to unnecessary time slots.

To this end, we especially focus on frameless ALOHA [67], where the frame length is automatically determined on the fly. Frameless ALOHA has a potential for fulfilling the above requirements; the combination of simple probabilistic transmission and SIC works without any difficulty even with massive number of users, as frameless ALOHA (and other coded ALOHA schemes) is designed via density evolution analysis, presuming infinitely large number of users and frame length. Moreover, the frameless structure adaptively determines the frame length according to the channel traffic, so that the fluctuating traffic can be automatically tracked. However, it is a critical problem that the achievable throughput performance of frameless ALOHA is lower than *framed* schemes such as IRSA, as frameless ALOHA can only control the transmission probability, but not the degree distribution. IRSA is obviously considered to achieve higher throughput performance than frameless ALOHA, as the IRSA can design the degree distribution itself. Another problem of frameless ALOHA is the error floor, which is caused by the probabilistic transmission. Because of the error floor, a fraction of users cannot be retrieved after the frame is terminated, resulting in instability of the system. Hence, it is an urgent issue to establish a multiple access scheme suitable for massive multiple access networks, satisfying the above-mentioned requirements. In this dissertation, we tackle this issue by proposing several novel graph-based random

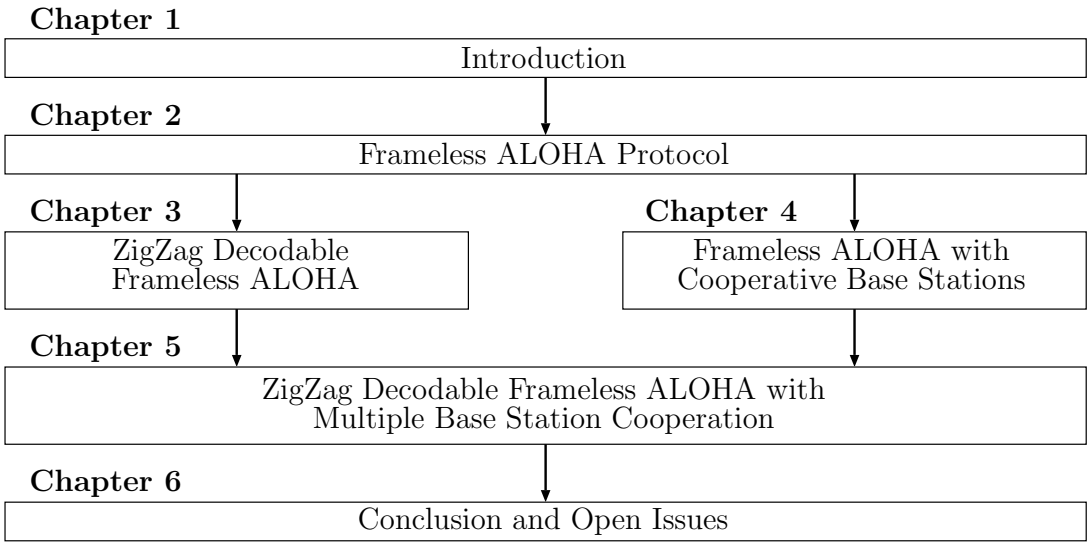

Fig. 1.4 Outline of this dissertation. Chapter 1 is followed by five chapters.

access schemes, which solve the problems of frameless ALOHA: *the low throughput* and *the error floor*, while showing that *the fluctuating traffic* can be dealt with.

1.4 Organization of This Dissertation

In Chapter 1, we have described the advances in wireless communications leading to massive wireless communications, which results in the necessity of designing efficient medium access control protocols. The focus and the aim of this dissertation has also been laid out. Figure 1.4 shows the outline of this dissertation. The remainder of this dissertation is organized as follows.

Chapter 2: Frameless ALOHA Protocols

Chapter 2 explains the conventional frameless ALOHA protocol, including the theoretical analysis of PLR performance. Moreover, we propose an optimization scheme for the transmission probability so as to maximize the throughput performance.

Chapter 3: ZigZag Decodable Frameless ALOHA

We discuss the application of ZD into frameless ALOHA in Chapter 3, introducing ZDFA and E-ZDFA. In ZigZag decodable frameless ALOHA, we consider to apply ZigZag decoding (ZD) [86], which was proposed to combat the hidden node problem of

WLANs by resolving colliding packets from hidden nodes. In ZD, collided users are required to immediately retransmit their packets, resulting in two sets of two colliding packets. ZD utilizes the difference in arrival timing of each packet, where the process of collision cancel can be interpreted as segment-wise SIC. Introducing ZD into frameless ALOHA, *ZigZag decodable frameless ALOHA (ZDFA)* is first proposed. Deriving the exact theoretical PLR and throughput performance of ZDFA, it is revealed that the straightforward application of ZD into frameless ALOHA degrades the throughput performance.

We then modify the protocol, namely *enhanced ZigZag decodable frameless ALOHA (E-ZDFA)*, by exploiting the frameless nature, which turns out to enhance the throughput performance. Specifically, E-ZDFA requires some retrieved users to halt retransmission in order to suppress collision and encourage singleton reception or the minimum collision, *i.e.* collision of two packets which can be retrieved via ZD. Moreover, the transmission probability is dynamically increased so as to prevent wasting time slots, as the number of contending users becomes less due to the retransmission canceling. An approximated PLR analysis for E-ZDFA is presented, and based on the approximate analysis, the transmission probability is optimized so that the throughput performance is maximized. Numerical examples confirm that E-ZDFA outperforms the conventional frameless ALOHA. Especially for the moderate number of users, *e.g.* thousand users exist in the network, it is shown that E-ZDFA largely improves the throughput performance over conventional framed coded ALOHA schemes.

Chapter 4: Frameless ALOHA with Cooperative Base Stations

Although E-ZDFA achieves higher throughput and lower error floor than the original frameless ALOHA, E-ZDFA also increases the complexity of the receiver caused by the introduction of ZD. To alleviate the additional complexity at the receiver, we focus on *multiple base station (BS) network*, which is a feasible situation for massive wireless communications. Supposing backhaul networks among BSs, frameless ALOHA with multiple BS cooperation is proposed, where BSs share successfully retrieved packets with each other, which accelerates the SIC at each BS.

To fully exploit the multiple BS nature, we propose to classify users into multiple groups depending on which BSs the user can communicate with, and each group has its own transmission probability. It is noteworthy that, in our proposed protocol, all the BSs and users share the same frequency band, so that no resource allocation such as frequency division is considered.

The related work to our work is that of IRSA with multiple cooperative BSs, namely spatio-temporal cooperation, studied in [87]. In [87], the PLR performance of the system has been approximately analyzed, assuming a Poisson point process (PPP) network. The exact analysis for the PLR performance has not been derived, as the SIC is performed over multiple BSs with backhaul network, so that the connection between each BS has to be considered. In this chapter, we derive the exact PLR representation by taking into account the network topology, while an algorithm to obtain the analytical equations for arbitrary number of BSs is given. It is found that frameless ALOHA with cooperative BSs achieves higher throughput performance than resource-allocation scenario, where the frequency band is divided for each BS so as to prevent interference among BSs.

Chapter 5: ZigZag Decodable Frameless ALOHA with Multiple Base Station Cooperation

Finally, tolerating the computational cost at BSs, we joint the two proposed scheme to propose *ZigZag decodable frameless ALOHA with multiple BS cooperation* (ZDFA-coop), where multiple BS cooperation and SIC work together. It is shown that the application of ZD is capable of increasing the throughput performance even in a multiple BS environment, revealing that ZDFA-coop outperforms frameless ALOHA with multiple BS cooperation. Furthermore, a practical situation, where the number of users fluctuates, is considered in this chapter, and ZDFA-coop is compared with conventional schemes, namely IRSA with degree distribution optimized in [63] and spatio-temporal cooperation [87]. Numerical results confirm that ZDFA-coop outperforms conventional schemes in terms of throughput performance.

Chapter 6: Conclusion and Open Issues

The dissertation is concluded in Chapter 6, while addressing remaining future works.

Chapter 2

Frameless ALOHA Protocol

In this chapter, the conventional frameless ALOHA protocol [67] is explained. After introducing the system model considered, probabilistic transmission of users is described, followed by the packet retrieval of the receiver via successive interference cancellation (SIC). Then, theoretical packet loss rate (PLR) analysis based on density evolution is introduced.

2.1 Network and Channel Model

Let us consider a network with N users and a common base station (BS), where each user aims to deliver its own packet to the BS. Each user possesses one packet to be transmitted at the beginning of the transmission, and it is supposed that new packets are not generated throughout the transmission. In order to focus on the evaluation of the protocol, noise-free channels are assumed, which are achieved by assuming that sufficient received power is available resulting in *interference-limited* channels. Moreover, it is assumed that all the channel coefficients between users and the BS is constant throughout the transmission and perfectly known at the BS. The channel model described here is also known as *protocol model* introduced in [35].

All the users and the BS are synchronized in time so that all the transmission of users is slot-wise. Upon transmission, time slots are organized as a *frame*, where the frame length, *i.e.* the number of time slots, is denoted by T.

2.2 Probabilistic Transmission

At each time slot, users randomly decide whether or not to transmit their packets using the transmission probability p, which is given by

$$p = \frac{G}{N}, \tag{2.1}$$

where G is called *target degree* and indicates the number of users simultaneously transmitting in one time slot.

It is noteworthy that we can control the throughput performance by controlling the target degree. The probabilistic transmission of users continues until the sufficiently large fraction of users are retrieved at the BS, which is assessed by the given threshold $\alpha \in (0, 1]$. Specifically, transmission is terminated when $\lfloor \alpha N \rfloor$ users are successfully retrieved. In particular, $\alpha = 1$ means that the transmission continues until all the users are retrieved. The frame length T is not determined *apriori*, but adaptively determined as the BS terminates the frame after retrieving sufficiently large fraction of users. This is why this protocol is called *frameless*.

2.3 Successive Interference Cancellation

Received packets may contain collisions, and thus the BS uses SIC so as to resolve and retrieve collided packets. The SIC for frameless ALOHA is equivalent to the peeling decoder for low-density parity check (LDPC) codes [23] and can be described by the following steps:

(i) Retrieve the transmitted packets from singleton slots. The slots are assumed to be empty.

(ii) Subtract the packets from all the received signals in which the packets are included.

After step (ii), some collided packets become singletons, and the above operations are repeated until all the singleton slots vanish. In order to execute step (ii), it is assumed that each packet includes information indicating the time slot in which it is transmitted. Note that the retrieved packets might be included in future received packets. To this end, if each user identification (ID) is used as a seed for a random generator for choosing time slots in which to transmit, the receiver can determine all the future transmissions and subtract signals from all the received packets [88].

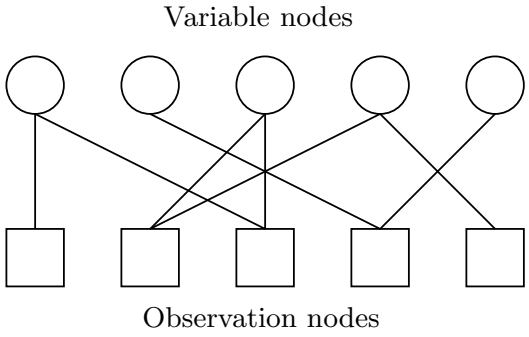

Fig. 2.1 An example of bipartite graph of frameless ALOHA.

2.4 Bipartite Graph Representation and Degree Distributions

Transmission of users can be visually represented by a *bipartite graph*. In frameless ALOHA, the bipartite graph consists of two kinds of nodes, namely *variable nodes* and *observation nodes*, as shown in Fig. 2.1. Variable nodes correspond to users or transmitted packets, and observation nodes represent received packets or time slots. The variable node and the observation node is connected with an edge if the corresponding user has transmitted the packet at the corresponding time slot. The number of edges connected to each node is referred to as *degree*. The degree of variable nodes denotes how many times the corresponding user transmits the packet during the frame, and the degree of observation nodes is the number of users simultaneously transmitting in the corresponding time slot.

Since users randomly transmit their packets, the resulted bipartite graph is also constructed randomly, which can be characterized by *degree distributions*. Because of the probabilistic transmission of users, degree of variable nodes and observation nodes follows binomial distribution with parameters T (or N) and p. Given the frame length T, the probability that a user transmits a packet k times, namely L_k, is given by

$$L_k = \binom{T}{k} p^k (1-p)^{T-k}. \tag{2.2}$$

Similarly, the probability that k users simultaneously transmit in the same slot, namely R_k, is given by

$$R_k = \binom{N}{k} p^k (1-p)^{N-k}. \tag{2.3}$$

Using L_k and R_k, *node-perspective* degree distributions are defined in the manner of polynomials. Specifically, using a dummy variable x, node-perspective degree distribution of variable nodes and observation nodes are defined as

$$L(x) \triangleq \sum_{k=0}^{T} L_k x^k, \tag{2.4}$$

and

$$R(x) \triangleq \sum_{k=0}^{N} R_k x^k, \tag{2.5}$$

respectively.

While node-perspective degree distributions characterize degrees of nodes, *edge-perspective* degree distributions can be used to represent the degree of the node with which the focused edge is connected. Specifically, considering an edge in the bipartite graph, the probability that the edge is connected with degree-k variable node is given by

$$\lambda_k = \frac{kTL_k}{\sum_{l=0}^{T} lTL_l} = \frac{kL_k}{\sum_{l=0}^{T} lL_l}, \tag{2.6}$$

where the numerator kTL_k denotes the average number of edges connected with degree-k variable nodes, and the denominator $\sum_{l=0}^{T} lTL_l$ is the average number of edges including in the bipartite graph.

The probability for observation nodes can be similarly defined. The probability that the edge is connected with degree-k variable node is given by

$$\lambda_k = \frac{kNR_k}{\sum_{l=0}^{N} lNR_l} = \frac{kR_k}{\sum_{l=0}^{N} lR_l}. \tag{2.7}$$

Similarly to node-perspective degree distributions, edge-perspective degree distributions of variable nodes and observation nodes are defined as

$$\lambda(x) = \sum_{k=1}^{T} \lambda_k x^{k-1}, \tag{2.8}$$

and

$$\rho(x) = \sum_{k=1}^{N} \rho_k x^{k-1}, \tag{2.9}$$

respectively, where the term x^{k-1} denotes that the node has $(k-1)$ other edges when the edge is connected with degree-k node, and it can be observed that

$$\lambda(x) = \frac{L'(x)}{L'(1)}, \tag{2.10}$$

and

$$\rho(x) = \frac{R'(x)}{R'(1)}. \tag{2.11}$$

2.5 Theoretical Analysis for Packet Loss Rate

The asymptotic PLR performance via SIC can be theoretically derived using density evolution [67, 25], which is originally used to analyze the decoding performance of low-density parity-check codes. In density evolution, SIC is considered as a message passing algorithm, where two kinds of messages, "0" for un-retrieved and "1" for retrieved, are passed between variable nodes and observation nodes. At the variable nodes, for each connected edge, the edge carries message "1" if at least one of the other edges carries the message "1" into the variable nodes in the last iteration, *i.e.*, the user corresponding to the variable node can be retrieved when the packet becomes singleton at least one time slot. Otherwise, if all of the other edges carry the message "0", the edge carries the message "0" as the packet has not been retrieved yet. Upon receiving messages from variable nodes, each edges carries a message from observation nodes. Focus on an edge connected to the observation node. The edge carries the message "1" to the connected variable if and only if all of the other connected edges carries the message "1", since in that case the time slot corresponding to the observation node becomes singleton. Otherwise, the edge carries the message "0."

Now let us consider how to theoretically analyze the message passing algorithm described above. Let x_l denote the probability that the edge carries the message "0" from variable nodes to observation nodes. Similarly, let w_l denote the probability that the edge carries the message "0" from observation nodes to variable nodes. Since SIC starts from singleton observation nodes, the analysis starts from the calculation of w_l. Consider an observation node with degree-k. The edge connected with the observation node carries the message "1" iff all of the other edges have carried the message "1" into the observation node in the last iteration, and the probability is given by $(1-x_{l-1})^{k-1}$ for $l \geq 1$. The observation node process is depicted in Fig. 2.2-(a), where the observation node has degree-3. Moreover, by averaging over the degree, the edge carries the message "1" into variable nodes with probability $\sum_{k=1}^{N} \rho_k (1-x_{l-1})^{k-1} = \rho(1-x_{l-1})$. Hence,

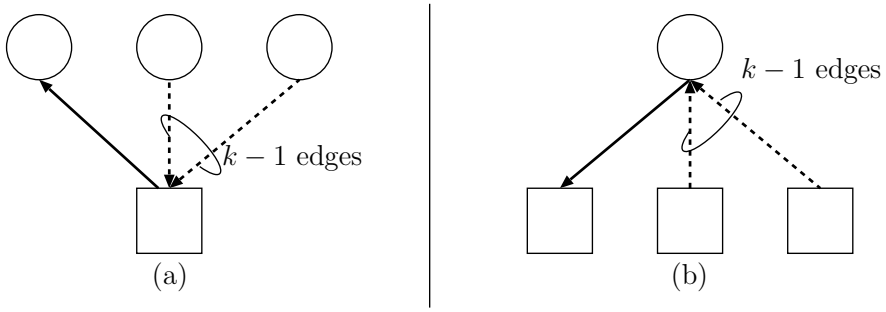

Fig. 2.2 Illustration of density evolution calculation. (a) Observation node calculation. The solid arrow carries the message "0" when at least one edge out of the other $(k-1)$ edges have carried the message "0" into the observation node in the previous iteration. (b) Variable node calculation. The solid arrow carries the message "0" iff all of the other $(k-1)$ edges have carried the message "0" in the previous iteration.

the probability w_l is calculated as

$$w_l = 1 - \rho(1 - x_{l-1}), \tag{2.12}$$

where $x_0 = 1$ since none of the packets has been retrieved at the beginning of SIC.

Let us consider the calculation of x_l. If the variable node has degree-k, the connected edge carries the message "0" into the observation node iff the other $(k-1)$ edges have carried the message "0" into the variable node in the previous iteration, and the probability is given by $(1-w_l)^{k-1}$. The variable node process is illustrated in Fig. 2.2-(b). Since the edge is connected with degree-k variable node with probability λ_k, averaging over k yields

$$x_l = \lambda(w_l). \tag{2.13}$$

After a sufficiently large number of iterations, the packet is lost, *i.e.* still being not retrieved, iff all the edges connected to the corresponding variable node carry the message "0." The probability of that event at the T-th time slot, namely the PLR, is obtained as

$$p_{\mathrm{e}}(T) = L(w_l). \tag{2.14}$$

It is noteworthy that the analysis above implicitly an assumes infinitely large number of nodes in the graph so that the degree distribution of the graph becomes typical. Finite length analysis of frameless ALOHA can be found in [70], where the PLR performance is exactly derived with respect to the number of users and time slots. Although such finite length analysis is useful to design systems with not-so-large

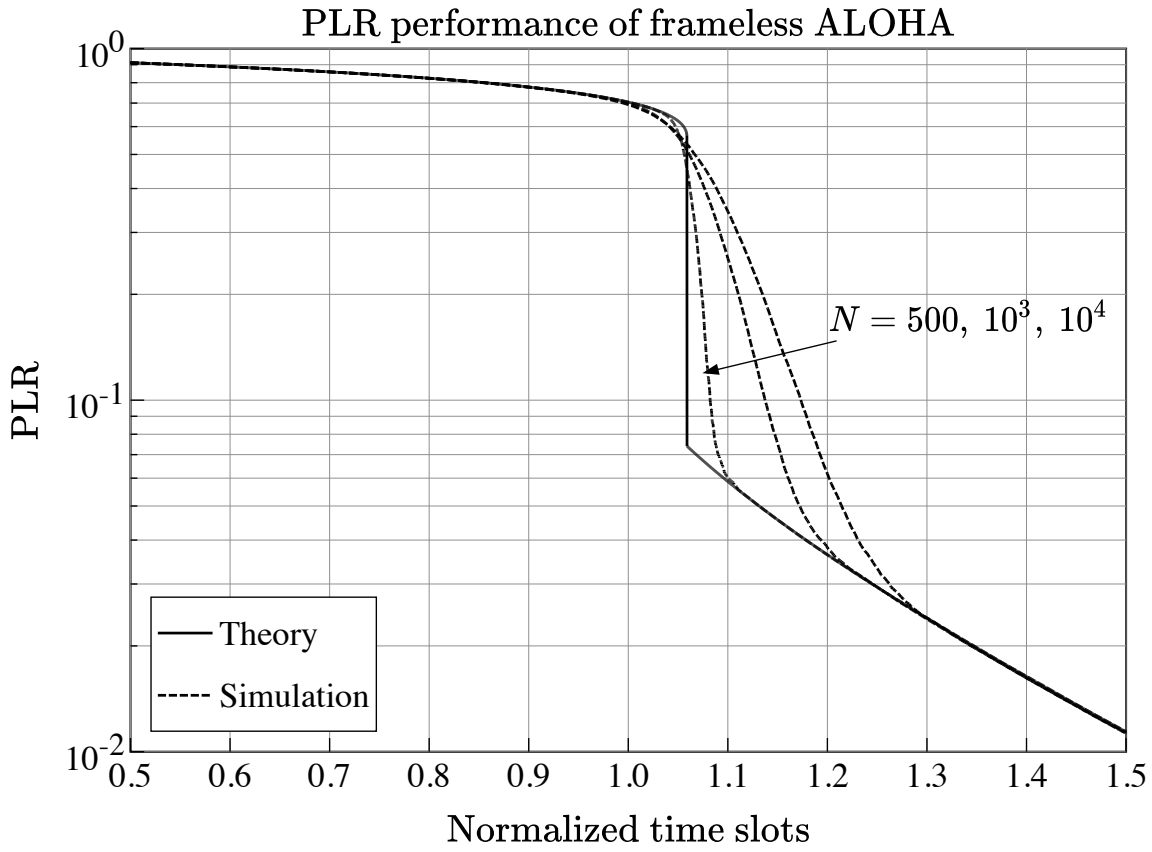

Fig. 2.3 PLR performance of frameless ALOHA. The target degree of $G = 3.09$ is used for all curves. Theoretical analysis shows good agreement with simulated PLR performance.

number of users, we here use the asymptotic analysis so as to consider massive wireless networks where the number of users is larger than one thousand.

Figure 2.3 shows an example of the PLR performance of frameless ALOHA, where the target degree is set to $G = 3.09$. The horizontal axis corresponds to the normalized number of time slots, *i.e.* T/N, and it is observed that the PLR performance drastically improves around the point of $T/N = 1.06$ (waterfall region). This is because the SIC is a kind of belief propagation algorithm, similar to the decoder of LDPC codes. For comparison, results of computer simulations with various number of users are shown. Since the theoretical analysis presumes asymptotic setting, the result of computer simulations approaches the theoretical analysis as the number of users increases.

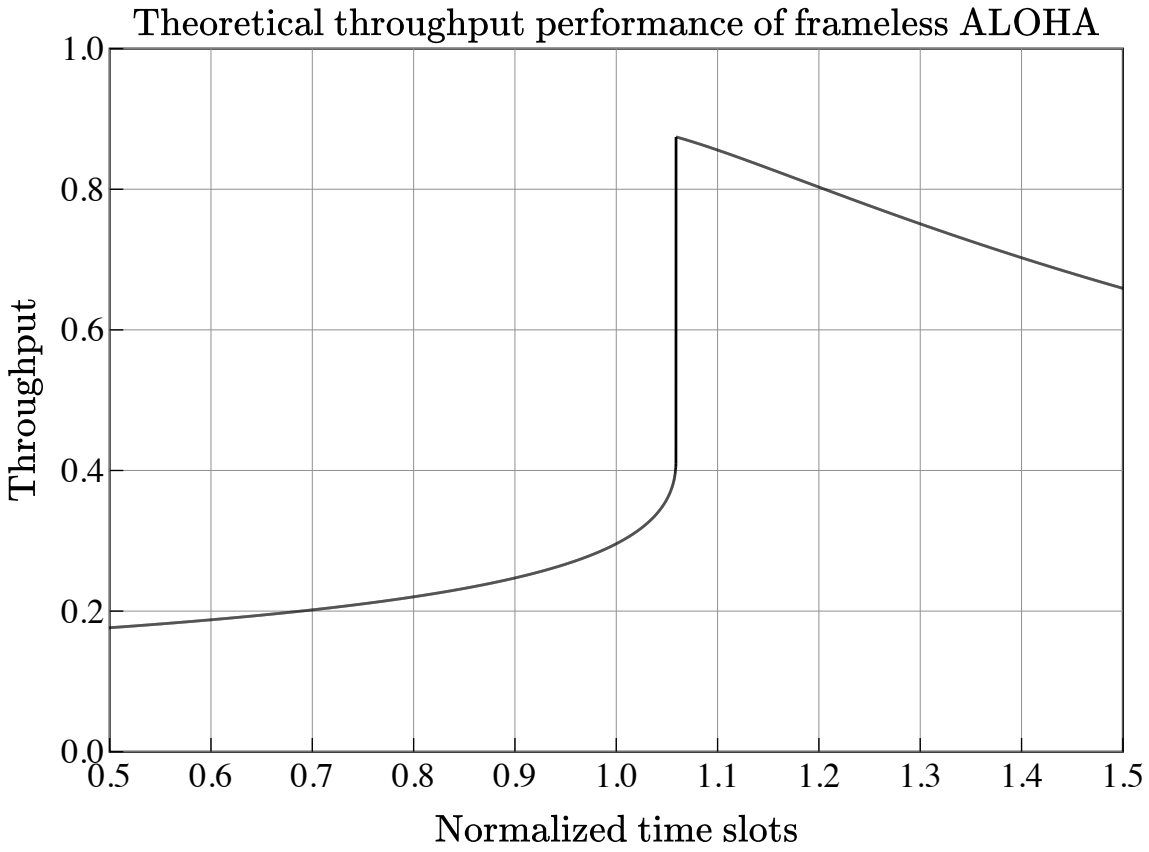

Fig. 2.4 Theoretical throughput performance of frameless ALOHA corresponding to the theoretical PLR curve of Fig. 2.3. It is noteworthy that the throughput performance has a peak.

2.6 Throughput Performance and Optimization

It would be of interest to maximize the efficiency of the transmission. To this end, throughput is a useful metric to measure the efficiency of the protocol. Throughout the dissertation, the throughput is defined as the fraction of retrieved users and the number of elapsed time slots. Hence, throughput is a function of time slots, namely

$$\begin{aligned} S(T) &\triangleq \frac{\text{The number of retrieved packets within } T \text{ slots}}{T} \\ &= \frac{N(1-p_{\mathrm{e}}(T))}{T}. \end{aligned} \tag{2.15}$$

Figure 2.4 shows the theoretical throughput performance, which corresponds to the theoretical PLR shown in Fig. 2.3. It is observed that there is a peak in the throughput performance, where the peak is corresponding to the waterfall region of the PLR.

Based on the theoretical analysis on the PLR and throughput performance of frameless ALOHA, we would like to maximize the throughput performance. Given N, the throughput represented by (2.15) is determined by two kinds of variables: T and $p_{\mathrm{e}}(T)$. Recall that the PLR $p_{\mathrm{e}}(T)$ is calculated via density evolution, which includes degree distributions. As degree distributions of frameless ALOHA is determined by the transmission probability and consequently the target degree, there should exist the target degree which maximizes the throughput performance. In this dissertation, we define the *optimal target degree* as the one which yields the highest throughput performance. Then, we formulate the optimization problem to maximize the throughput. While throughput can be represented as a function of time slots, frameless ALOHA protocol is terminated upon retrieving sufficiently large number of users. Therefore, the practically achieved throughput is a random variable with respect to the instant realization of bipartite graph (or transmission schedule of users). It is hence difficult to derive the average throughput performance of frameless ALOHA.

At this point, we propose to maximize the peak throughput, so as to maximize the resulted average throughput performance. As seen in Fig. 2.3, the actual PLR performance and consequently throughput performance shows good agreement with the theoretical analysis for large number of users, and the waterfall region is also reproduced. Then, it can be considered that the frameless ALOHA transmission would be terminated when the PLR attains the waterfall region, retrieving sufficiently large number of users. This optimization policy can be verified by the achieved throughput performance as shown in Fig. 2.5, where the achieved throughput performance versus the number of users is plotted. From the figure, it is observed that the average throughput performance approaches the theoretical peak throughput, and thus the optimization policy is valid for large number of users.

With all of the above in mind, we can formulate the optimization problem to maximize the average throughput performance as follows

$$\max_{G} \quad \sup_{T} S(T) \tag{2.16}$$

$$\text{s.t.} \quad 1 - p_{\mathrm{e}}(T^*) \geq \alpha, \tag{2.17}$$

where $T^* = \arg\sup_T S(T)$.

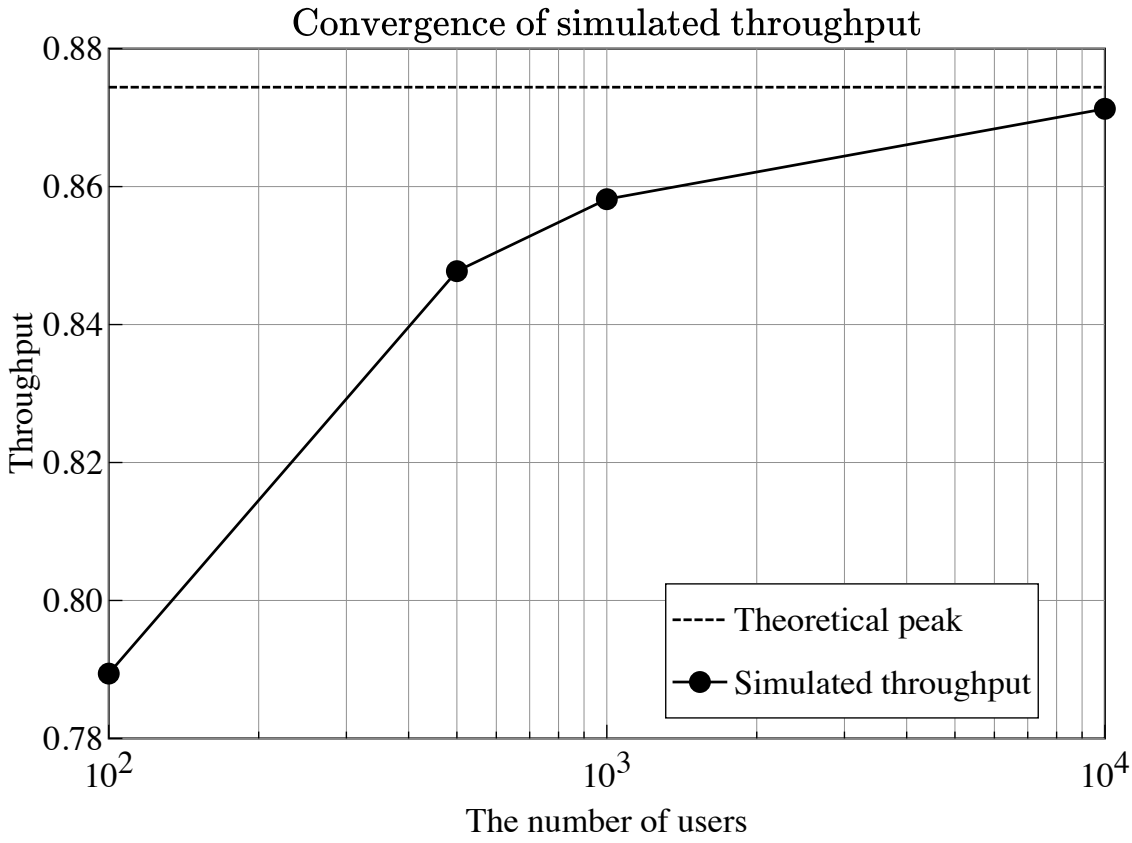

Fig. 2.5 Average throughput performance and theoretical peak throughput of frameless ALOHA with $G = 3.09$. As the number of users increases, simulated throughput performance converges the theoretical peak throughput.

The optimization problem, however, cannot necessarily be a convex optimization, as both the objective function and the constraint include iterative calculation with degree distribution. Hence, in order to solve the optimization problem, differential evolution [89, 90] is used here, which is a type of genetic algorithm. It is noteworthy that differential evolution has been widely used to optimize the degree distribution of LDPC codes so as to maximize the decoding threshold [25]. Solving the optimization above, we have obtained the optimal target degree of $G = 3.09$, with the peak throughput of 0.874.

2.7 Eliminating the Error Floor

As we have seen so far, simple probabilistic transmission causes an error floor problem, where a fraction of packets cannot be recovered because of the possibility that the

packets were not transmitted during the frame. In [74], *improved frameless ALOHA* has been proposed to eliminate the error floor while keeping the frameless nature. In this approach, the target frame length is calculated from the number of users so that every user determines the number of retransmissions and transmits at least once during the frame, eliminating the error floor. If there still exists some unresolved users after the target frame length, the users continue transmission following the original frameless ALOHA. However, additional overhead is needed to inform all the receivers of which user is not decoded yet.

The error floor problem also exists in Luby-transform (LT) codes [64] which belong to a class of rateless codes and are based on the same decoding procedure as that of frameless ALOHA. In order to overcome the error floor of LT codes, raptor codes have been proposed in [65], where error correcting codes are concatenated to LT codes. It is a natural conclusion that frameless ALOHA can utilize erasure correcting codes to eliminate the error floor. In this section, we consider to concatenate an erasure correcting code to frameless ALOHA.

2.7.1 Coded Frameless ALOHA

In order to eliminate the error floor of frameless ALOHA, we propose *coded frameless ALOHA*, in which users transmit encoded packet segments instead of the original packets. Erasure correcting codes are used to decode the remaining packets upon SIC, because the remaining packets are assumed to be erased.

Each user's packet is encoded via erasure correcting codes independently, and the codeword, the length of which is N_p in bits, is further divided into B *segments* of the same length. In each time slot, encoded segment is transmitted instead of the original packet. The segment to be transmitted is chosen randomly when the user decides to transmit, and the probability that each segment will be transmitted is given by p/B. In practice, each transmitted segment has a header part that includes information about the sender as well as other information. Thus, packet division may cause a larger overhead due to additional headers. For the sake of simplicity, the effect of packet headers is not considered, assuming the length of the header is zero. Moreover, in the paper, an asymptotic situation is considered, where the codeword is divided into segments with one bit, *i.e.* $B = N_p$. This assumption is not practical due to the huge number of overhead, but is useful to reveal the ultimate performance of the system. If the codeword is divided into segments consisting of multiple bits, erasure events on codeword bits cannot be assumed to be independent, as multiple bits simultaneously

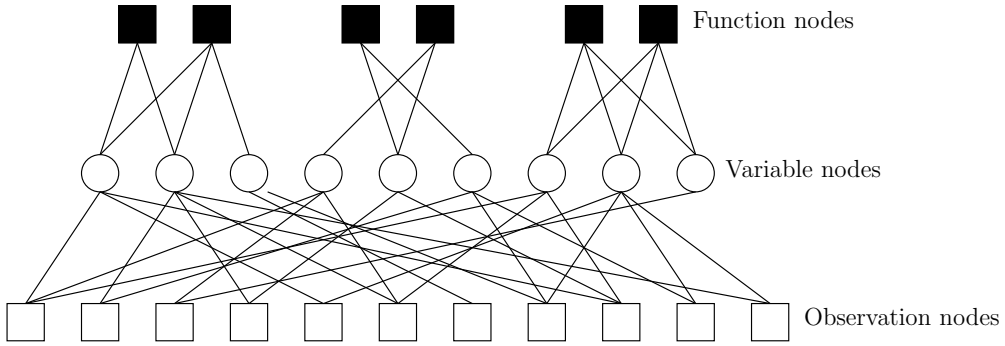

Fig. 2.6 Graph representation of coded frameless ALOHA. The upper part with the black function nodes and variable nodes compose the Tanner graph for the LDPC code, and the lower part with the white observation nodes and variable nodes compose the bipartite graph for frameless ALOHA.

erase. The correlated erasure channel yields worse decoding performance, and hence, the asymptotic situation can be regarded as the bound for the practical performance.

Using graph-based codes allows us to represent coded frameless ALOHA with a single graph. Hereinafter, let us consider the use of LDPC codes [18]. LDPC codes can be represented by a bipartite graph called a *Tanner graph*, where variable nodes correspond to codeword bits, and function nodes correspond to parity checks. Variable nodes in a Tanner graph are also variable nodes in the bipartite graph for frameless ALOHA, as shown in Fig. 2.6. In the tripartite graph of coded frameless ALOHA in the present paper, variable nodes correspond to codeword bits.

For the lower part of the graph corresponding to frameless ALOHA transmission, the degree distributions $L^{\mathrm{ch}}(x)$ and $R^{\mathrm{ch}}(x)$ are obtained by replacing p in (2.4) and (2.5) with p/B. The edge perspective degree distributions $\lambda^{\mathrm{ch}}(x)$ and $\rho^{\mathrm{ch}}(x)$ are defined in the same manner as (2.8) and (2.9). For the upper part of the graph corresponding to the LDPC code, the variable and function node degree distributions are arbitrarily defined as $L^{\mathrm{co}}(x) \triangleq \sum_{k=\mathtt{l}_{\min}}^{\mathtt{l}_{\max}} L_k^{\mathrm{co}} x^k$ and $R^{\mathrm{co}}(x) \triangleq \sum_{k=\mathtt{r}_{\min}}^{\mathtt{r}_{\max}} R_k^{\mathrm{co}} x^k$ respectively, where $\mathtt{l}_{\min}(\mathtt{r}_{\min})$ is the minimum degree of each column (row), and $\mathtt{l}_{\max}(\mathtt{r}_{\max})$ is the maximum degree of each column (row).

The rate of the LDPC code is obtained by [23]

$$R = 1 - \frac{\sum_{k=\mathtt{l}_{\min}}^{\mathtt{l}_{\max}} k L_k^{\mathrm{co}}}{\sum_{k=\mathtt{r}_{\min}}^{\mathtt{r}_{\max}} k R_k^{\mathrm{co}}}. \tag{2.18}$$

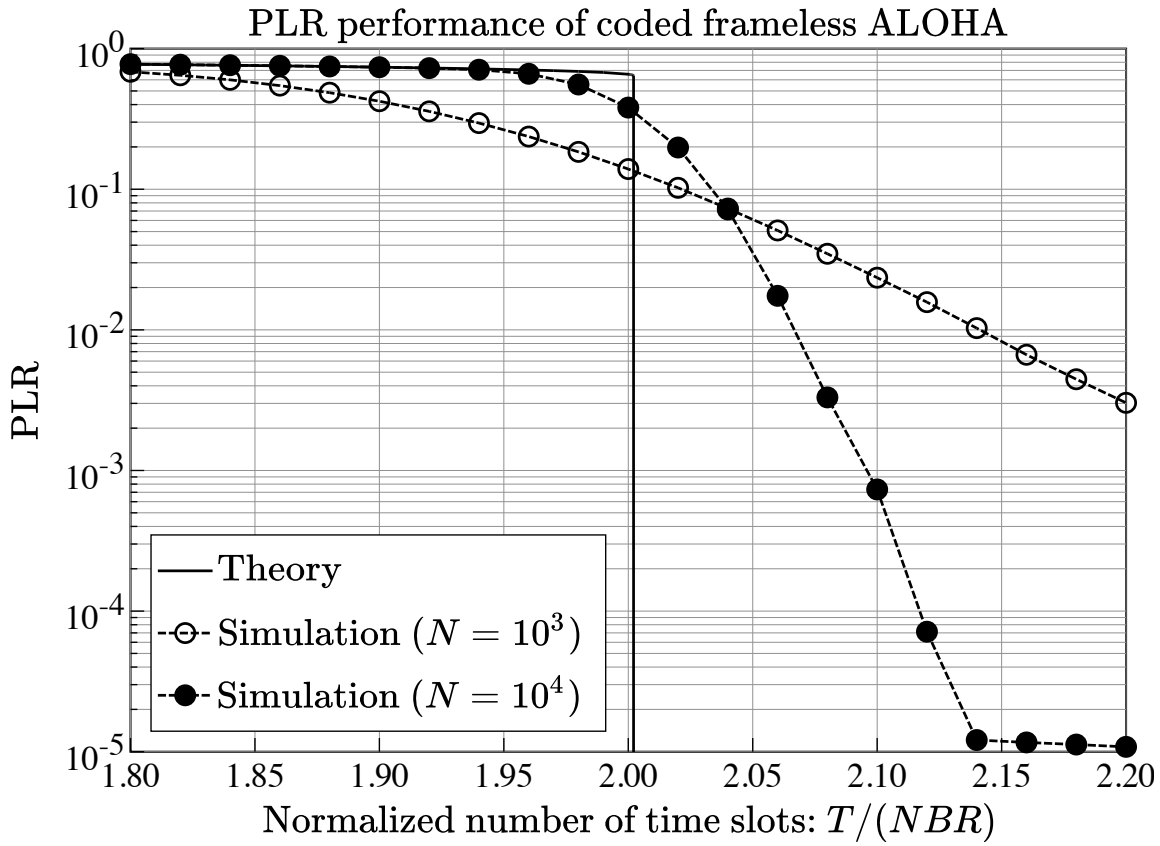

Fig. 2.7 Comparison of theoretical and simulated PLR performance of coded frameless ALOHA with $G = 3.09$ and (3,6)-regular LDPC codes.

The PLR analysis of coded frameless ALOHA can be simply obtained by concatenating density evolution analysis of the original frameless ALOHA and the LDPC code; the probability that each variable node fails to be decoded is obtained by multiplying results from both analyses. Then we have

$$x_l = L^{\mathrm{co}}(w_l^{\mathrm{co}})L^{\mathrm{ch}}(w_l^{\mathrm{ch}}), \tag{2.19}$$

$$w_l^{\mathrm{co}} = 1 - \rho^{\mathrm{co}}(1 - x_{l-1}), \tag{2.20}$$

$$w_l^{\mathrm{ch}} = 1 - \rho^{\mathrm{ch}}(1 - x_{l-1}). \tag{2.21}$$

The theoretical PLR is given by $p_{\mathrm{e}}(T) = x_l$ for sufficiently large l. In order to verify the analysis, theoretical PLR and computer-simulated PLR are compared in Fig. 2.7, where (3,6)-regular LDPC codes and the target degree of $G = 3.09$ are used. As the number of actual users increases, the PLR performance approaches the theoretical

performance. The remaining error floor in the simulated curve is due to the short loops in the parity check matrix, which will vanish as the codeword length increases.

Using the theoretical PLR given in (2.19), the theoretical throughput is defined as a fraction of successfully decoded segments and elapsed slots considering the coding rate, that is

$$S(T) = R\frac{NB(1-p_{\mathrm{e}}(T))}{T}. \tag{2.22}$$

The number of time slots is denoted by T, where each user transmits one segment in the slot. Thus, in order to transmit NB segments, $T \geq NB$ slots are needed.

The following theoretical representation of the throughput enables the optimization problem to be formulated in order to find the optimal target degree and degree distributions of LDPC codes so that the achievable throughput is maximized:

$$\max_{L^{\mathrm{co}}(x),R^{\mathrm{co}}(x),G} \quad \sup_{T} S(T) \tag{2.23}$$

$$\text{s.t.} \quad p_{\mathrm{e}}(T) < 1-\alpha \tag{2.24}$$

$$0 < R \leq 1 \tag{2.25}$$

$$G_{\min} \leq G \leq G_{\max} \tag{2.26}$$

$$\sum_{\mathtt{l}_{\min}}^{\mathtt{l}_{\max}} L_k^{\mathrm{co}} = \sum_{\mathtt{r}_{\min}}^{\mathtt{r}_{\max}} R_k^{\mathrm{co}} = 1. \tag{2.27}$$

In the optimization problem, target degree and degree distribution of the code are optimized.

2.7.2 Numerical Examples

In order to reveal the achievable performance of coded frameless ALOHA, target degree and degree distributions are theoretically optimized. Differential evolution [89], which is a genetic algorithm, has been used to solve the optimization problem since the problem is a multi-modal optimization. Parameters are as follows: $(G_{\min}, G_{\max}) = (1, 4)$, $(\mathtt{l}_{\min}, \mathtt{l}_{\max}) = (1, 10)$, $(\mathtt{r}_{\min}, \mathtt{r}_{\max}) = (1, 40)$, $\alpha = 1 - 10^{-5}$, $N = 10^4$, and $B = 100$.

The optimal target degree for the proposed coded frameless ALOHA is $G = 2.81$, whereas the optimal target degree for the original frameless ALOHA is approximately $G = 3.09$ [91, 68]. Although a smaller target degree generates an earlier waterfall region and a higher error floor, the earlier waterfall can potentially achieve higher throughput performance. This hidden potential is maximized by the use of erasure correcting codes, while the erasure correction capability overcomes the inherent error floor. Moreover,

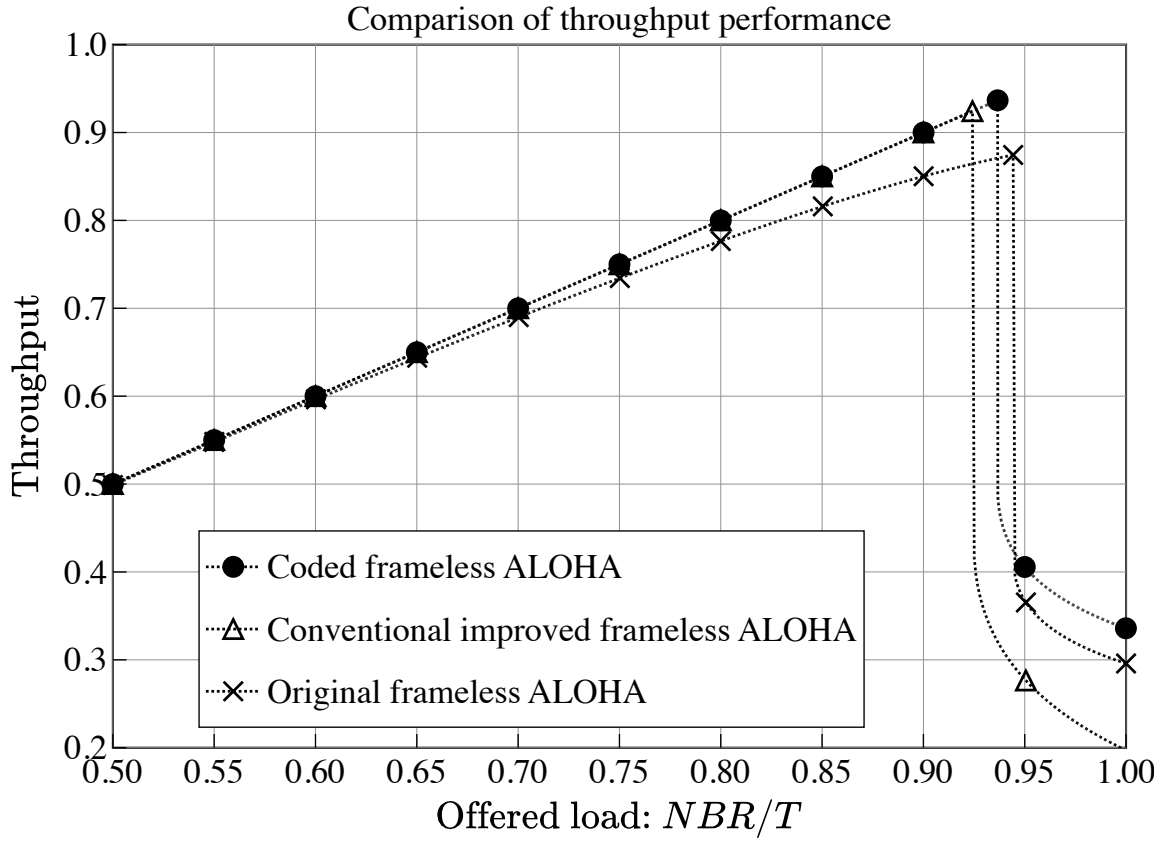

Fig. 2.8 Theoretical throughput performance of coded frameless ALOHA with optimized degree distributions. Coded frameless ALOHA outperforms conventional frameless ALOHA schemes.

the optimal variable node degree distribution is $L^{\text{co}}(x) = 0.91x + 0.09x^2$, and the optimal function node degree distribution is

$$\begin{aligned} R^{\text{co}}(x) =& 0.05x^2 + 0.01x^3 + 0.02x^4 + 0.01x^8 + 0.02x^9 + \\ & 0.03x^{10} + 0.01x^{11} + 0.03x^{12} + 0.01x^{13} + 0.05x^{14} + \\ & 0.09x^{16} + 0.02x^{17} + 0.10x^{18} + 0.13x^{19} + 0.13x^{20} + \\ & 0.12x^{21} + 0.09x^{22} + 0.02x^{23} + 0.05x^{25} + 0.01x^{27}, \end{aligned}$$

where the rate is $R = 0.94$.

Presence of degree-1 codeword bits is an unreasonable setting in the general case because the erasure correction capability would be very poor. Surprisingly, the collaboration with SIC, however, allows the code to work very well.

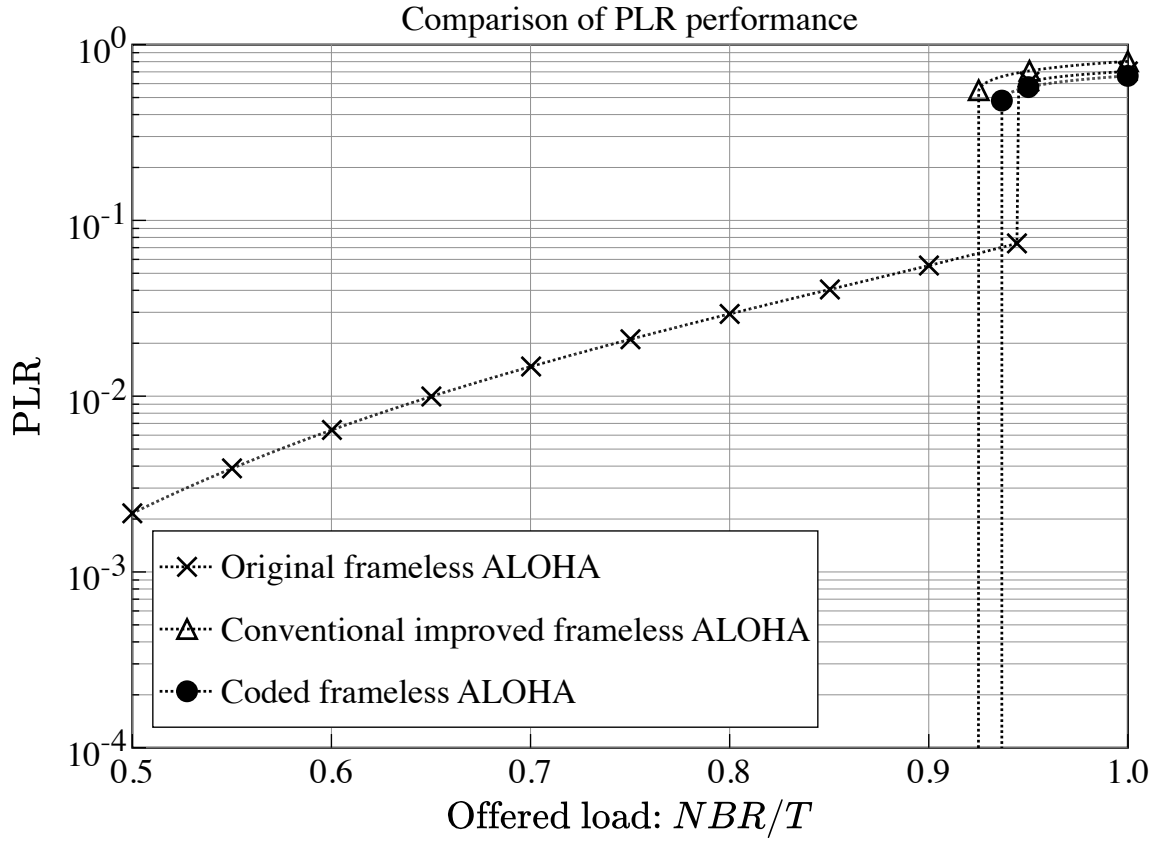

Fig. 2.9 Theoretical PLR performance of coded frameless ALOHA with optimized degree distributions. Coded frameless ALOHA and improved frameless ALOHA are observed to eliminate the error floor of the original frameless ALOHA.

The theoretical PLR and throughput performance of coded frameless ALOHA are compared with the original frameless ALOHA, conventional improved frameless ALOHA [74].Figures 2.8 and 2.9 are the theoretical throughput and PLR performance, respectively. The horizontal axes indicate the normalized load, *i.e.*, the fraction of transmitted information packets and time slots, given as NBR/T. It is observed from Fig. 2.8 that our proposed coded frameless ALOHA can achieve higher throughput than improved frameless ALOHA, while completely eliminating the error floor as shown in Fig. 2.9.

However, in order to practically achieve the performance revealed here, encoded data should be divided into single bits. Such fragmentation would lead to larger overhead, since each transmitted packet has to equip preamble. Hence, the performance gain obtained via concatenating an erasure correcting code would be canceled with the additional overhead caused by packet dividing. Although it is also possible to divide

packets into segments consisting of multiple bits, the resulting PLR performance becomes worse, as a multiple codeword bits erase simultaneously when a segment fails to be retrieved via SIC. In the following chapter, we consider to achieve higher throughput utilizing different improvement.

2.8 Chapter Summary

In this chapter, conventional frameless ALOHA protocol was described. Based on the density evolution analysis, an optimization problem for the target degree so as to maximize the average throughput was proposed, where maximization of the theoretical peak throughput was used as the utility function. The optimization scheme proposed here can be used in arbitrary uplink multiple access network using frameless ALOHA.

Moreover, we addressed the elimination of the error floor, by concatenating erasure an correcting code, proposing namely coded frameless ALOHA. Coded frameless ALOHA was observed to eliminate the error floor under the asymptotic setting where the codeword was divided into single bit to be transmitted. As the asymptotic setting would cause huge signaling overhead and thus poor throughput, we concluded that coded frameless ALOHA was impractical.

Chapter 3

ZigZag Decodable Frameless ALOHA

We consider to apply ZigZag decoding (ZD) into frameless ALOHA. As ZD resolves collision of two packets, the combination of ZD and successive interference cancellation (SIC) is expected to provide lower packet loss rate (PLR) performance than the conventional frameless ALOHA. A straightforward implementation is firstly considered, namely *ZigZag decodable frameless ALOHA (ZDFA)*, while deriving the exact theoretical expression for the PLR performance, and it is shown that the straightforward implementation results in poor PLR and throughput performance than the conventional scheme. Then, we propose a sophisticated implementation so called *enhanced ZigZag decodable frameless ALOHA (E-ZDFA)*, where the transmission probability is dynamically increased so as to improve the throughput by enhancing chances for un-retrieved users to transmit. It is revealed through computer simulations that E-ZDFA achieves higher throughput performance than the original frameless ALOHA, while lowering the error floor.

3.1 Introduction

The SIC process of coded ALOHA, including frameless ALOHA, is identical to belief BP decoding over a binary erasure channel, namely peeling decoder, and hence analytical tools for codes-on-graphs are available for coded ALOHA. While the peeling decoder can only start decoding from *degree-1 check nodes*, *i.e.*, parity checks, including only one unknown codeword bits, more powerful decoders that can start decoding from check nodes with higher degree have been proposed. For instance, Olmos *et al.* [92] proposed a tree-structure expectation propagation (TEP) decoder, in which a check node with two unknown codeword bits, *i.e.*, *a degree-2 check node*, can be used as a starting point of decoding. The TEP decoder was shown to yield a better bit-error-rate

performance than that of the BP decoder. However, the TEP decoder requires the structure of the bipartite graph, and this requirement cannot be fulfilled in frameless ALOHA, which continues probabilistic transmission, in which the bipartite graph is constructed on the fly. Notably, the result of the TEP decoder showed that the idea of directly resolving collided packets would improve the decoding performance.

For multiple access, ZigZag decoding (ZD) has been proposed to demodulate two colliding packets as a solution to the hidden terminal problem [86]. In ZD, colliding users are requested to immediately retransmit their packets by the receiver so as to receive two colliding packets. Then, if the two packets are received with different delays, data packets can partially be demodulated from each received packet. The demodulated part can be used to cancel collision in part in the other colliding packet; as a result, two colliding packets can be retrieved in a ZigZag manner. As TEP decoder improves the decoding performance of LDPC codes, ZD is considered to improve the packet-retrieval performance of frameless ALOHA.

Oinaga *et al*. [93] proposed ZigZag decodable coded slotted ALOHA (ZDCSA), in which ZD is straightforwardly introduced into IRSA. The authors compared ZDCSA with conventional IRSA and showed that ZDCSA achieves better throughput performance when the number of users is *moderately* large, *i.e.*, 1000. However, they also pointed out that the asymptotic throughput of ZDCSA is lower than that of IRSA. This is because ZD requires packet retransmission, resulting in the degradation of throughput performance. Moreover, as IRSA determines the number of retransmissions and slots in which each user transmits its packet in advance, the latter slots are used for transmission of already-retrieved users, for which the throughput performance is also degraded.

To this end, this chapter proposes ZDFA, in which ZD is introduced into frameless ALOHA [67]. First, a straightforward implementation of ZD into frameless ALOHA is discussed, where it is revealed that the asymptotic throughput performance degrades along with the ZDCSA scenario [93] because of additional time slots. Then, we exploited the frameless nature to propose a sophisticated implementation, namely, E-ZDFA, in which the transmission probability is dynamically increased to enhance the chances for unretrieved users to transmit. Simultaneously, users retrieved via ZD or received without collision, *i.e.*, retrieved upon being received, are acknowledged by the receiver through two-bit feedback to stop retransmission in following slots. The error floor of E-ZDFA was theoretically derived in this study, confirming that E-ZDFA has the potential to retrieve more users than the original frameless ALOHA. Computer simulations were conducted, which show that a suitably chosen transmission probability

outperforms the throughput performance of the frameless ALOHA and IRSA with the degree distribution obtained in [63].

3.2 System Model

Our model comprises a network with N transmitting users and a common BS. Each user has an own packet at the beginning of the communication, and new packets are supposed to not be generated (no backlogging). Throughout the study, a noise-free channel was considered, in which the transmitted packet can be successfully retrieved by the receiver without collision. Packets that collide are considered to be lost, as, for mathematical tractability reasons, the capture effect [69] is not considered. As this model is considered to be the worst-case scenario, it provides a lower-bound of the throughput performance in practical situations, in which the capture effect would be available.

Moreover, the BS was assumed to be able to distinguish the following conditions for each time slot:

(a) No users have transmitted.

(b) Only one user has transmitted, *i.e.*, the time slot is a singleton.

(c) Two users have transmitted and collided.

(d) Three or more users have transmitted and packets have collided.

Especially, the BS should detect condition-(c) so that ZD can be operated. This was realized by supposing that each packet contains a unique word, which identifies the transmitter. The BS can detect collision of two packets by calculating the correlation between the received packet and unique words [86], and the BS then acknowledges the collision of two packets when the correlation has two peaks. This assumption is practical, as each transmitted packet should contain information indicating the transmitter of the packet.

Time slots comprise two kinds of *subslots*, *i.e.*, uplink subslot (US) and downlink subslot (DS), as shown in Fig. 3.1. Users transmit their packets in the US, and the BS broadcasts feedback signal to the following DS. A detailed explanation about feedback signals from the BS is provided in the subsequent sections. Upon transmission, slots are organized into a *frame*.

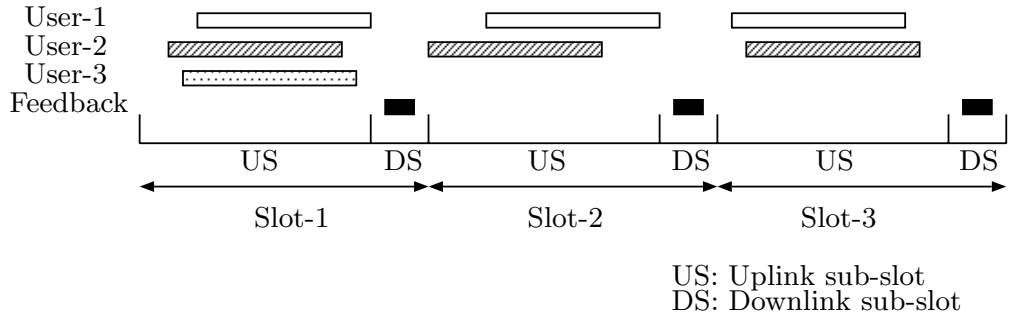

Fig. 3.1 Illustration of time slots and subslots.

3.3 ZigZag Decodable Frameless ALOHA

This section explains the application of ZD into frameless ALOHA. Next, we discuss a simple implementation, in which ZD is straightforwardly introduced into frameless ALOHA, and propose a sophisticated implementation, in which the transmission probability is dynamically increased.

3.3.1 ZigZag Decoding

To perform ZD, when a collision of two users is detected, the BS requires the users to retransmit immediately in the next time slot. Throughout the study, we assumed that packets collide with *segment-wise* delay and the possible back-off is segment-wise, where the slot is supposed to be further divided into segments. Figure 3.2 depicts how ZD proceeds, with each packet consisting of four segments. Upon detecting a collision of two packets, the BS broadcasts a feedback signal, which requires the colliding users to immediately retransmit the packets. Then, users who have transmitted the packets retransmit their packets in the next slot, while other users refrain from transmitting packets. Figure 3.2-(a) shows that the first segment of packet-1 (gray colored) and the last segment of packet-2 (white colored) are received without collision. If the difference between the arrival of two packets is different in two received packets, as shown in the figure, then the retrieved segment of packet-1 is collided in the second slot, where the BS can cancel retrieved segment from slot-2, as shown in Fig. 3.2-(b). Upon canceling segments, new segments become collision-free, and the same procedure is iterated. The cancellation can be performed if packets are received with different delays in two slots. We simply modeled ZD as a random variable without considering the actual arrival

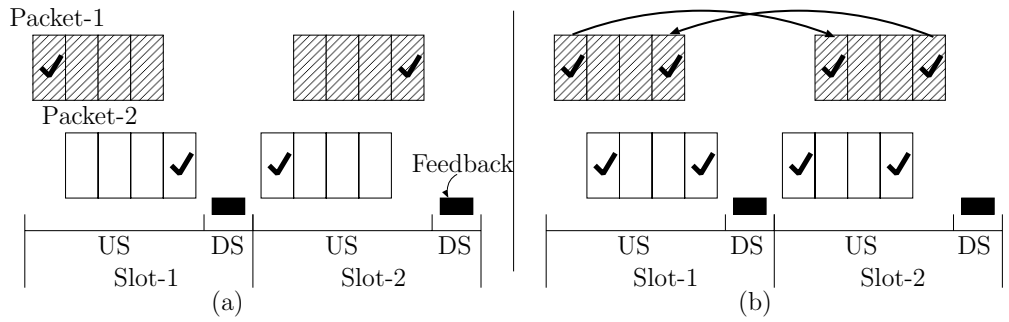

Fig. 3.2 Illustration of ZD. (a) Two packets collide in slot-1, and are retransmitted in the next slot. The first segment of packet-1 and the last segment of packet-2 are free of collision in slot-1; thus, they are retrievable. (b) By canceling the retrieved segments, the third segment of packet-2 becomes free of collision in slot-1, while the second segment of packet-2 becomes free of collision in slot-2.

timing. The two retransmitted packets are retrieved with probability ω; however, ZD failed to retrieve both the packets with probability $(1-\omega)$.

3.3.2 Straightforward Implementation

Let us first consider a straightforward implementation of ZD into frameless ALOHA, where the scheme is termed *ZDFA*. In this scenario, users operate in the same manner as in the original frameless ALOHA, except for the requested retransmission caused by the feedback signal from the BS. When the BS broadcasts the two-bit feedback signal upon detecting collision of two packets, the colliding users immediately retransmit their packets in the next time slot, while the other users refrain from transmitting. When the slot ends, all the users restart the probabilistic transmission.

Theoretical Analysis for Packet Loss Rate

Let us consider the theoretical expression for the PLR of ZDFA. Transmission of users can be depicted via bipartite graph as well as the original frameless ALOHA. The bipartite graph consists of *variable nodes*, *observation nodes*, and edges between two kinds of nodes. Variable and observation nodes correspond to transmitted packets and time slots, respectively, and the edge denotes that the packet of the connected variable node is transmitted in the slot of the connected observation node. Moreover, *degree* of the node is defined as the number of edges connected to the node; degree of variable node shows the number of times the corresponding user has transmitted during the frame, and degree of observation node indicates the number of users that

have transmitted in the slot. For the sake of visibility, the additional slot for ZD is omitted in the graph, as the additional slots always appear after two packets collide.

Similar to the original frameless ALOHA, density evolution [23] can be used to analyze the asymptotic performance. Recall that, given the number of time slots T, the PLR performance of the original frameless ALOHA can be given by

$$p_{\mathrm{e}}(T) = L(1 - \rho(1 - x_l^{(T)})), \tag{3.1}$$

where $x_l^{(T)}$ denotes the probability that the edge is connected to the variable node of an unretrieved user at the l-th iteration and given by

$$\begin{aligned} x_l^{(T)} &= \lambda(1 - \rho(1 - x_{l-1}^{(T)})) \\ &= \lambda \left(1 - \rho_1 - \sum_{k=2}^{N} \rho_k (1 - x_{l-1}^{(T)})^{k-1} \right). \end{aligned} \tag{3.2}$$

Regarding ZDFA, additional packet retrieval through ZD should be considered. Note that $(1 - \rho(1 - x_{l-1}^{(T)}))$ in (3.2) gives the probability that the edge is connected to the observation nodes corresponding to the colliding slots. In the original frameless ALOHA, BS can resolve the collision only when slots become singletons. In contrast, in ZDFA, BS can also resolve the collision when slots contain collision of two packets. This modification can be reflected in the analysis yielding

$$x_l^{(T)} = \lambda \left(1 - \rho_1 - \rho_2 \left(\omega + (1 - \omega)(1 - x_{l-1}^{(T)}) \right) - \sum_{k=3}^{N} \rho_k (1 - x_{l-1}^{(T)})^{k-1} \right), \tag{3.3}$$

and if ω is 1, *i.e.*, ZD always succeeds[1], (3.3) is simplified to

$$x_l^{(T)} = \lambda \left(1 - \rho_1 - \rho_2 - \sum_{k=3}^{N} \rho_k (1 - x_{l-1}^{(T)})^{k-1} \right). \tag{3.4}$$

In (3.3) and (3.4), additional slots dedicated to ZD for immediate retransmission are implicitly ignored, and thus the theoretical PLR curve shows an earlier waterfall region than the exact PLR performance. Therefore, the penalty for the additional slots should be included. If there are T independent slots in which users can perform probabilistic transmission, the average number of resulted slots including required retransmission is calculated as $(T + TR_2)$, where R_2 is the probability that the observation node has

[1]Probability ω can be regarded as the probability of the number of segments being sufficiently large.

degree-2. Then, the PLR performance of ZDFA can be given by

$$p_{\mathrm{e}}^{(\mathrm{ZD})}(T+TR_2) = L\left(1-\rho_1-\rho_2-\sum_{k=3}^{N}\rho_k(1-x_l^{(T)})^{k-1}\right), \tag{3.5}$$

or if there are T time slots in total (including required retransmission), we have

$$p_{\mathrm{e}}^{(\mathrm{ZD})}(T) = L\left(1-\rho_1-\rho_2-\sum_{k=3}^{N}\rho_k(1-x_l^{\left(\frac{T}{1+R_2}\right)})^{k-1}\right). \tag{3.6}$$

Throughput Performance of ZigZag Decodable Frameless ALOHA

This study focused on the achievable throughput performance of ZDFA. By using (3.6), the throughput performance at the T-th slot, namely $S(T)$, is defined as

$$S(T) \triangleq \frac{N(1-p_{\mathrm{e}}^{(\mathrm{ZD})}(T))}{T}. \tag{3.7}$$

The throughput performance (and consequently PLR performance) of ZDFA is determined by the target degree, which is optimized to maximize the throughput performance. According to [94], the average throughput performance of frameless ALOHA can be maximized by finding the optimal target degree which maximizes the *peak* throughput. At the peak point, the corresponding PLR should be less than the given threshold. It is worth noting that the retrieval of all the users would result in a large delay because of the probabilistic transmission [67]. In this study, the optimization policy used in [94] was followed, and the optimal target degree for ZDFA was obtained using the following optimization problem:

$$\max_{G} \quad \sup_{T} S(T) \tag{3.8}$$

$$\text{s.t.} \quad p_{\mathrm{e}}^{(\mathrm{ZD})}(T^*) \leq 1-\alpha, \tag{3.9}$$

where $T^* = \arg\sup_T S(T)$ and α denotes the threshold on the fraction of retrieved users.

By using brute-force search over G, $G = 3.76$ was revealed to achieve the highest throughput performance, where the corresponding peak throughput was 0.856, while the original frameless ALOHA with the optimal target degree of $G = 3.09$ achieved the peak throughput of 0.867 [94]. The result reveals that straightforward implementation of ZD into frameless ALOHA causes degradation of the throughput performance. Figure

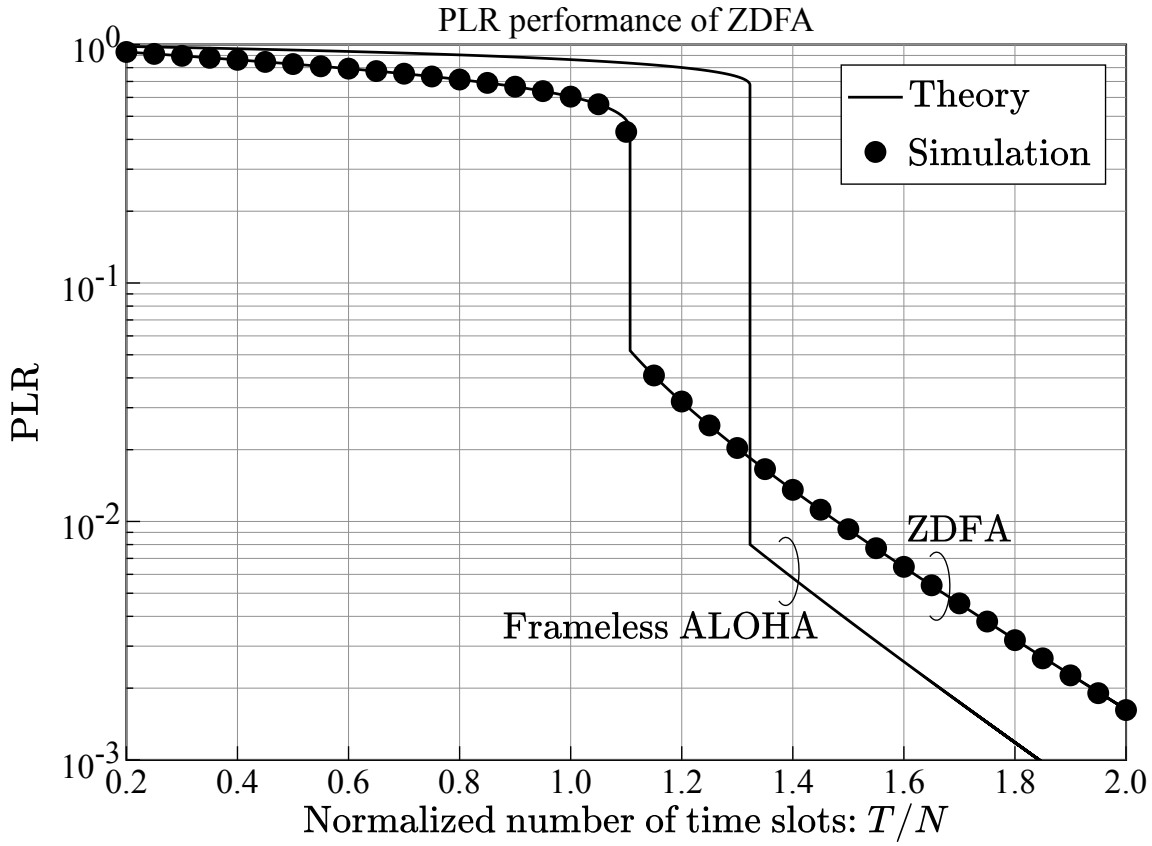

Fig. 3.3 Comparison of PLR performance of ZDFA and the original frameless ALOHA. The target degree of $G = 3.76$ is used for all curves, and $N = 10^4$. ZDFA has higher error floor than frameless ALOHA.

3.3 depicts the PLR performance of ZDFA with $G = 3.76$, where the number of users is supposed to be 10^4. For comparison, the PLR performance of the original frameless ALOHA with the optimal target degree $G = 3.76$ is shown. We confirmed that our derived analysis (3.5) coincides with the result of computer simulations, verifying that the theoretical analysis provides the exact PLR performance of ZDFA. The PLR performance of frameless ALOHA should have an error floor caused by the probability that the user never transmits during the frame. Hence, for frameless ALOHA, a higher transmission probability results in lower error floor. However, in Fig. 3.3, ZDFA shows higher error floor than the original frameless ALOHA while ZDFA with $G = 3.76$ uses the same transmission probability as frameless ALOHA with $G = 3.76$. This is because ZDFA uses some slots for the required retransmission to perform ZD, where other users are prohibited to transmit. In other words, even if the frame length is T, users do not always have T chances to transmit their packets, thus resulting in

a high error floor. Although the occurrence of waterfall in ZDFA is earlier than in frameless ALOHA, a higher error floor limits the number of retrieved users, and hence the resulting throughput performance is lower than that of frameless ALOHA. In other words, lowering the error floor of ZDFA is an obvious solution to the degradation of the throughput performance.

3.3.3 Enhanced ZigZag Decodable Frameless ALOHA

To solve the aforementioned problem of lower throughput performance in ZDFA as compared to frameless ALOHA, we propose *E-ZDFA*, which lowers the error floor by utilizing additional one-bit feedback from the BS. E-ZDFA exploits three additional features: *retransmission canceling*, *transmission probability updating*, and *predictive-canceling*. Specifically, the BS uses a feedback signal when a single user has been retrieved from collision-free slot or two users have been retrieved through ZD. With the feedback, the retrieved user can acknowledge that its own packet has been successfully retrieved. Then, the user stops retransmitting in the following slots to suppress collision. Simultaneously, other users also acknowledge that one (or two) user(s) has (have) been retrieved, and the number of contending users decreases; if the feedback indicating the retrieval of the transmitted packet is received after receiving the feedback requiring retransmission, the number of retrieved packets is considered to be two, as the BS broadcasts the feedback requiring retransmission upon detecting collision between two packets; otherwise, only one user is retrieved via collision-free reception. Next, transmission probability in E-ZDFA is dynamically updated, *i.e.*, increased to encourage transmission of other users. Moreover, as the BS knows when the retrieved packets are transmitted, it is able to cancel retrieved packets as soon as the packet arrives, thus performing ZD. The three aforementioned features work together to lower the error floor, and exploit higher throughput performance than that in the original frameless ALOHA.

Feedback Signal Utilization

In E-ZDFA, the BS broadcasts a feedback signal to users when the transmitted packets are retrieved via ZD, as well as when only one packet is received and retrieved. It is worth noting that the feedback signal does not require to specify which user is retrieved, and hence the feedback only requires additional one-bit; regardless of whether the transmitted packet(s) is (are) retrieved. Users who have acknowledged that their packets are retrieved cancel their retransmission in the following slots (*retransmission*

canceling). Note that, in the original frameless ALOHA, the retransmission canceling does not improve throughput performance, neither does it lower the error floor, as the SIC and retransmission canceling are interchangeable. However, in case of ZD, the retransmission canceling should be performed first, and it plays an important role in lowering error floor and increasing throughput by retrieving more users.

Owing to retransmission canceling, the channel load decreases as the frame size increases, and users are able to transmit more frequently. Hence, E-ZDFA dynamically increases the transmission probability of users (*transmission probability updating*). Note that all the users are able to know the number of users who have stopped retransmission by observing the feedback from the BS. Let us denote $N_{\text{ret}}^{(T)}$ by the number of users acknowledged by the BS as retrieved until the T-th slot. Then, instead of the original transmission probability of $p = G/N$, the probability at the T-th slot is dynamically updated as

$$p^{(\text{EZ})}(T) = \frac{G}{N - N_{\text{ret}}^{(T)}}. \tag{3.10}$$

Conventional frameless ALOHA also uses a feedback signal, which indicates the end of a frame; the feedback signal only requires one-bit. In E-ZDFA, the BS broadcasts a feedback signal to inform users about the following four conditions:

- The transmitted packet(s) is (are) retrieved.
- Two packets are collided, and the corresponding users are required to retransmit.
- The frame is ended as the desired PLR has been achieved at the BS.
- The frame is continued as the desired PLR has not been achieved.

Therefore, the feedback signal of E-ZDFA only requires at most two bits, which can be neglected for evaluating throughput performance.

Predictive Cancelling of Packets

Although the feedback signal can stop retransmission of retrieved users, users retrieved via SIC do not stop retransmission as they cannot acknowledge whether their packets have been retrieved. However, BS can recall that each packet contains the information indicating the time slots in which the packet is transmitted; thus, the BS can predict when retrieved packets are transmitted. This feature allows the BS to cancel retrieved packets as soon as a packet is received (*predictive-canceling*).

Figure 3.4 illustrates predictive-canceling. In Fig. 3.4-(a), three users transmit in a time slot, and one of them has already been retrieved through SIC. As the BS knows

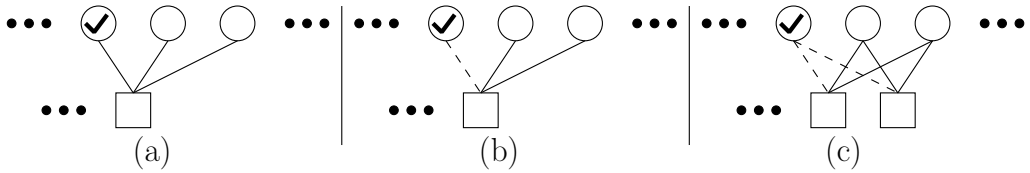

Fig. 3.4 Illustration of predictive-canceling. (a) Three users transmit simultaneously, and one has already been retrieved via SIC. (b) The BS can cancel the packet as it knows that the packet will be transmitted in this slot. The slot can be regarded as degree-2 slot. (c) The BS requires the users to retransmit packets immediately to perform ZD.

that the slot contains the retrieved packet, the BS cancels the packet, as shown in Fig. 3.4-(b). Then, the slot becomes degree-2 so that the BS broadcasts the second feedback requiring the *three* users to immediately retransmit the packets in the next slot. After canceling the retrieved packet from the received packet, the BS performs ZD to these two slots, as shown in Fig. 3.4-(c). Suppose that ZD has succeeded and the BS broadcasts the fourth feedback, users can guess that two packets are retrieved via ZD and increase $N_{\mathrm{ret}}^{(T)}$ by two.

Error Floor Analysis for Enhanced ZigZag Decodable Frameless ALOHA

Owing to the retransmission canceling and transmission probability updating, the degree distribution of E-ZDFA varies dynamically as the number of slots increases. As a result, it is difficult to track the exact behavior of degree distributions; hence, density evolution cannot be straightforwardly applied into E-ZDFA. A simple yet informative approach to analyze the system is to derive the error floor of E-ZDFA. Frameless ALOHA protocols have an error floor because of the probabilistic transmission, and the error floor is calculated by considering the probability that the user never transmits during the frame. Higher error floor yields an unstable system, where non-negligible fraction of users are not retrieved upon terminating the frame. At this point, our proposed E-ZDFA dynamically updates the transmission probability and is expected to have lower error floor than the original frameless ALOHA. Therefore, instead of the exact PLR analysis, we theoretically derived the error floor of E-ZDFA by analyzing $N_{\mathrm{ret}}^{(T)}$.

Let us define $N^{(T)} \triangleq N - N_{\text{ret}}^{(T)}$ as the number of contending users at the T-th slot. Hence, the probability that k users transmit at the k-th slot, namely $R_k^{(T)}$ is given by

$$R_k^{(T)} = \binom{N^{(T)}}{k} \left(p^{(\text{EZ})}(T)\right)^k \left(1 - p^{(\text{EZ})}(T)\right)^{N^{(T)}-k}. \tag{3.11}$$

The probability of a single user being retrieved from collision-free reception is $R_1^{(T)}$, and the probability that two users are retrieved via ZD is $\omega R_2^{(T)}$. Moreover, the probability that retrieved packets are included in a received signal should be considered. Thus, the density evolution analysis for ZDFA was used to estimate the number of retrieved packets. Let us denote the approximated PLR at the T-th slot by $\beta(T)$, which is defined as in (3.6) by using density evolution. When the slot has degree-k, the probability that $(k-1)$ edges have been retrieved so that the remaining packet can be retrieved is

$$\binom{k}{1} \beta(T) \left(1 - \beta(T)\right)^{k-1}, \tag{3.12}$$

and similarly, the probability of two packets remaining is

$$\binom{k}{2} \left(\beta(T)\right)^2 \left(1 - \beta(T)\right)^{k-2}. \tag{3.13}$$

Then, $N_{\text{ret}}^{(T)}$ is calculated as

$$\begin{aligned} N_{\text{ret}}^{(T)} \approx & N_{\text{ret}}^{(T-1)} + R_1^{(T)} + 2\omega R_2^{(T)} \\ & + \sum_{k=3}^{N^{(T)}} R_k^{(T)} \left(\binom{k}{1} \beta(T) \left(1 - \beta(T)\right)^{k-1} + 2\omega \binom{k}{2} \left(\beta(T)\right)^2 \left(1 - \beta(T)\right)^{k-2} \right), \end{aligned} \tag{3.14}$$

where $N_{\text{ret}}^{(T)}$ is updated while the inequality

$$\frac{N_{\text{ret}}^{(T)}}{N} + \left(1 - \beta(T)\right) \leq 1 \tag{3.15}$$

is satisfied. Furthermore, if $N_{\text{ret}}^{(T)}/N + (1 - \beta(T)) > 1$, $N_{\text{ret}}^{(T)}$ is not updated and the same transmission probability is used in following slots.

By using (3.14), the transmission probability at the T-th slot can be theoretically calculated. Finally, the error floor for the PLR performance of E-ZDFA is given by

$$p_{\mathrm{e,LB}}(T + T\bar{R}_2^{(T)}) = \prod_{t=1}^{T}(1 - p^{(\mathrm{EZ})}(t)), \tag{3.16}$$

or equivalently

$$p_{\mathrm{e,LB}}(T) = \prod_{t=1}^{\frac{T}{1+\bar{R}_2^{(T)}}} (1 - p^{(\mathrm{EZ})}(t)), \tag{3.17}$$

where $\bar{R}_2^{(T)}$ is the average fraction of additional slots occurring with T original slots and given by

$$\bar{R}_2^{(T)} = \frac{\sum_{t=1}^{T} R_2^{(t)}}{T}. \tag{3.18}$$

3.4 Numerical Examples

3.4.1 Throughput and Packet Loss Rate Performance

We here evaluated the achievable throughput performance of E-ZDFA. While ZDFA, which does not consider retransmission canceling, transmission probability updating, and predictive canceling, can be theoretically analyzed via density evolution, E-ZDFA cannot be analyzed via density evolution because of these additional features. Hence, we cannot theoretically optimize the target degree so as to maximize the throughput performance. Therefore, in order to investigate the achievable throughput performance of E-ZDFA, let us consider to use computer simulations to seek the target degree that maximizes the average throughput. Although such heuristic search does not necessarily yield the global-optimum of the target degree, the solution guarantees how much performance gain can be *at least* achieved via E-ZDFA. By using the brute-force search, the target degree of $G = 3.32$ yielded the highest throughput of 0.929, which outperforms the peak throughput of conventional frameless ALOHA, namely 0.867.

Figure 3.5 depicts the PLR performance of E-ZDFA with $G = 3.32$. For comparison, PLR performance of ZDFA (without additional feedback) with $G = 3.32$ and the original frameless ALOHA with the optimized target degree $G = 3.09$ are also depicted. Note that the PLR curves in Fig. 3.5 are obtained through computer simulations, not including the theoretical error floor analysis. The comparison of E-ZDFA and ZDFA showed that transmission probability updating lowers the error floor, while showing an

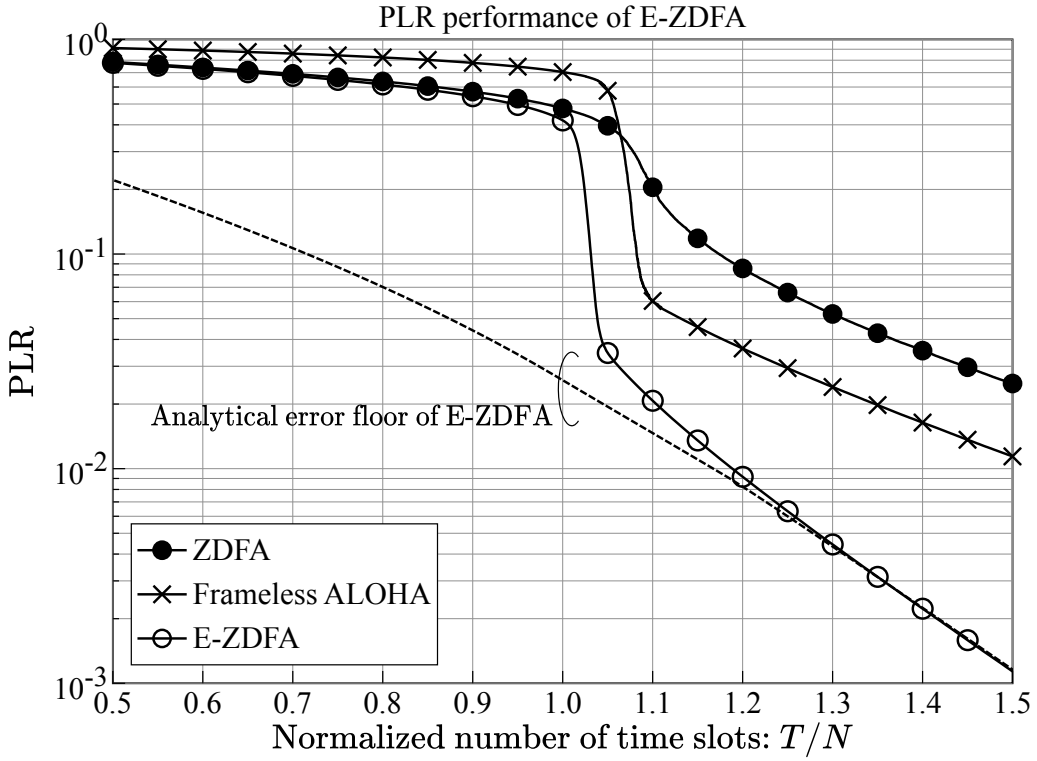

Fig. 3.5 PLR performance of E-ZDFA. E-ZDFA, frameless ALOHA, and ZDFA use the target degree of $G = 3.32$, $G = 3.09$, and $G = 3.32$, respectively. The number of users is 10^4. E-ZDFA is observed to achieve lower error floor than the original frameless ALOHA and ZDFA, while showing earlier waterfall region.

earlier waterfall region. Moreover, E-ZDFA is observed to have a lower error floor than conventional frameless ALOHA owing to the additional features. Notably, the PLR of E-ZDFA approaches the theoretical error floor given in (3.17) with increasing number of time slots, where the error floor achieves lower PLR than ZDFA and frameless ALOHA.

3.4.2 Comparison with State-of-the-Art Approaches

E-ZDFA automatically determines the suitable frame length due to the frameless structure and achieves the designed throughput performance for any number of users. This section shows the comparison of E-ZDFA with state-of-the-art coded ALOHA scheme, namely IRSA with degree distribution derived in [63], in terms of average

throughput. In this study, the degree distribution for IRSA is used as

$$\begin{aligned} L(x) =& 0.494155x^2 + 0.159085x^3 + 0.107372x^4 + 0.070336x^5 + 0.045493x^6 \\ &+ 0.019898x^7 + 0.024098x^{11} + 0.008636x^{12} + 0.005940x^{13} + 0.008749x^{15} \\ &+ 0.002225x^{18} + 0.001261x^{20} + 0.002607x^{22} + 0.008092x^{23} + 0.002287x^{24} \\ &+ 0.012274x^{25} + 0.002530x^{26} + 0.003094x^{27} + 0.002558x^{28} + 0.005891x^{29} \\ &+ 0.013419x^{30}, \end{aligned} \tag{3.19}$$

where the peak throughput is 0.977.

With this degree distribution, each user decides the number of retransmissions and then selects time slots to transmit the packet from the frame. Therefore, while E-ZDFA and frameless ALOHA automatically determine the frame length, IRSA requires the BS to determine the frame length *prior to transmission*. Moreover, the suitable frame length varies with the number of users, and the BS should obtain the appropriate frame length before the beginning of every frame. In the evaluation, for each number of users, the frame length that yields the highest throughput is obtained via brute-force search; the throughput performance of IRSA is maximized at every point. Although this setting is a bias in favor of IRSA, our proposed E-ZDFA still achieves higher throughput performance than IRSA for a practical number of users, *i.e.*, $N \leq 1000$.

Figure 3.6 shows the throughput performance against the number of users in the network, When $N = 10^4$, IRSA shows the highest throughput performance as it asymptotically exhibits the throughput of 0.977. However, when the number of users decreases, the throughput of IRSA worsens than E-ZDFA even for a suitable frame length. The original frameless ALOHA also outperforms IRSA for $N \leq 500$. This is because the degree distribution of IRSA is optimized so that the peak throughput is maximized in the asymptotic setting, where numbers of users and time slots are infinite. Therefore, if the number of users is not sufficiently large for a typical actual degree distribution in the graph, the performance significantly degrades. In contrast, E-ZDFA and frameless ALOHA show less degradation of throughput than IRSA as the degree of frameless ALOHA schemes follows binomial distribution, which has a gentler slope than the optimized degree distribution of (3.19). Therefore, frameless ALOHA schemes can reproduce the designed degree distribution even when the number of users is not very large; thus, the achieved throughput performance is close to the designed performance. In other words, E-ZDFA and frameless ALOHA are more suitable for multiple access in the network with fluctuating demands than IRSA. Furthermore,

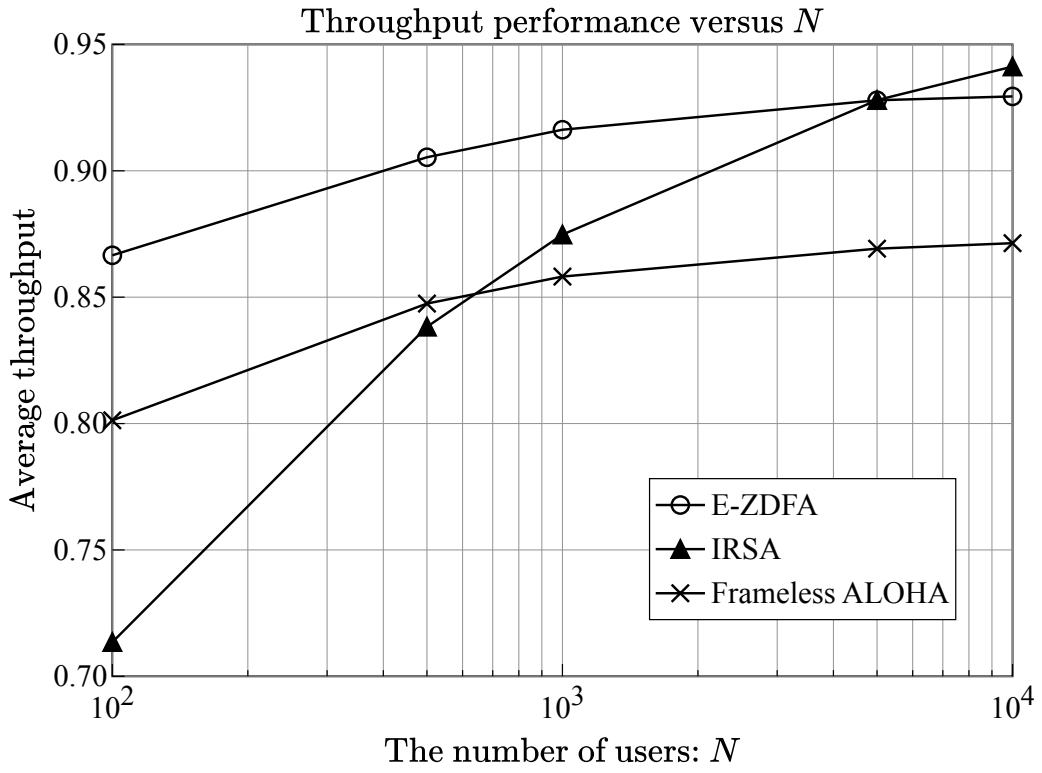

Fig. 3.6 Throughput performance versus the number of users. E-ZDFA and frameless ALOHA use the target degree of $G - 3.32$ and $G = 3.09$, respectively, while IRSA uses the optimized degree distribution of (3.19). IRSA has the highest throughput performance when $N = 10^4$, while the throughput of IRSA degrades as the number of users decreases. E-ZDFA achieves higher throughput performance than IRSA with practically large number of users.

owing to the use of ZD, E-ZDFA always achieves higher throughput than the original frameless ALOHA.

3.4.3 Effect of Threshold on Packet Loss Rate

Let us consider how the threshold on PLR, namely α, affects the throughput of E-ZDFA, by comparing with that of frameless ALOHA. Recall that frameless ALOHA protocols are terminated when $\lfloor \alpha N \rfloor$ packets are retrieved at the BS. Owing to the probabilistic transmission of users, larger α is considered to require larger number of time slots, and hence the throughput would be degraded. At this point, as E-ZDFA achieves lower error floor than the original frameless ALOHA, E-ZDFA is expected to be more robust against the increase of α than frameless ALOHA.

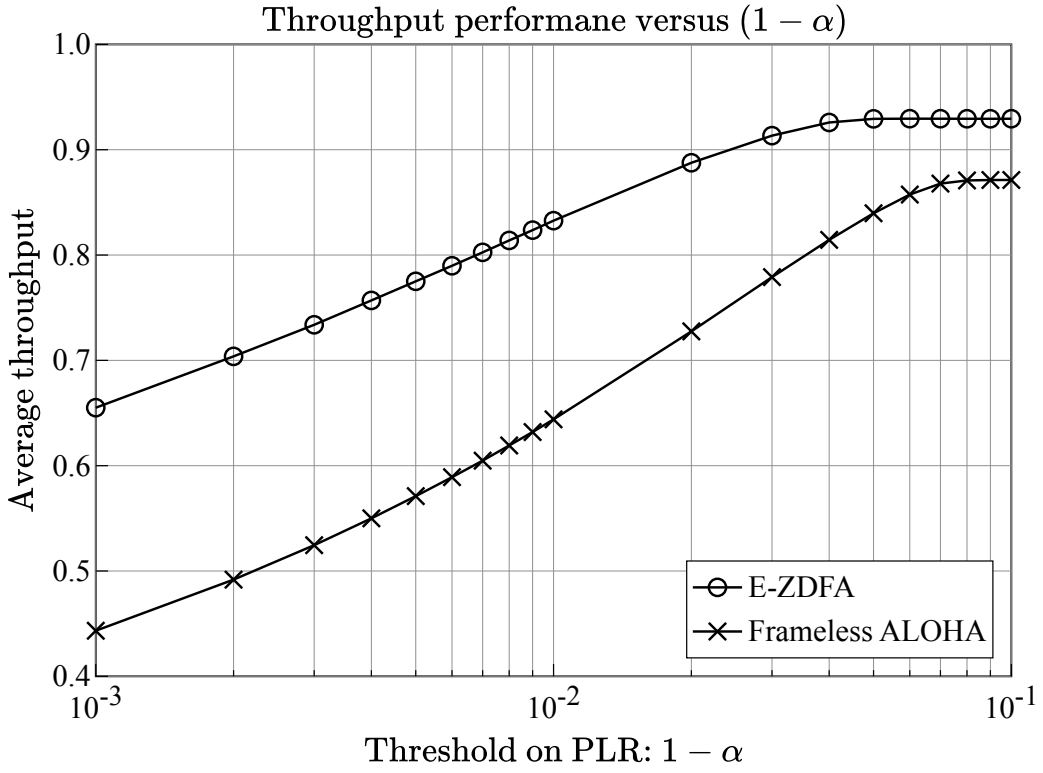

Fig. 3.7 Throughput performance versus the threshold on PLR, namely $(1-\alpha)$. E-ZDFA and frameless ALOHA use the target degree of $G-3.32$ and $G=3.09$, respectively, and the number of users is 10^4. E-ZDFA achieves higher throughput performance for arbitrary value of $(1-\alpha)$.

Figure 3.7 shows the throughput performance of E-ZDFA with different values of α, where the horizontal axis corresponds to the required PLR, namely $(1-\alpha)$, and the number of users is set to $N=10^4$. The threshold on PLR can be regarded as the *guaranteed PLR*, as the transmission continues until the PLR achieves threshold. From the figure, E-ZDFA is shown to achieve higher throughput than the original frameless ALOHA for all α. Moreover, the degradation of throughput according to the increase of α (decrease of $1-\alpha$) is suppressed as E-ZDFA achieves lower error floor than frameless ALOHA, as already discussed earlier. Thus, the result confirms that E-ZDFA is capable of achieving higher throughput than frameless ALOHA, while achieving arbitrary PLR.

Although E-ZDFA has been shown to achieve higher *average throughput* than the original frameless ALOHA, the variance of throughput should be small so as to realize stable system. Figure 3.8 shows the variance of throughput of E-ZDFA and frameless ALOHA. For most values of α, E-ZDFA achieves lower variance than

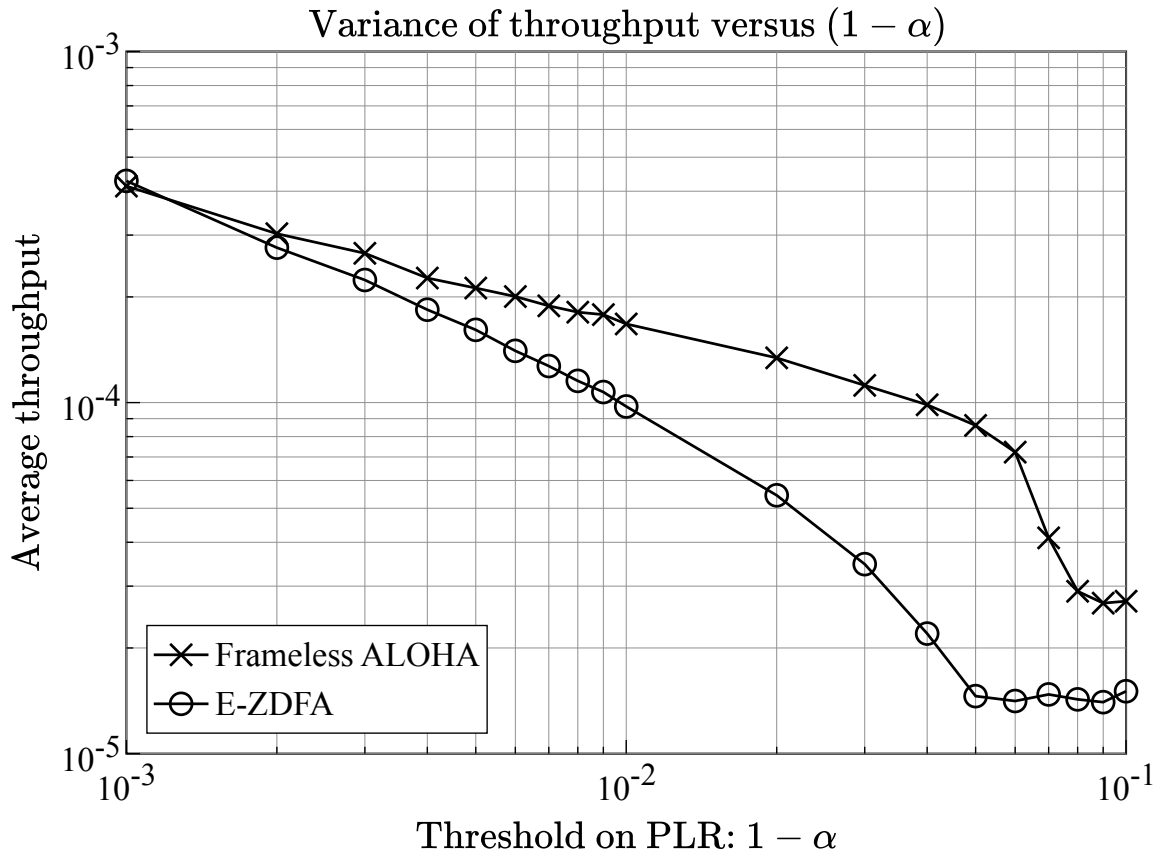

Fig. 3.8 Variance of throughput versus $(1-\alpha)$. E-ZDFA is observed to achieve lower variance than the original frameless ALOHA for arbitrary $(1-\alpha)$.

frameless ALOHA. This is also due to the fact that E-ZDFA has lower error floor. At the point of $1.0-\alpha = 10^{-3}$, *i.e.* 99.9% of users are required to be retrieved, the variance of E-ZDFA becomes slightly higher than frameless ALOHA. However, the gap between them is only 10^{-4} and is negligible, while the gap between achieved throughput is 0.11 as seen in Fig. 3.7. Hence, we can conclude that our proposed E-ZDFA is not only capable of achieving higher throughput than the original frameless ALOHA, but also robust against the requirement for the PLR performance.

3.4.4 Throughput Performance in the Presence of Positive Probability of ZD Failure

Finally, we evaluated the throughput performance of E-ZDFA in a practical situation, where ZD fails to retrieve packets with positive probability $(1-\omega)$. Consider a large-scale network, *e.g.*, $N = 1000$, and the threshold on PLR is set to $\alpha = 0.8$. In

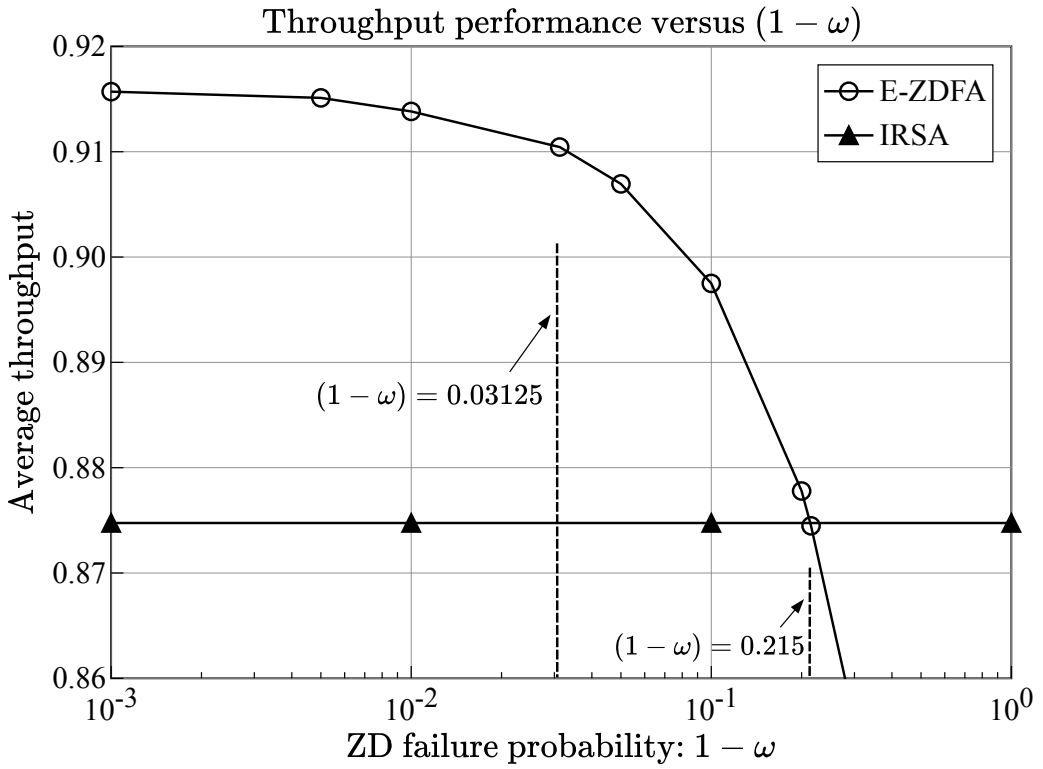

Fig. 3.9 Throughput performance versus the probability of the failure of ZD, namely $(1-\omega)$. E-ZDFA uses the target degree of $G-3.32$, and IRSA uses the degree distribution of (3.19). In order to outperform IRSA by E-ZDFA, the required probability is 0.215.

practicality, the difference between the arrivals of packets is realized by the random selection of back-off patterns by users. Hence, the probability of the failure of ZD is obtained through the number of possible patterns. Specifically, if the number of back-off patterns is denoted by CW, then the probability is calculated as

$$1-\omega = \frac{1}{\mathrm{CW}}. \tag{3.20}$$

Figure 3.9 shows the throughput performance of E-ZDFA for various values of $(1-\omega)$. For comparison, IRSA with the degree distribution [63] is also depicted. E-ZDFA can be observed to outperform IRSA when $(1-\omega) \geq 0.215$, and the corresponding value of CW is approximately 4.65. Therefore, to outperform the conventional IRSA, only five back-off patterns are required. Especially, it was addressed by Gollakota and Katabi [86] that CW is initialized to 32 in standard 802.11, resulting in $(1-\omega) = 1/32 = 0.03125$. As shown in the figure, $(1-\omega) = 0.03125$ yields throughput of 0.91. Therefore, even in a practical situation, our proposed E-ZDFA outperforms the state-of-the-art IRSA.

3.5 Chapter Summary

In this chapter, we investigated the application of ZD into frameless ALOHA, and revealed that the straightforward application of ZD causes higher error floor than in the original frameless ALOHA, thus resulting in lower throughput performance. To deal with the error floor problem, we proposed E-ZDFA, which utilizes one-bit additional feedback. This additional feature allows E-ZDFA to achieve lower error floor and higher throughput performance than state-of-the-art IRSA and frameless ALOHA. Moreover, E-ZDFA was confirmed to be robust against the requirement of PLR.

This chapter revealed that our proposed E-ZDFA outperformed conventional IRSA in terms of throughput with practically large number of users, *e.g.*, approximately 1000. It is worth noting that, in networks with practical scale, E-ZDFA achieves the highest throughput performance than conventional schemes. Hence, we conclude that this chapter largely contributes to the improvement of random access protocols in terms of throughput.

Chapter 4

Frameless ALOHA with Cooperative Base Stations

Although ZigZag deciding (ZD) enables frameless ALOHA to improve its throughput performance, the base station (BS) is required to implement ZigZag decoding, which would be an additional cost compared to the conventional schemes. Moreover, because of the massive number of contending users, the number of unique preambles equipped at the start of packets would be also massive, which may result in huge computation to detect collision. These problems motivate us to consider another frameless ALOHA scheme, which can achieve higher throughput performance while not increasing the complexity. Herein, we consider the problem of cooperative multi-access in the presence of overlapped coverage areas. Assuming a frameless ALOHA transmission scheme, we derive exact analytical throughput expressions for throughput in the aforementioned scenarios as a function of the frame length of the system and for arbitrary average numbers of users transmitting in each slot (target degree). After obtaining these original expressions, we then formulate a utility function whose maximization (obtained, *e.g.*, through genetic algorithms) yields unequal and optimum target degrees to be employed by users in each group in order to maximize the peak throughput of the whole system, while satisfying a given prescribed outage. A comparison of the resulting cooperative multiple BS multi-access scheme against optimized single-BS frameless ALOHA systems — which presume the perfect isolation of users at each BS and an equal optimum target degree for all users — indicates a significant gain in overall throughput, thereby revealing that a "*multi-access diversity gain*" can be reaped by allowing groups of users from different BSs to overlap.

4.1 Introduction

While cooperation of BSs has been well studied in the context of cellular systems [95], [96], the application of multiple BS cooperation into wireless sensor networks (WSNs) or WLANs, is recently gathering interests [97], [98]. Multiple BS cooperation obviously enhances the connectivity of a wireless network. Moreover, the cooperation so as to increase throughput has been actively discussed. In [99], an interference cancellation-based non-orthogonal multiple-access (NOMA) scheme with multiple BSs was proposed. That scheme exploits the difference between received power among multiple BSs in order to retrieve colliding packets, and jointly optimizes the power allocation of users as well as the BS association to ensure that the capacity of each BS is maximized while minimizing total transmission power. In addition, an opportunistic transmission method in a multi-cell network is discussed in [100], where each user simultaneously considers whether 1) the channel gain to the receiver is sufficiently large, and 2) the interference that a user causes to other receivers is sufficiently small. These schemes attempt to maximize network throughput by considering the signal power and signal-to-interference-plus-noise ratio (SINR), which is achieved by focusing on the physical layer rather than the medium access control (MAC) layer itself. When it comes to the MAC layer, inter-slot SIC (hereafter termed SIC) over a multiple-BS network was recently studied by [87]. In that study, the authors proposed improving SIC performance via multiple BS cooperation via a system in which users transmit their packets using the *framed* ALOHA strategy described by [57], and BSs share retrieved packets using a backhaul network that allows each BS to cancel the shared packets. Moreover, supposing that users and BSs are deployed following a PPP, analytical expressions for the packet loss rate (PLR) and throughput are derived, with the analysis results used to optimize the number of user retransmissions. The main conclusion reached in [87] is that it is nearly optimal for all the users to transmit twice during the frame.

However, while the work of [87] is very informative, it faces several practical limitations. For instance, regarding the user transmission protocol, the framed structure requires a suitable number of time slots, which is a challenging requirement for multiple-BS networks since each BS will have a different number of users. Moreover, the optimized transmission strategy might be sub-optimal in practice due to the PPP assumption. Furthermore, the proposed optimization method presupposes that the average number of BSs connected to each user is identical, while in practice the number of BSs and the retransmission numbers are different for each user.

In this chapter, we derive an exact theoretical PLR expression for coded ALOHA with multiple BS cooperation. Specifically, we assume the use of frameless ALOHA [67], which is a recently proposed coded ALOHA scheme in which the frame length is automatically determined on the fly under the constraint that sufficiently large packet numbers are retrieved. This frameless ALOHA scheme is well suited for multiple-BS networks because its *frameless* structure is realized via probabilistic user retransmissions that are based on a given transmission probability, thus avoiding the problem of frame length determination that arises in framed schemes. In contrast to the approximated analysis of [87], the exact analysis takes into account the connectivity of users and BSs so that packet sharing among BSs can be precisely tracked. Our proposed analysis is then employed to optimize the average number of user retransmissions so as to maximize the network throughput. A comparison of the resulting cooperative multiple-BS multi-access scheme against optimized single-BS frameless ALOHA systems — which presumes perfect user isolation at each BS and an equal and optimum average number of retransmissions for all users — indicates a significant gain in the overall throughput, thus revealing that a "*multi-access diversity gain*" can be reaped by allowing user groups from different BSs to overlap. The theoretical analysis of throughput is further used to quantitatively evaluate the multi-access diversity gain, with the results confirming that the gain grows as the number of BSs increases. Numerical examples demonstrate that the proposed frameless ALOHA with optimized parameters exhibits higher maximum throughput performance than the state-of-the-art multiple BS random access scheme proposed in [87]. The contributions of this chapter are summarized as follows:

- We derive an exact theoretical throughput expression for frameless ALOHA with multiple BS cooperation and demonstrate its application to the optimization of transmission probabilities in order to maximize the achievable throughput.
- Simple lower and upper bounds for cooperative throughput are introduced to calculate the throughput performance for a large number of BSs in order to guarantee that the multi-access diversity gain increases as the number of BSs increases.
- The results show that our proposed scheme outperforms the conventional scheme in [87] in terms of maximum throughput.

This chapter contributes to the increase of throughput of systems with multiple BSs; not only cellular networks, but also relatively small yet dense networks, *e.g.*, WLANs.

The remainder of the chapter is organized as follows. Section 4.2 introduces the system model and describes frameless ALOHA with multiple BS cooperation. In section

4.3, a theoretical throughput analysis of frameless ALOHA with and without multiple BS cooperation is presented. The results are then used to obtain the multi-access diversity gain. While the analysis results can be applied to an arbitrary number of BSs, we specifically demonstrate its utility in a three-BS network. Moreover, the upper and lower bounds of the multi-access diversity gain are introduced. Section 4.4 shows some numerical results related to the target degree optimization and the average throughput performance, as well as a comparison with a state-of-the-art scheme named *spatio-temporal cooperation* [87]. Those results show that our proposed scheme achieves a higher throughput performance. Finally, we conclude the chapter in Section 4.6.

4.2 System Model

4.2.1 Network Model

Throughout this chapter, we will consider a network with N users and M BSs. Each user has one packet at the start of a frame, and no new packets are generated during the frame. Moreover, users do not have specific destinations and strive to deliver their packets to any BSs that can receive the packets. Each user transmits the same packet in all the time slots of the frame. Users are categorized into multiple groups depending on which BS(s) they are able to communicate with. Let I denote the number of user groups. It is assumed that each user can communicate with at least one BS. Thus, there exists at most $2^M - 1$ user groups, where N_i denotes the number of users in the i-th user group. Hereinafter, u_i denotes the i-th user group, and s_j denotes BS-j. Figure 4.1 shows an example of a network model for $M = 2$.

Not only do users need to be associated with the network, they also need to know which user group they are participating in and the number of users in the group in order to calculate the transmission probability, as will be described later. To this end, each user at first broadcasts a short packet to the BSs in order to announce its intention to participate in the network prior to transmitting data. This short packet transmission is conducted before the data transmission, and we assume that the network association will be ideally finished, *i.e.*, the short packet is received at the BSs without any errors. The BSs share the received short packets with each other in order to calculate the number of users for each group. Finally, the BSs report the number of users in each group, and which group users belong, to the users. Although users may be allocated randomly in practice, this chapter only considers an analysis for a deterministic allocation because our analysis method can be applied to any network

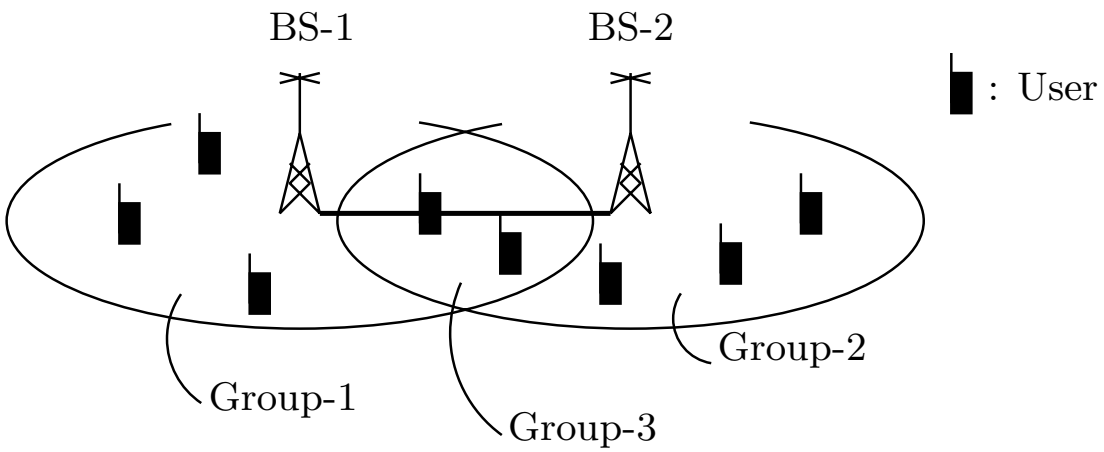

Fig. 4.1 An example of a network model for $M = 2$. Users in group-3 (u_3) can communicate with both BSs, which are connected via a backhaul network.

simply by changing the number of users in each group. It is assumed that all of the BSs are connected to each other via a backhaul network, so they can communicate with each other without errors. Additionally, all the users and BSs are assumed to be temporally synchronized so that each transmission occurs in a time slot.

4.2.2 Frameless ALOHA Transmission

In every time slot, each user decides whether or not to transmit its own packet using a transmission probability. The transmission probability of u_i is given by $p_i = G_i/N_i$, where G_i is called the *target degree*, which is defined as the average number of users in u_i transmitting in one time slot. As stated above, before they can calculate p_i, users need to know their group index i and N_i. Target degrees can be arbitrarily set and are shared among each user group. Although target degrees can be changed at every time slot, as mentioned in [67], that study also shows that even a constant target degree yields a throughput performance comparable with that for multiple target degrees. Thus, hereafter we only consider constant target degrees for each user group.

Frameless ALOHA transmission can be represented by a bipartite graph that consists of edges and two kinds of nodes: *variable nodes* and *observation nodes*. Variable nodes and observation nodes correspond to information packets and received packets, respectively. Note that since M BSs in the network simultaneously receive packets, M observation nodes exist for each time slot. When the frame length is T, there are MT observation nodes in the transmission graph. The user transmission is depicted by an edge between the variable and observation nodes. The number of edges

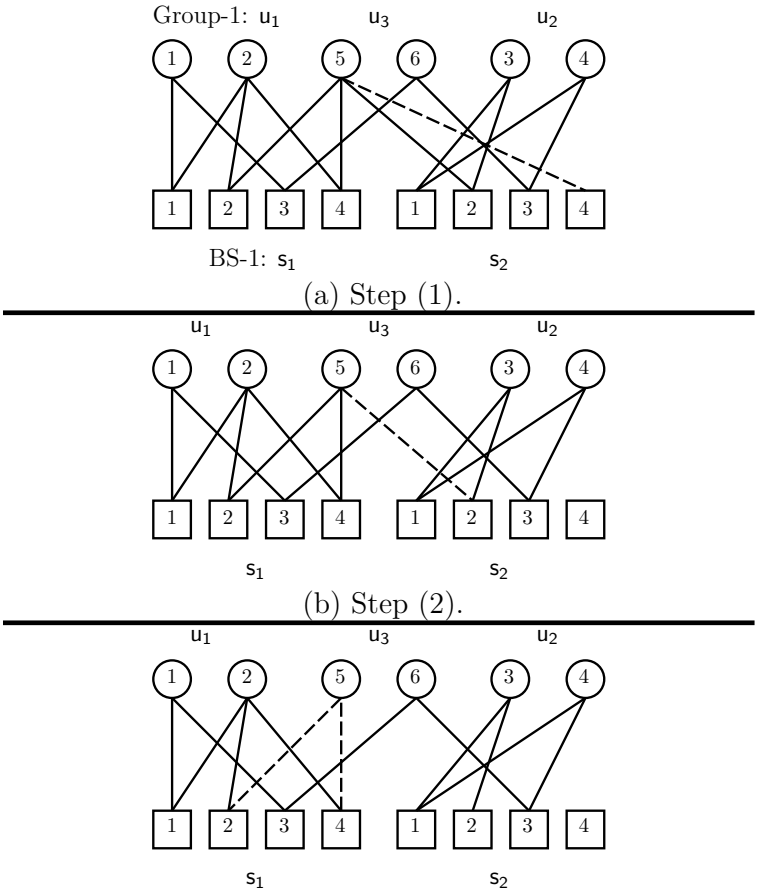

(a) Step (1).

(b) Step (2).

(c) Packet sharing of BSs.

Fig. 4.2 Transmission graph and SIC. (a) An example of a transmission graph. The user-5 packet can be retrieved at s_2. (b) The user-5 packet is subtracted from corresponding received packets. (c) The use of multiple BS cooperation makes it possible for s_1 to subtract the user-5 packet from the corresponding received packets.

connected to each node is called the *degree* of the node. Note that the degree of a variable node corresponds to the number of user transmissions in the frame, while the degree of an observation node corresponds to the number of users transmitting in the time slot. Hereinafter, we refer to the bipartite graph as a *transmission graph* in order to emphasize that the graph visually represents the user *transmissions*. In order to help readers to visually understand the bipartite graph, an example of a transmission graph with $M = 2$ BSs is shown in Fig. 4.2. In the example, user-5 belonging to u_3 transmits the packet in slot-2 and slot-4. Since packets transmitted by users in u_3 can be received at both s_1 and s_2, the variable node of user-5 is connected with observation nodes of slot-2 and slot-4 of s_1 and s_2.

4.2.3 Packet Retrieval with Multiple Base Station Cooperation

Since users transmit their packets independently, some users may transmit simultaneously in the same slot, thus leading to *packet collisions*. Packets that collide are considered to be lost since, for mathematical tractability reasons, the capture effect [69] is not considered. Since this model is considered to be the worst-case scenario, it provides a lower-bound to throughput performance in practical situations where the capture effect would be available. Hence, the model is both relevant and useful because it permits an achievable performance to be obtained, and has been used in numerous conventional studies, *e.g.* [56, 57, 87]. It is worth noting that users existing near the boundary of coverage areas would cause interference to the other BS, while the other BS cannot retrieve the packet because of low-received power. However, as the number of retransmission of users is not large, where the average number of retransmission is given by G_i, we assume that the effect of this interference can be negligible, so that the model performs as the worst-case scenario. It is further assumed that BSs are able to distinguish the conditions for each time slot: (i) no users have transmitted, (ii) only one user has transmitted, *i.e.*, the time slot is a singleton, and (iii) some users have transmitted and packets have collided. However, even if the BS detects a collision, it cannot identify which user's packets have collided, or how many packets have collided. Frameless ALOHA employs SIC in order to retrieve the original packets from collisions. The SIC for frameless ALOHA is equivalent to the peeling decoder for low-density parity check (LDPC) codes [23]. As depicted in Fig. 4.2, the SIC process can be described using the following steps:

(i) Retrieve the transmitted packets from singleton slots as depicted in Fig. 4.2–(a). The slots are assumed to be empty.

(ii) Subtract the packets from all the received signals in which the packets are included.

After step (ii), some collided packets become singletons, *e.g.*, the second time slot of s_2 becomes a singleton in Fig. 4.2–(b), and the above operations are repeated until all the singleton slots vanish. In order to execute step (ii), it is assumed that each packet includes information indicating the time slot in which it is transmitted. Note that the retrieved packets might be included in future received packets. To this end, if each user identification (ID) is used as a seed for a random generator for choosing time slots in which to transmit, the receiver can determine all the future transmissions and subtract signals from all the received packets [88]. We assume that a backhaul network is used among the participating BSs in order to immediately share successfully

retrieved packets, so that the received packets are subtracted from all the received signals in which shared packets are included, thus leading to additional singleton time slots, as shown in Fig. 4.2–(c). The combination of shared packets among BSs with SIC is equivalent to the decoding process in *spatio-temporal cooperation*, which was proposed by [87]. In frameless ALOHA, the frame length can be arbitrarily extended to retrieve more transmitted packets. However, a large number of time slots may be required to retrieve all the transmitted packets, which could result in significant delays. In this chapter, it is assumed that the frame is terminated when $\lfloor \alpha N \rfloor$ packets are successfully retrieved, thus providing a point where the threshold $\alpha \in (0, 1]$ can be set arbitrarily.

Upon transmission, slots are organized into a *frame*, with the start and end of the frame reported by the receiver via a beacon. The name *frameless* comes from the fact that the frame length is not *a priori* fixed. Users whose packets were not retrieved in the previous frame will retransmit the same packets in the next frame. Thus, there is only one feedback from BSs, where the feedback signal stops user transmissions. To this end, after each slot, it is presumed that the users will wait a short period for the feedback signal. If users do not receive the feedback signal, they continue the frameless ALOHA transmission.

4.2.4 Degree Distributions

Let us denote the number of time slots by T. *Degree distributions* characterize the randomly constructed transmission graph and can be used to theoretically analyze the PLR for frameless ALOHA. We define $L_{i,k}$ as the probability that the variable node for a user in u_i has a degree-k, *i.e.*, that the user in u_i has transmitted the packet k times during T slots. The probability $L_{i,k}$ is given by

$$L_{i,k} = \binom{T}{k} p_i^k (1 - p_i)^{T-k}. \tag{4.1}$$

Furthermore, $R_{i,k}$ is the probability that k users in u_i transmit in the slot. Then, the probability is given by

$$R_{i,k} = \binom{N_i}{k} p_i^k (1 - p_i)^{N_i-k}. \tag{4.2}$$

Using the probabilities, *node-perspective* degree distributions are defined as

$$L_i(x) \triangleq \sum_{k=0}^{T} L_{i,k} x^k, \tag{4.3}$$

and

$$R_i(x) \triangleq \sum_{k=0}^{N_i} R_{i,k} x^k, \tag{4.4}$$

where x is a dummy variable.

The node-perspective degree distributions yield *edge-perspective* degree distributions as

$$\lambda_i(x) \triangleq \sum_{k=1}^{T} \lambda_{i,k} x^{k-1} = L_i'(x)/L_i'(1), \tag{4.5}$$

and

$$\rho_i(x) \triangleq \sum_{k=1}^{N_i} \rho_{i,k} x^{k-1} = R_i'(x)/R_i'(1). \tag{4.6}$$

Hereafter, for the sake of brevity, we will use the symbol u_i to refer either the user group or a packet of the user in the group, according to context. The coefficient in (4.5), namely $\lambda_{i,k}$, denotes the probability that the transmitted packet u_i is retransmitted k times during the frame. Similarly, $\rho_{i,k}$ in (4.6) denotes the probability that the transmitted packet u_i has collided with other $(k-1)$ packets transmitted by users in u_i in the slot.

4.3 Throughput Analysis

In this section, we will attempt to quantitatively determine how much performance improvement can be achieved via multiple BS cooperation. To this end, we derive theoretical expressions for the frameless ALOHA throughput with and without multiple BS cooperation. Given a number of time slots T, the throughput $S(T)$ is defined as the fraction of successfully retrieved packets and time slots, and is given by

$$S(T) \triangleq \frac{N_{\text{ret}}(T)}{T}, \tag{4.7}$$

where $N_{\text{ret}}(T)$ denotes the number of retrieved packets within T slots, and $0 \leq N_{\text{ret}}(T) \leq N$.

Moreover, we introduce a metric named *multi-access diversity gain* to evaluate the performance improvement achieved via multiple BS cooperation. We define S^{c} and S^{nc} as the throughput performance for frameless ALOHA with and without multiple BS cooperation, respectively. Then, the multi-access diversity gain Γ is defined as

$$\Gamma \triangleq \frac{S^{\mathrm{c}}}{S^{\mathrm{nc}}}. \tag{4.8}$$

To theoretically calculate throughput performance, $N_{\mathrm{ret}}(T)$ should be theoretically obtained in (4.7). To this end, denoting by $p_{\mathrm{e}}(T)$ the PLR with T time slots, $N_{\mathrm{ret}}(T)$ is given by $N_{\mathrm{ret}} = N(1 - p_{\mathrm{e}}(T))$, where the PLR $p_{\mathrm{e}}(T)$ needs to be theoretically derived. In the following subsection, a theoretical PLR expression for frameless ALOHA with multiple BSs is derived while considering two scenarios: non-cooperative BSs and cooperative BSs.

4.3.1 Analysis of Non-Cooperative Packet Retrieval

In situations without multiple BS cooperation, each BS locally attempts to retrieve transmitted packets. Since packets are retrieved via an iterative SIC process, a theoretical PLR can be obtained via iterative calculations. The idea behind the calculation is similar to the original density evolution [23]. Specifically, in order to obtain the PLR of u_i, two kinds of variables, namely $x_{i,j}^{(l)}$ and $w_{i,j}^{(l)}$, are iteratively calculated for each j in a way that ensures the users in u_i can communicate with s_j. The former, $x_{i,j}^{(l)} \in [0, 1]$, is the probability that the packet u_i will not be retrieved at s_j in the l-th iteration. This event occurs when all the retransmitted packets have collided. Then, $x_{i,j}^{(l)}$ is given by

$$x_{i,j}^{(l)} = \begin{cases} \lambda_i(w_{i,j}^{(l)}), & \text{for } l \geq 1 \\ 1, & \text{for } l = 0, \end{cases} \tag{4.9}$$

where $x_{i,j}^{(0)} = 1$ indicates that no packet has been retrieved at the beginning of the retrieval process, and $\lambda_i(w_{i,j}^{(l)}) = \sum_{k=1}^{T} \lambda_{i,k} \times (w_{i,j}^{(l)})^{k-1}$ corresponds to the probability that all the incoming $(k-1)$ edges are still colliding.

The latter, $w_{i,j}^{(l)} \in [0, 1]$, is the probability that the packet u_i has collided at s_j in the l-th iteration. To calculate $w_{i,j}^{(l)}$, we consider the probability that the transmitted packet becomes un-collided. The probability of all users in u_i except the specified user being retrieved is $\rho_i(1 - x_{i,j}^{(l-1)}) = \sum_{k=1}^{N_i} \rho_{i,k} \times (1 - x_{i,j}^{(l-1)})^{k-1}$, and the probability that all users in u_m have been retrieved is $R_m(1 - x_{m,j}^{(l-1)}) = \sum_{k=0}^{N_m} R_{m,k} \times (1 - x_{m,j}^{(l-1)})^{k}$. Then,

$w_{i,j}^{(l)}$ is given by

$$w_{i,j}^{(l)} = 1 - \rho_i(1 - x_{i,j}^{(l-1)}) \prod_{m:\mathsf{u}_m \in \mathcal{U}(\mathsf{s}_j)\setminus\{\mathsf{u}_i\}} R_m(1 - x_{m,j}^{(l-1)}), \tag{4.10}$$

where $\mathcal{U}(\mathsf{s}_j)$ is a set of user groups established in a way that permits users in the group to communicate with s_j. After a sufficiently large number of iterations, retrieval of the packet u_i only fails when the packet retrieval attempt fails at all the BSs. Hence, the theoretical PLR of u_i, say $p_{\mathrm{e},i}(T)$, is obtained by

$$p_{\mathrm{e},i}(T) = L_i(w_i), \tag{4.11}$$

$$w_i \approx \prod_{j:\mathsf{s}_j \in \mathcal{S}(\mathsf{u}_i)} w_{i,j}^{(l)}, \tag{4.12}$$

where $\mathcal{S}(\mathsf{u}_i)$ is a set of BSs to which the users in u_i are connected.

The calculation of $p_{\mathrm{e},i}(T)$ in (4.11) is identical to the original frameless ALOHA analysis, while the calculation of w_i is approximated. The approximation comes from the assumption in (4.12), which states that the potential of a packet u_i to become a singleton at each slot is independent of each BS. However, this is not actually the case since the packets of groups in the overlapped areas should be received simultaneously at multiple BSs. Nevertheless, the use of this approximation allows us to simplify the theoretical expression, as shown in (4.12), while still providing an accurate result.

4.3.2 Analysis of Cooperative Packet Retrieval

In order to clarify how to theoretically analyze the PLR for a frameless ALOHA with multiple cooperating BSs, we derive the exact theoretical expression for the PLR for a specific case with $M = 3$. When making comparisons with the non-cooperative case, it is necessary to consider the effect of packet sharing among BSs. Thus, important additional terms appear in the analytical equation. When $M = 3$, there exists at most $2^3 - 1 = 7$ user groups.

When packet sharing is employed, a packet transmitted from the overlapped coverage area should be retrieved simultaneously at all participating BSs. This implies that the retrieval process for each BS is *not actually independent*, unlike the non-cooperative case where the retrieval process is performed *independently* at each BS.

Moreover, a packet can sometimes be retrieved even if it has collided with other packets. In Fig. 4.3, some users in u_1, u_2, and u_7 have transmitted their packets, while presuming that no users in u_4, u_5, and u_6 have transmitted packets, nor of u_3. Although

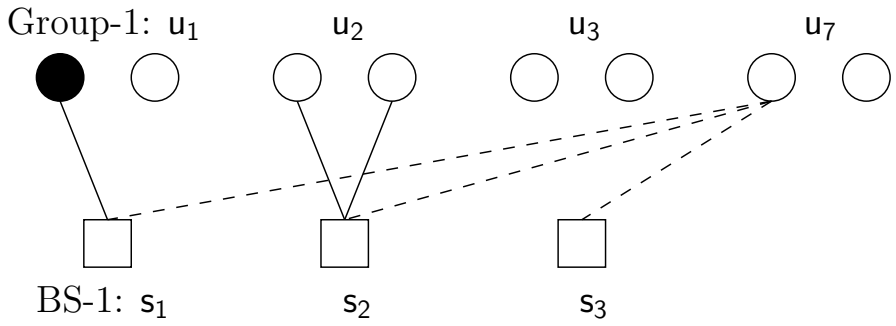

Fig. 4.3 An example of a transmission graph where a collided packet u_1 (represented by a filled circle) can be retrieved.

the packet u_1 has collided with the packet u_7, the colliding packet is retrieved at s_3, ultimately making it possible to retrieve the packet u_1.

The theoretical PLR for frameless ALOHA with multiple BS cooperation obtained via iterative calculation of two kinds of variables, namely $x_i^{(l)}$ and $w_i^{(l)}$, is needed, as is the analysis of non-cooperative cases. The calculation of $x_i^{(l)}$ is identical to the non-cooperative case, that is

$$x_i^{(l)} = \begin{cases} \lambda_i(w_i^{(l)}), & \text{for } l \geq 1 \\ 1, & \text{for } l = 0. \end{cases} \tag{4.13}$$

As shown in Fig. 4.3, other important terms result when it comes to $w_i^{(l)}$with the multiple BS cooperation because of further packet retrieval. We can describe $w_i^{(l)}$ by following the intuitive representation

$$w_i^{(l)} = 1 - (P_i^{(\mathrm{r0})} + P_i^{(\mathrm{r1})}), \tag{4.14}$$

where $P_i^{(\mathrm{r0})}$ is the probability that the packet is free from collision (also included in the analysis of non-cooperative case), and $P_i^{(\mathrm{r1})}$ is an additional term, *i.e.*, the probability that the packet can be retrieved after it has collided with other packets.

The variable $w_i^{(l)}$ can be obtained by finding all the patterns where the packet u_i has been retrieved. Specifically, for $M = 3$, we have

$$\begin{aligned} w_1^{(l)} =& 1 - \mathrm{r}_1 \left(\mathrm{R}_4\mathrm{R}_6\mathrm{R}_7 + \mathrm{C}_4\mathrm{R}_2\mathrm{R}_5\mathrm{R}_6\mathrm{R}_7 + \mathrm{C}_4\mathrm{C}_5\mathrm{R}_2\mathrm{R}_3\mathrm{R}_6\mathrm{R}_7 + \mathrm{C}_6\mathrm{R}_3\mathrm{R}_4\mathrm{R}_5\mathrm{R}_7 + \mathrm{C}_6\mathrm{C}_5\mathrm{R}_2\mathrm{R}_3\mathrm{R}_4\mathrm{R}_7 \right. \\ & \left. + \mathrm{C}_4\mathrm{C}_6\mathrm{R}_2\mathrm{R}_3\mathrm{R}_5\mathrm{R}_7 + \mathrm{C}_7\left(\mathrm{R}_4\mathrm{R}_5\mathrm{R}_6\left(1 - \bar{\mathrm{R}}_2\bar{\mathrm{R}}_3\right) + \mathrm{C}_4\mathrm{R}_2\mathrm{R}_3\mathrm{R}_5\mathrm{R}_6 + \mathrm{C}_6\mathrm{R}_2\mathrm{R}_3\mathrm{R}_4\mathrm{R}_5\right)\right), \end{aligned} \tag{4.15}$$

$$w_4^{(l)} = 1 - \mathrm{r}_4(\mathrm{R}_7(\mathrm{R}_5\mathrm{R}_6(1-\bar{\mathrm{R}}_1\bar{\mathrm{R}}_2) + (1-\mathrm{R}_5-\mathrm{C}_5)\mathrm{R}_1\mathrm{R}_6 + (1-\mathrm{R}_6-\mathrm{C}_6)\mathrm{R}_2\mathrm{R}_5 + \mathrm{C}_5\mathrm{R}_6(\mathrm{R}_1+\bar{\mathrm{R}}_1\mathrm{R}_2\mathrm{R}_3) + \mathrm{C}_6\mathrm{R}_5(\mathrm{R}_2+\bar{\mathrm{R}}_2\mathrm{R}_1\mathrm{R}_3)) + \mathrm{C}_7\mathrm{R}_3\mathrm{R}_5\mathrm{R}_6(1-\bar{\mathrm{R}}_1\bar{\mathrm{R}}_2)), \quad (4.16)$$

and

$$w_7^{(l)} = 1 - \mathrm{r}_7(\mathrm{R}_4\mathrm{R}_5\mathrm{R}_6(1-\bar{\mathrm{R}}_1\bar{\mathrm{R}}_2\bar{\mathrm{R}}_3) + \mathrm{R}_4\mathrm{R}_5\bar{\mathrm{R}}_6\mathrm{R}_2 + \mathrm{R}_4\bar{\mathrm{R}}_5\mathrm{R}_6\mathrm{R}_1 + \bar{\mathrm{R}}_4\mathrm{R}_5\mathrm{R}_6\mathrm{R}_3). \quad (4.17)$$

An algorithm that can be used to calculate $w_i^{(l)}$ for an arbitrary number of BSs will be discussed in the next section. For a sufficiently large l, the PLR for u_i is theoretically calculated as

$$p_{\mathrm{e},i}(T) = L_i(w_i^{(l)}), \quad (4.18)$$

and the average PLR is given by

$$p_{\mathrm{e}}(T) = \sum_{i=1}^{I} \frac{N_i}{N} p_{\mathrm{e},i}(T). \quad (4.19)$$

Generalized Analysis

The equations (4.13), (4.14), (4.18), and (4.19) still hold for general cases of $M > 1$. Moreover, we can straightforwardly calculate (4.13), (4.18), and (4.19) for any given network with an arbitrary M. The calculation of (4.14), however, cannot be solved in a straightforward manner, as $P_i^{(\mathrm{r0})}$ and $P_i^{(\mathrm{r1})}$ consist of a large number of probabilities indicating specific patterns where the specified packet can be retrieved. The specific form of $w_i^{(l)}$ depends on the number of BSs and the consequent network topology, and can only be obtained by searching all the cases where the packet u_i can be retrieved. Since the number of terms included in $P_i^{(\mathrm{r0})}$ and $P_i^{(\mathrm{r1})}$ is large[1], it is important to take all the patterns into consideration in order to fully reveal the throughput performance. If some patterns are ignored in the analysis, the analytical performance becomes worse than the practical performance. To this end, we introduce a *walk graph* representation of multiple BS networks that visualizes a snapshot at the time slot. The walk graph consists of two kinds of nodes, namely user nodes and BS nodes, which correspond to user groups and BSs, respectively. User nodes can be connected to BS nodes that allow communications with the corresponding user group, providing the following three conditions are present:

[1]For instance, when $M = 4$, the number of terms included in $P_i^{(\mathrm{r0})}$ is 69,356, and the number of terms included in $P_i^{(\mathrm{r1})}$ is 6,108[101].

1. When no users in the group have transmitted in the slot (or all the transmitted packets from the group in the slot have been retrieved), the user node has no edges.

2. If a single packet has been transmitted in the slot (or packets from multiple users have been transmitted and all except the packet of a single user have been retrieved), the user node and the BS nodes are connected with one edge.

3. The user node has two edges that extend to each connectable BS node when a collision has occurred.

Now, let us define three sets of user nodes, namely $\mathcal{U}_0$, $\mathcal{U}_1$, and $\mathcal{U}_2$, which include user nodes with no edges, a single edge, and two edges in the walk graph, respectively. For example, the walk graph corresponding to the situation of Fig. 4.3 is shown in Fig. 4.4, where $\mathcal{U}_0 = \{\mathsf{u}_3, \mathsf{u}_4, \mathsf{u}_5, \mathsf{u}_6\}$, $\mathcal{U}_1 = \{\mathsf{u}_1, \mathsf{u}_7\}$, and $\mathcal{U}_2 = \{\mathsf{u}_2\}$. The walk graph takes $3^I = 3^{2^M-1}$ patterns, depending on the condition of each user node, and the probability of the instant walk graph can be obtained using degree distributions. The probability that the user node has no edges with each connectable BS node is given by

$$\mathrm{R}_i \triangleq R_i(1 - x_i^{(l-1)}), \tag{4.20}$$

and the probability that the user node has a single edge with each connectable BS node is

$$\mathrm{C}_i \triangleq \sum_{k=1}^{N_i} \binom{N_i}{k} p_i^k (1-p_i)^{N_i-k} k x_i^{(l-1)} (1 - x_i^{(l-1)})^{k-1}. \tag{4.21}$$

Hence, the occurrence probability of the realization of walk graph g, such as $\Pr(g)$, is given by

$$\Pr(g) = \prod_{i:\mathsf{u}_i \in \mathcal{U}_0} \mathrm{R}_i \prod_{j:\mathsf{u}_j \in \mathcal{U}_1} \mathrm{C}_j \prod_{k:\mathsf{u}_k \in \mathcal{U}_2} (1 - \mathrm{R}_k - \mathrm{C}_k). \tag{4.22}$$

When we focus on the user group u_u, the probability that only the specified user will remain un-retrieved in the slot is given by

$$\mathrm{r}_u \triangleq \rho_u(1 - x_u^{(l-1)}). \tag{4.23}$$

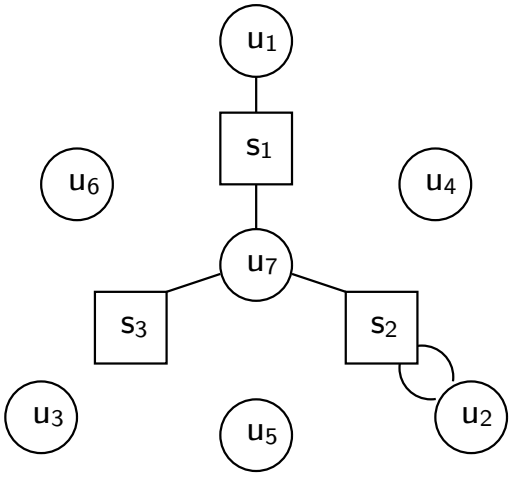

Fig. 4.4 A walk graph of the frameless ALOHA with three cooperative BSs.

Algorithm 1 Calculation of $w_i^{(l)}$

Set $d_i = 1$, $P_i^{(\mathrm{r})} = 0$
for all $g \in \mathcal{G}_{d_i=1}$ **do**
  Carry out SIC on the walk graph g
  if Succeeded **then**
    $P_i^{(\mathrm{r})}$ += $\Pr(g)$
  end if
end for
$w_i^{(l)} = 1 - P_i^{(\mathrm{r})}$

Therefore, given that only the specified user in u_u has transmitted, the probability of the walk graph g is given by

$$\Pr(g) = \mathrm{r}_u \prod_{i:\mathsf{u}_i \in \mathcal{U}_0} \mathrm{R}_i \prod_{j:\mathsf{u}_j \in \mathcal{U}_1 \setminus \{\mathsf{u}_u\}} \mathrm{C}_j \prod_{k:\mathsf{u}_k \in \mathcal{U}_2} (1 - \mathrm{R}_k - \mathrm{C}_k). \tag{4.24}$$

Note that the walk graph has 3^I patterns since there are I user groups that accept three kinds of conditions depending on the number of edges. Thus, the probability $P_i^{(\mathrm{r}0)}$ ($P_i^{(\mathrm{r}1)}$) can be obtained by calculating the sum of all the probabilities of walk graphs where the specified user can be retrieved from singleton slots (collided slots). Let us define $\mathcal{R}_i^{(\mathrm{r}0)}$ as a set of walk graphs where the packet u_i can be retrieved from singleton slots, and $\mathcal{R}_i^{(\mathrm{r}1)}$ as a set of walk graphs where the packet can be retrieved

from collided slots. Then, $P_i^{(\mathrm{r}0)}$ and $P_i^{(\mathrm{r}1)}$ are obtained by $P_i^{(\mathrm{r}0)} = \sum_{g \in \mathcal{R}_i^{(\mathrm{r}0)}} \Pr(g)$ and $P_i^{(\mathrm{r}1)} = \sum_{g \in \mathcal{R}_i^{(\mathrm{r}1)}} \Pr(g)$.

Finally, $w_i^{(l)}$ is obtained by (4.14), which can be rewritten as

$$w_i^{(l)} = 1 - \sum_{g \in \mathcal{R}_i} \Pr(g) \triangleq 1 - P_i^{(\mathrm{r})}, \tag{4.25}$$

where $\mathcal{R}_i = \mathcal{R}_i^{(\mathrm{r}0)} \cup \mathcal{R}_i^{(\mathrm{r}1)}$.

Whether or not the instant walk graph belongs to $\mathcal{R}_i$ is determined by the use of an algorithm similar to SIC. Since it is also a bipartite graph, SIC can be straightforwardly applied to the walk graph. If the specified packet is retrieved, the instant graph is in $\mathcal{R}_i$. Now, let us denote the degree of user node i as d_i, and a universal set of walk graphs as $\mathcal{G}$. Furthermore, we define $\mathcal{G}_{d_i=a}$ as a set of walk graphs that satisfy $d_i = a$. Then, Algorithm I shows how to search all of the appropriate cases of u_i for the arbitrary number of M.

Using the algorithm, the theoretical PLR performance and consequently the throughput performance can be derived for any number of BSs. This information is then used to obtain the multi-access diversity gain. However, finding all the patterns where the specified packet can be retrieved is NP-hard, and the algorithm requires an exhaustive search over 3^I candidate walk graph patterns. Specifically, for $M = 4$, the analysis requires evaluation over 10^7 graphs, and the size increases to about 10^{14} when $M = 5$. Hence, exact analyses involving cases of $M > 4$ would be impossible due to their complexity. However, it is worth noting that we can utilize various search algorithms, *e.g. backtracking*, to solve combinatorial search problems with low relatively complexity.

4.3.3 Approximated Analysis for General Case

In order to alleviate the exponential complexity of calculating the exact throughput performance, we next derive the upper and lower throughput bounds for multiple BS cooperation.

Upper Bound

With a single BS, the highest throughput performance is 1.0, which can be achieved by TDMA[2]. Assuming a symmetric network with M BSs where the numbers of users in every networks are same, the highest throughput performance is similarly M, which

[2]When a capture effect is available, multiple packets can be retrieved from a single time slot, resulting in a throughput performance higher than 1.0[69].

Table 4.1 Optimal target degrees for $M \leq 4$.

M	$\lvert\mathcal{S}(\mathsf{u}_i)\rvert = 1$	$\lvert\mathcal{S}(\mathsf{u}_i)\rvert = 2$	$\lvert\mathcal{S}(\mathsf{u}_i)\rvert = 3$	$\lvert\mathcal{S}(\mathsf{u}_i)\rvert = 4$	Peak	Average
1	3.10	-	-	-	0.874	0.867
2	1.81	1.68	-	-	1.676	1.673
3	1.11	0.94	0.78	-	2.366	2.363
4	0.69	0.52	0.46	0.46	2.940	2.936

can be achieved when there exists no users in the overlapped coverage area. This idea yields a simple upper bound of the throughput performance as follows. Denote by S_1 the maximized throughput performance of frameless ALOHA with a single BS. Specifically, it has been seen in previous chapter that frameless ALOHA asymptotically achieves a throughput of about $S_1 = 0.87$. Then, the throughput of frameless ALOHA with multiple BS cooperation is upper-bounded as

$$S^{\mathrm{c}} \leq MS_1. \tag{4.26}$$

Using the upper bound of the throughput, the upper bound of the multi-access diversity gain can be obtained by dividing (4.26) by the throughput performance of a non-cooperative case obtained using (4.11).

Lower Bound

In order to obtain the lower throughput bound, we derive the *upper* PLR bound for frameless ALOHA with cooperative multiple BSs by assuming a toy model as follows. When focusing on the packet u_i, only the retrieved packets of the users in u_i are shared among the BSs, not the packets of users in the other groups. This is equivalent to ignoring the probability $P_i^{(\mathrm{r1})}$ in (4.14). Hence, from the viewpoint of throughput, this toy model is obviously inferior to the actual network model where multiple BS cooperation is available. In the following paragraphs, we explain how the lower bound of the throughput is derived by the upper bound of the PLR. The upper bound of the PLR is obtained by bounding $P_i^{(\mathrm{r})}$ from the *lower* side, where we use the lower bound for a union probability, as proposed in [102], to reduce the resulting computational complexity. Consider a union probability of n random variables, *i.e.*, the probability that at least one of n events, namely $A_i, i \in [1, n]$, has occurred, which is represented by $\Pr(\bigcup_{i=1}^{n} A_i)$. Using a $1 \times n$ vector $\mathbf{p} = (\Pr(A_1), \ldots, \Pr(A_n))$ and an $n \times n$ square

matrix $\mathbf{Q} = \{\Pr(A_i \cap A_j)\}$, the union probability is lower-bounded as

$$\Pr(\bigcup_{i=1}^{n} A_i) \geq \mathbf{p}\mathbf{Q}^{-1}\mathbf{p}^{\mathrm{t}}, \tag{4.27}$$

where $\mathbf{Q}^{-1}$ is an inverse matrix of $\mathbf{Q}$, and t denotes transposition [102].

We were motivated to employ the lower bound of (4.27) not only because it is elegant, but also because it is more accurate than the well-known Bonferroni lower bound. Consider applying the bound to the calculation of $P_i^{(\mathrm{r})}$. The probability $P_i^{(\mathrm{r})}$ can be rewritten as the union probability, specifically

$$P_i^{(\mathrm{r})} = \Pr(\bigcup_{j:\mathsf{s}_j \in \mathcal{S}(\mathsf{u}_i)} \mathsf{u}_i \text{ is retrieved at } \mathsf{s}_j). \tag{4.28}$$

Then, we can apply the lower bound to the calculation of $P_i^{(\mathrm{r})}$. Based on the toy model introduced given above, the probability of the packet u_i being retrieved at s_j is given by

$$P_i^{(\mathrm{r})}(\mathsf{s}_j) = \mathrm{r}_i \prod_{k:\mathsf{u}_k \in \mathcal{U}(\mathsf{s}_j)\setminus\{\mathsf{u}_i\}} \mathrm{R}_k, \tag{4.29}$$

where $P_i^{(\mathrm{r})}(\mathsf{s}_j)$ denotes the probability that the packet u_i has been retrieved at s_j, and $\mathcal{U}(\mathsf{s}_j)$ is a set of user groups that has been set up so that all group users can communicate with s_j.

The probability corresponds to cases where the packet u_i is retrieved at s_j since the packet is received without any collisions in the actual network model. It is obvious that the bound ignores cases where the specified packet u_i is retrieved after the packet has collided. Moreover, based on the toy model, the joint probability corresponding to cases where the packet u_i is retrieved at both s_{j_1} and s_{j_2} is given by

$$P_i^{(\mathrm{r})}(\mathsf{s}_{j_1}, \mathsf{s}_{j_2}) = \mathrm{r}_i \prod_{k:\mathsf{u}_k \in \mathcal{U}(\mathsf{s}_{j_1}) \cup \mathcal{U}(\mathsf{s}_{j_2})\setminus\{\mathsf{u}_i\}} \mathrm{R}_k, \tag{4.30}$$

where $P_i^{(\mathrm{r})}(\mathsf{s}_{j_1}, \mathsf{s}_{j_2})$ denotes the probability that the packet u_i is retrieved at both s_{j_1} and s_{j_2}. By substituting (4.29) and (4.30) into (4.27), where elements of $\mathbf{p}$ and diagonal elements of $\mathbf{Q}$ are given by (4.29), and non-diagonal elements of $\mathbf{Q}$ are given by (4.30), we can obtain the lower bound for $P_i^{(\mathrm{r})}$. Note that the size of $\mathbf{Q}$ is $|\mathcal{S}(\mathsf{u}_i)| \times |\mathcal{S}(\mathsf{u}_i)|$,

Table 4.2 Optimal target degrees for several networks.

Network type	N_1	N_3	G_1	G_3	Peak	Average
(a)	0	10,000	-	3.098	0.874	0.867
(b)	100	10,000	1.388	3.094	0.893	0.890
(c)	1,000	10,000	1.621	3.063	1.064	1.060
(d)	10,000	10,000	1.812	1.680	1.676	1.673
(e)	10,000	1,000	3.051	1.869	1.836	1.829
(f)	10,000	100	3.096	0.302	1.758	1.746
(g)	10,000	0	3.098	-	1.748	1.736

and none of the diagonal elements of $\mathbf{Q}$ are zero as long as $G_i > 0$. Using (4.29) and (4.30), the upper PLR bound can be derived by lower-bounding $P_i^{(\mathrm{r})}$.

Thanks to the simplification of (4.29) and (4.30), an exhaustive search over 3^{2^M-1} candidates in the exact analysis is replaced with only, at most, $M(M+1)/2$ terms[3]. On the other hand, the simplification may loosen the upper bound of the PLR. As mentioned above, in order to obtain the exact PLR performance, all of the patterns should be taken into account. Hence, if we want to make the bound tighter, we need to consider more terms, which requires a larger computational cost, and it is hard to formulate a tight bound at a low computational cost. However, the fact remains that the upper bound of the PLR (*i.e.*, the lower bound of the throughput) reveals the guaranteed performance gain, and hence, the lower throughput bound is valuable.

4.4 Numerical Examples

In this section, we examine frameless ALOHA with multiple BS cooperation and give some numerical examples. Specifically, the optimization problem on target degrees, which maximizes the average throughput, is introduced. The optimization problem is based on the previously derived theoretical throughput expressions. Furthermore, the performance improvement via multiple BS cooperation, namely *multi-access diversity gain*, was evaluated, and it was revealed that the gain increases almost linearly as the number of BSs increases. Moreover, frameless ALOHA using the optimized target degrees is compared with a state-of-the-art random-access scheme that also uses multiple BS cooperation, with the results showing that the optimized frameless ALOHA scheme

[3]The number of terms varies depending on how many BSs the specified user group can communicate with. For u_i, the number of terms is $|\mathcal{S}(\mathsf{u}_i)|(|\mathcal{S}(\mathsf{u}_i)|+1)/2$.

significantly outperforms the conventional multiple BS cooperation scheme thanks to the frameless structure and the exact analysis of PLR.

4.4.1 Target Degree Optimization

The throughput at the T-th time slot $S(T)$ has been defined as the fraction of retrieved information packets and elapsed time slots, which is shown in (4.7). The equation of (4.7) can be rewritten as $S(T) = \sum_i N_i(1 - p_{\mathrm{e},i}(T))/T$. The average throughput performance of the original (single-BS) frameless ALOHA peaks as the number of time slots increases, and it has been shown that the actual throughput performance converges to the theoretical performance as the number of users increases. Additionally, the average throughput performance converges to the peak throughput value when there is a sufficiently large number of users [67, 91]. Hence, in order to maximize the average throughput, the optimization problem is formulated to find the target degree vector $\mathbf{G}_{\mathrm{opt}} = \{G_{1,\mathrm{opt}}, \ldots, G_{I,\mathrm{opt}}\}$ which maximizes the peak throughput, that is

$$\max_{\mathbf{G}} \quad \sup_{T} S(T) \tag{4.31}$$

$$\text{s.t.} \quad 1 - p_{\mathrm{e}}(T^*) > \alpha, \tag{4.32}$$

where $T^* = \arg\sup_T S(T)$.

Using the theoretical analysis of PLR, target degrees can be optimized for arbitrary networks with an arbitrary number of BSs. Consider the target degree optimization for networks with $I = 2^M - 1$ user groups with $M \leq 4$. The threshold is set to $\alpha = 0.8$ and the frame terminates when 80% of all the packets have been successfully retrieved. Without the loss of generality, it is constrained that $G_i = G_j$ for all i and j such that $|\mathcal{S}(\mathsf{u}_i)| = |\mathcal{S}(\mathsf{u}_j)|$. The optimization problem is a multi-modal problem with multiple target degrees to be optimized. In this chapter, the differential evolution [89], which is regularly used to optimize the degree distribution of graph-based codes such as LDPC codes [25], is employed to solve the problem. In the optimization example, 300 candidates are used, 0.2 is used as the mutant factor, and the update on candidates (generating mutants) are iterated 30 times. Details on the differential evolution algorithm can be found in [89]. In the subsections below, we first study optimization using several BS numbers while considering a symmetric network. Then, in order to show the relationship between the number of users in each network and the optimal target degrees, optimization for an asymmetric network is considered.

Optimization for Symmetric Networks

First, let us consider symmetric networks where $N_i = 10^4$ for all i. Table 4.1 shows the optimal target degrees and corresponding throughput performance for different BS numbers, where "Peak" denotes the theoretical peak throughput, and "Average" denotes the simulated average throughput performance. Note that achievable throughput with M BSs is M, at most. In our computer simulation, we presumed that $N_i = 10^4$ for each user group and confirmed that the theoretical peak throughput performance coincides with the actual average throughput performance of the computer simulation. The reason why the simulated performance values degrade slightly from theoretical performance values is that the theoretical analysis assumes the number of graph nodes to be infinite, so that the graph becomes typical. When multiple BSs exist in the network, target degrees of user groups in overlapped areas become smaller than that of the isolated user group. These results agree with the conclusion in [103], where it is suggested that users in overlapped areas should not transmit too much. Moreover, these results contradict the results of [87], where it is suggested that all the users should transmit with an equal probability in the presence of an SIC with multiple cooperating BSs. Throughput comparison with [87] will be discussed in Section 4.4.5.

Optimization for Asymmetric Networks

It may be of interest to note how the optimal target degrees and corresponding throughput performance vary when the number of users in each group differs. To clarify the discussion so far, let us consider networks with $M = 2$ BSs and consequently $I = 2^M - 1 = 3$ user groups. Specifically, u_1, u_2, and u_3. Groups-1 and 2 are able to communicate with BS-1 and 2 respectively, and u_3 can communicate with both BSs. Moreover, for the sake of simplicity, it is assumed that $N_1 = N_2$ and $G_1 = G_2$ so that we only need to mention N_1, not both N_1 and N_2. We optimized target degrees for several networks and listed the results in Table 4.2. We confirmed that theoretical peak throughput performances agree with simulated average throughput performances. In the following, the results are discussed in terms of two kinds of situations: $N_3 > N_1$ and $N_3 < N_1$.

When $N_3 > N_1$, where the number of users in the overlapped area is larger than that of users in isolated area, the peak throughput performance degrades as N_1 decreases. This is natural because the network approaches single BS network, where all the users can communicate with common BSs. Note that since network (a) is identical to a single BS network, the optimal target degree and the peak throughput are also identical

to the original frameless ALOHA. The optimal target degree of u_3 approaches the optimal value for single BS frameless ALOHA. *i.e.*, 3.098, as N_1 decreases. When it comes to u_1, the optimal target degree G_1 is decreased in order to bring it into balance with the increase of G_3. This is necessary because if the users in u_1 transmit frequently, the channel would become saturated and the SIC process would be stacked. Hence, in order to a achieve high throughput performance, the optimal G_1 must be decreased as the optimal G_3 in $N_3 > N_1$ is increased, As in the discussion above, when $N_3 < N_1$, the optimal target degree of u_1 approaches the optimal target degree of the original frameless ALOHA as N_3 decreases. In the most extreme case, *i.e.*, network (g), the optimal target degree is identical to the original frameless ALOHA, and the peak throughput is twice that of the original frameless ALOHA. Interestingly, the peak throughput values of networks (e) and (f) are both higher than that of (g). This is because packets transmitted from users in overlapped areas may be retrieved by other BSs while the average traffic load at each BS is the same as that for a single BS frameless ALOHA with an optimized target degree. An observation we can obtain here is that the number of users affects the throughput improvement via multiple BS cooperation. It is especially noteworthy that the existence of some users in overlapped areas increases rather than degrades throughput performance.

4.4.2 Comparison with Some Simple Schemes

We further show how much performance improvement is achieved by the proposed frameless ALOHA compared to non-cooperative frameless ALOHA schemes. For comparison purposes, two simple transmission schemes employing frameless ALOHA are considered while supposing that $M = 2$. Without loss of generality, let us consider again symmetric networks.

The simplest case is *perfect separation*, where each BS has its own frame. First, the users in u_1 and a portion of the users in u_3, namely $\mathsf{u}_{3,1}$ with $N_{3,1}$ users, transmit packets to s_1 with frameless ALOHA. Then, after the frame of s_1, the users in u_2 and the remaining users in u_3, namely $\mathsf{u}_{3,2}$ with $N_{3,2}$ users such that $N_{3,1} + N_{3,2} = N_3$, transmit to s_2. Perfect separation is equivalent to a frequency division model, where each BS uses its own frequency band.

Another case is *simultaneous transmission*, where all of the users transmit in the same frame while BSs retrieve packets without multiple BS cooperation. These two candidates use the optimal target degree $G = 3.098$, which is designed for $M = 1$, since BSs do not cooperate.

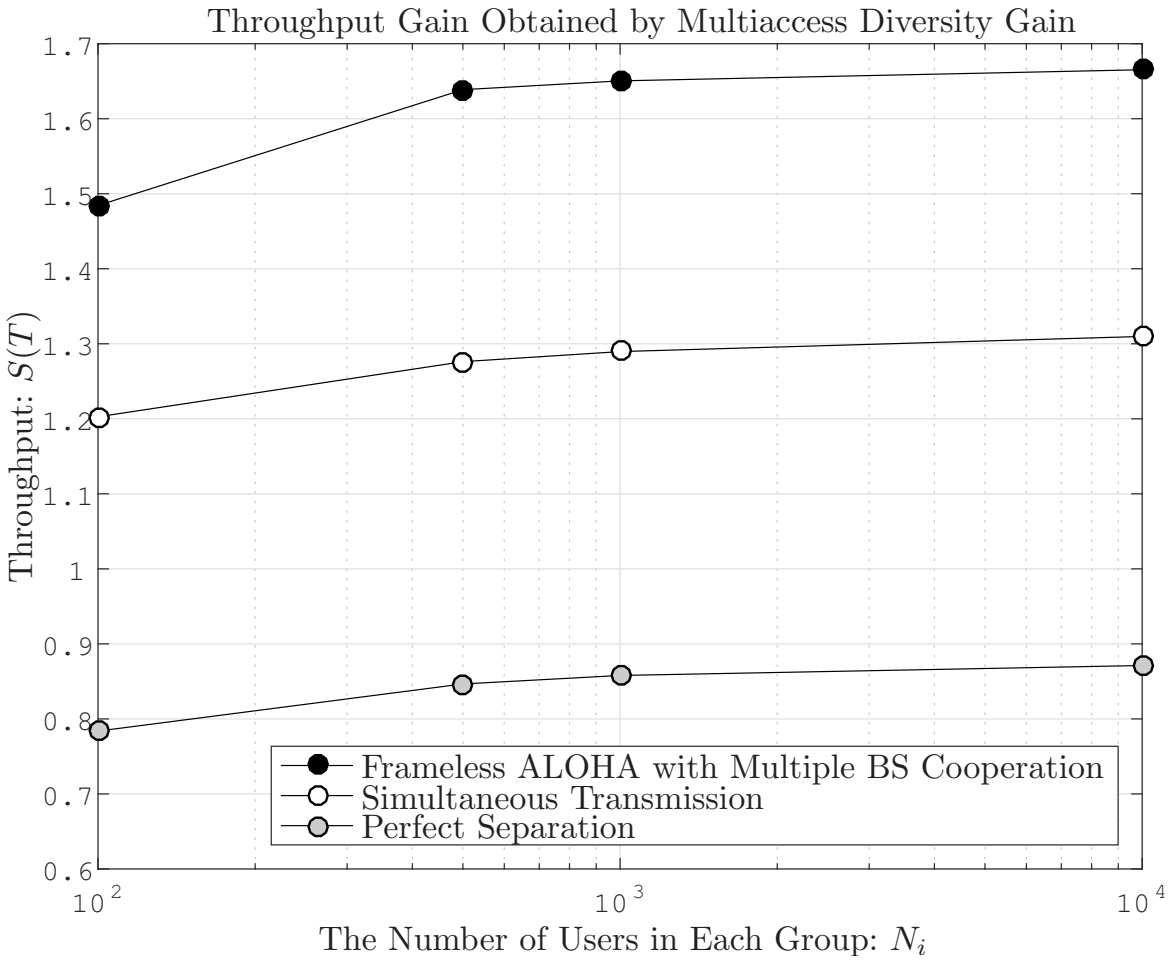

Fig. 4.5 Comparison of throughput performance of frameless ALOHA with multiple BS cooperation, perfect separation, and simultaneous transmission. Frameless ALOHA with multiple BS cooperation uses the optimized target degree, while simultaneous transmission and perfect separation uses identical target degree of $G = 3.09$.

Figure 4.5 shows the throughput performance of each scheme. Simultaneous transmission performs better than perfect separation because its features allow user in u_1 and u_2 to transmit simultaneously without interfering with each other and without any performance degradation. However, when combined with multiple BS cooperation and optimized target degrees, frameless ALOHA exhibits a throughput performance that is clearly higher than simultaneous transmission. An important observation to keep in mind is that the use of multiple cooperating BSs significantly improves the throughput performance due to the existence of *multi-access diversity gain*, which exploits the overlapped coverage areas. Furthermore, in the presence of SIC and multiple BS cooperation, coverage overlapping improves the throughput performance because of multi-access diversity gain, which is in contradiction to the

results in the classic multiple BS random access literature [103, 104]. However, it should also be noted that this contradiction arises because the literature had not yet considered interference cancellation, and the previously given advice that users in overlapped areas should be separated remains partially sound because excessive overlapping decreases throughput performance. Therefore, it can be concluded that, when multiple BS cooperation is available, multiple cells should be merged to facilitate maximum performance, rather than keeping each cell separate. We also examined multi-access diversity gain from the viewpoint of theoretical analysis. Recall that the main difference between cooperative and non-cooperative analysis is the calculation of $w_i^{(l)}$. From (4.14), the probability $w_i^{(l)}$ consists of two components: $P_i^{(\mathrm{r0})}$ and $P_i^{(\mathrm{r1})}$. In particular, the latter term corresponds to the probability that packets can be retrieved thanks to multiple BS cooperation, which cancels colliding packets. This is the exact outcome desired from multiple BS cooperation, and it is predicted that $P_i^{(\mathrm{r1})}$ *contributes significantly to multi-access diversity gain.* Figure 4.6 shows the evolution of $P_1^{(\mathrm{r0})}$ and $P_1^{(\mathrm{r1})}$ in the iterative calculation of $w_1^{(l)}$ and $x_1^{(l)}$, supposing that $M = 3$. Note that the resulting PLR decreases as $P_i^{(\mathrm{r0})}$ and $P_i^{(\mathrm{r1})}$ increase, which is obvious from (4.14). Interestingly, in contrast to the prediction, $P_i^{(\mathrm{r0})}$ plays a more important role than $P_i^{(\mathrm{r1})}$. Another important result of multiple BS cooperation is that packet sharing among BSs cancels more packets than in the non-cooperative case, thereby resulting in more singleton slots. When multiple BS cooperation is not available, each BS locally performs the SIC, as previously elucidated. In contrast, with cooperation, the SIC is performed *jointly* among BSs, thereby leading to the efficient retrieval of packets from overlapped areas. The idea is similar to the diversity techniques of a physical layer. One insight we can report here is that the gain is available as long as multiple cooperative BSs exist.

4.4.3 Evaluation of Multi-Access Diversity Gain

It has been confirmed that multiple BS cooperation enhances throughput performance more than separated-BS systems. Using (4.8), we will now examine how the multi-access diversity gain varies with M. Note that S^{nc} corresponds to the throughput of *simultaneous transmission* in the previous subsection, since simultaneous transmission achieves higher throughput than perfect separation.

In Fig. 4.7, the multi-access diversity gain Γ is depicted as a function of the number of BSs M, as well as the lower and upper bounds. The lower and upper bounds are given in Section 4.3.3. Note that target degrees used to obtain the lower bound are optimized point-by-point using the PLR upper bound. We confirmed that our proposed

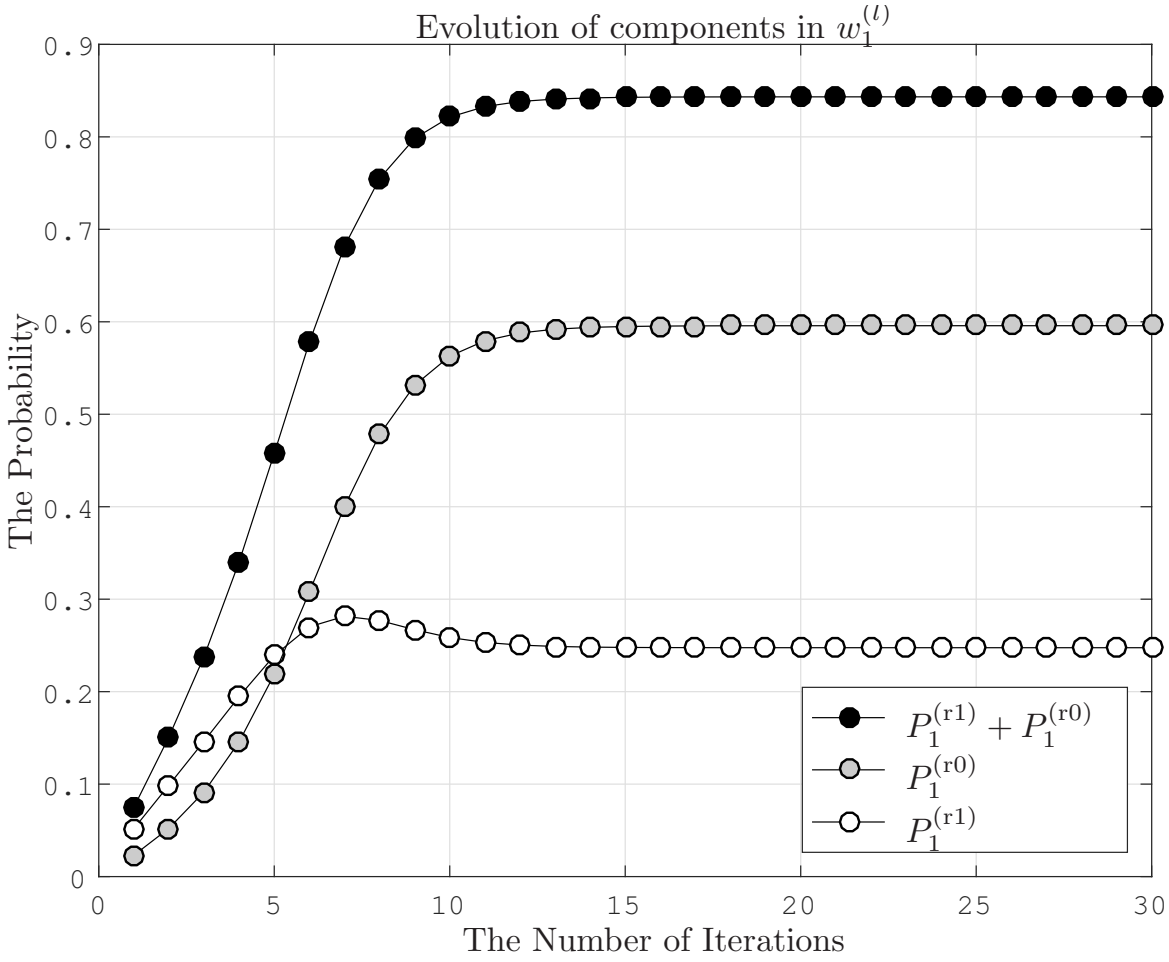

Fig. 4.6 Evolution of $P_1^{(\mathrm{r0})}$ and $P_1^{(\mathrm{r1})}$ in the iterative calculation.

theoretical analysis shows good agreement with the results of computer simulations. Due to computational costs, exact theoretical analysis and computer simulation results have only been obtained for $M \leq 4$. Although the upper bound is simple, we can obtain a meaningful insight that the achievable gain is at most linear. This is important, since the achievable limitation of the multiple BS cooperation is explicitly shown and we do not have to discover parameters such that the throughput is higher than MS_1. In other words, the upper bound can be seen as a *capacity* of the frameless ALOHA with multiple BS cooperation; the bound is an extreme goal which the system can achieve. Furthermore, it is worth noting that the increasing rate of the gain is maximized when the target degrees are optimized.

We also determined that the lower bound given by (4.27)–(4.30) is not tight. Although the bound is based on the lower bound of union probability, we can also make lower bounds by calculating (4.25) using an arbitrary subset $\mathcal{Q}_i \subset \mathcal{R}_i$ instead of $\mathcal{R}_i$. At

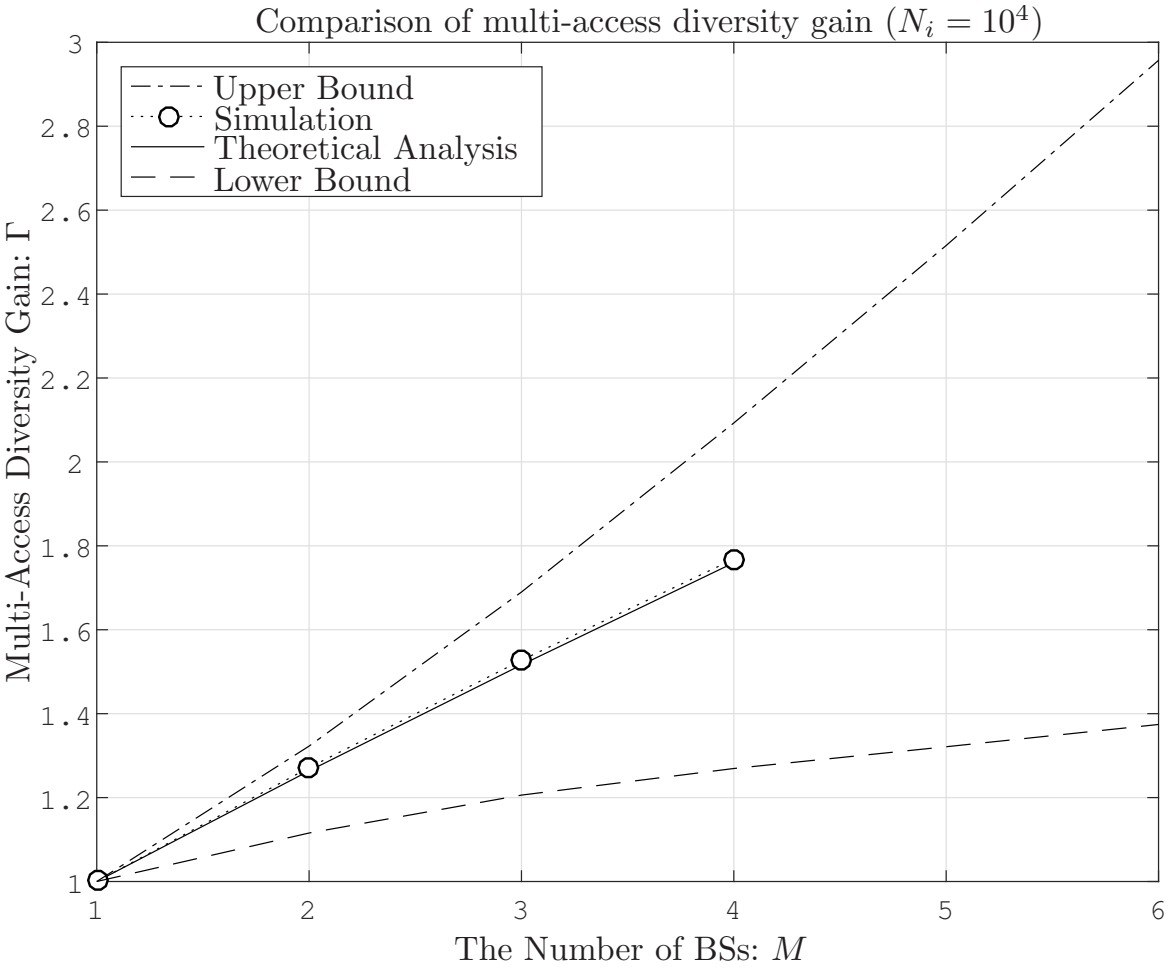

Fig. 4.7 Multi-access diversity gain Γ as a function of the number of BSs M. In theoretical analysis and simulation, the optimized target degrees are used for each point.

that point, the accuracy of the bound can be controlled by the size of $\mathcal{Q}_i$. The bound becomes identical to the exact analysis when $\mathcal{Q}_i = \mathcal{R}_i$, and the accuracy degrades as the size of $\mathcal{Q}_i$ decreases. However, as the number of BSs increases, producing accurate bounds requires enormous computational complexity. To this end, an affordable option is to use the matrix-based bound as the lower-bound of throughput performance for frameless ALOHA with multiple BS cooperation. Although the lower bound is not tight, the bound is remarkable since the bound *strictly exceeds* 1.0; we can *always increase* the throughput performance by multiple BS cooperation, and it is guaranteed that the throughput performance never degrades by the cooperation. This is a motivational insight, since we can obtain higher throughput gain as we deploy larger number of BSs.

It may be interesting to study how the multi-access diversity gain varies when the number of users in each group differs. For comparison purposes, we focus on three networks picked from Table 4.2: (c) $N_1 = N_2 = 10^3, N_3 = 10^4$, (d) $N_1 = N_2 = N_3 = 10^4$, and (e) $N_1 = N_2 = 10^4, N_3 = 10^3$. Recall that the gain of the symmetric network (d) is $\Gamma = 1.26$. In network-(e), where the number of users in the overlapped area is *smaller* than the number of isolated users, $S^{\mathrm{c}} = 1.84$, $S^{\mathrm{nc}} = 1.66$, and $\Gamma = 1.11$. The gain is smaller than that of the symmetrical network, meaning that the effect of multiple BS cooperation is slightly less than that of the symmetrical network. This is natural because the number of users that can be retrieved via multiple BS cooperation is smaller than can be retrieved by the symmetrical network. On the other hand, in network-(c), where the number of users in the overlapped area is *larger* than the number of isolated users, $S^{\mathrm{c}} = 1.06$, $S^{\mathrm{nc}} = 0.97$, and $\Gamma = 1.09$. The gain also decreases in comparison to the case of the symmetrical network because most of the users in the network belong to the overlapped area, which means that the network performance approaches that of a single BS case.

4.4.4 Effect of System Parameters

In this section, the effect of system parameters, *i.e.*, the number of users and the threshold, on the optimal target degree and multi-access diversity gain is discussed.

Effect of the Number of Users

The effect of the asymmetric network has been discussed previously. Note that the optimal target degree is affected by the *ratio* of the number of users in each group, but not the specific number of users. That is to say, the resulting optimal target degrees will be the same for two cases where $N_i = 10^4$ for all i and $N_i = 10^5$ for all i, as long as the number of users in each group is sufficiently large. If the number of users is small, then the assumption of density evolution that guarantees that the degree distribution of the graph is typical does not hold, leading to incorrect results[4].

Effect of Threshold α

Recall that α is the packet retrieval ratio required to finish the transmission frame. If α is too low, then the results would be equivalent to considering only the achieved throughput performance, but not the resulting PLR. Such optimization obviously results in *unfair* target degrees, which means that some user groups cannot deliver their

[4]Finite length analysis for frameless ALOHA can be found in [70].

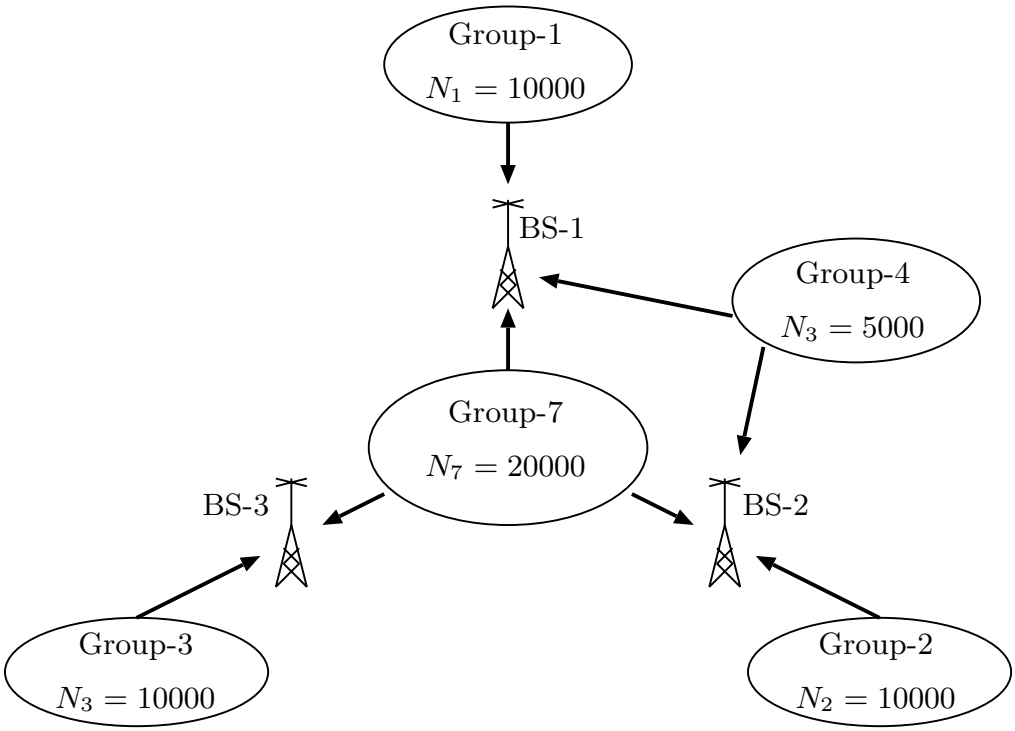

Fig. 4.8 The network model for $\delta = 2$.

packets to the BSs. On the other hand, optimization with too high an α yields poor throughput performance because frameless ALOHA uses probabilistic transmission, which leads to an error floor. That is, if we set the threshold at an extremely high value such as $\alpha = 1.0 - 10^{-5}$, obviously the frame length T must be large enough to achieve the required PLR, thereby resulting in decreased throughput performance.

Although the design of a practically optimal α was investigated in [68], our primary interest is to theoretically design and analyze the system. Thus, detailed discussions about parameters, *e.g.*, at what value should α be practically set in order to achieve a high throughput, are beyond the scope of this chapter. Moreover, it is worth noting that α can be designed independently for each group, leading to the design considering the fairness of user groups; system can be designed so as to achieve the desired PLR for each group.

4.4.5 Comparison with State-of-the-Art

A framed ALOHA protocol employing multiple BS cooperation and SIC, named *spatio-temporal cooperation*, was proposed in [87], and to the best of our knowledge, that scheme remains the state-of-the-art random access structure involving multiple BS cooperation. In this section, we have shown that our proposed frameless ALOHA with multiple BS cooperation achieves a higher throughput performance than spatio-temporal cooperation. In spatio-temporal cooperation, each user selects a temporal degree s according to a *degree distribution* $\Lambda = (\Lambda_1, \cdots, \Lambda_{s_{\max}})$ at the beginning of the frame, where Λ_s is the probability that the degree s is selected, and the maximum degree is denoted by $s_{\max}$.

The frame length is fixed *a priori* so that the user with the degree s transmits s times during the frame. Each user's transmission is heard by multiple BSs, and the average *spatial degree* δ is defined as the average number of BSs that can receive a packet from the user. Upon transmission, the BSs attempt to retrieve the transmitted packets using SIC, and successfully retrieved packets are shared among all the BSs. In [87], the degree distribution is optimized for some δ.

In order to compare our proposed frameless ALOHA with spatio-temporal cooperation, let us consider the network of $\delta = 2$, as shown in Fig. 4.8. For $\delta = 2$, the optimal degree distribution given in [87] is $\Lambda_2^* = 1$, which means that all the users transmit two times during the frame. The optimal target degrees of frameless ALOHA for the network can be obtained by the optimization problem given in (4.31), in which we need to optimize target degrees G_1, G_2, G_3, G_4, and G_7. Since u_1 and u_2 are symmetric with s_1 and s_2, *i.e.*, both groups are connected to a single BS that the users in u_4 and u_7 attempt to use simultaneously, it is assumed that $G_1 = G_2$.

The obtained optimal target degrees are $(G_1, G_3, G_4, G_7) = (1.42, 1.30, 0.47, 2.33)$. For comparison purposes, the normalized throughput performance versus the normalized load is evaluated for both schemes. The normalized load $\overline{G}$ is given by dividing the number of users in the network by the number of time slots and BSs, that is

$$\overline{G} \triangleq \frac{N}{MT}. \tag{4.33}$$

Normalized throughput $\overline{S}(\overline{G})$ is given by dividing throughput by the number of BSs, that is

$$\overline{S}(\overline{G}) \triangleq \frac{\sum_i N_i(1 - p_{\mathrm{e},i}(T))}{MT}. \tag{4.34}$$

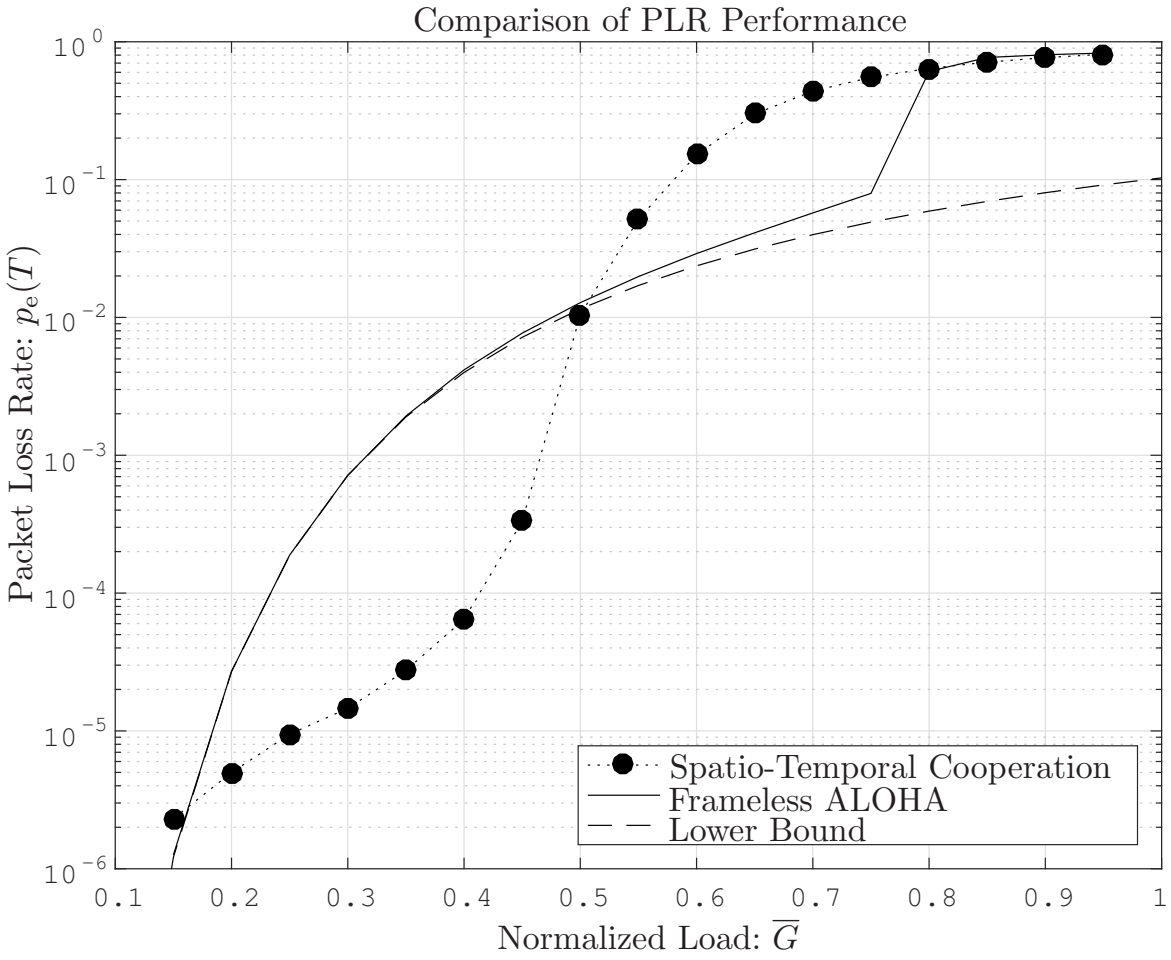

Fig. 4.9 Average PLR performance of frameless ALOHA with multiple BS cooperation and spatio-temporal cooperation for the network model shown in Fig. 4.8.

Figures 4.9 and 4.10 show, respectively, the normalized throughput performance and the average PLR performance of frameless ALOHA with multiple BS cooperation and spatio-temporal cooperation obtained via computer simulations. The PLR performance of frameless ALOHA is lower-bounded by the probability that the user never transmits in the frame, given by

$$p_{e_{LB}}(T) = \sum_{i=1}^{I} \frac{N_i}{N}(1-p_i)^T. \tag{4.35}$$

It is worth noting that the PLR performance suddenly drops at approximately $\overline{G} = 0.8$. The steep fall is called a *waterfall region*, and is a representative characteristic of a belief propagation (BP) decoder [23], and the SIC process can be interpreted as a BP decoder for binary erasure channels (BEC). Frameless ALOHA with multiple BS

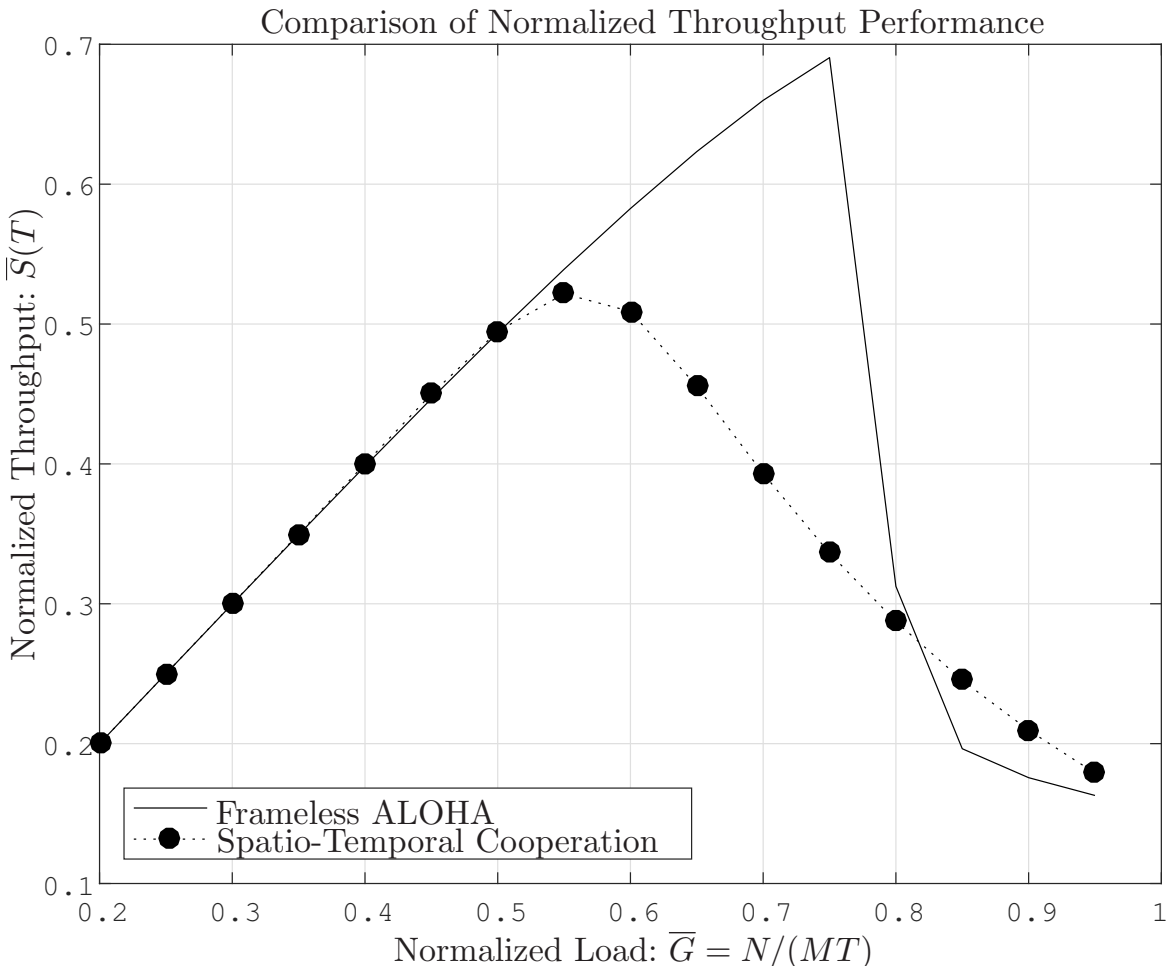

Fig. 4.10 Normalized throughput performance of frameless ALOHA with multiple BS cooperation and spatio-temporal cooperation for the network model shown in Fig. 4.8.

cooperation using the aforementioned optimized target degrees beats spatio-temporal cooperation from the viewpoint of both throughput and PLR in a practical area $0.5 \leq \overline{G} \leq 0.8$. Our observations show that our proposed scheme is capable of bearing a heavier load, and thus can achieve a higher throughput performance, *i.e.*, while the performance of spatio-temporal cooperation degrades after the point of $G = 0.55$, frameless ALOHA with the optimal target degrees achieves a high throughput until the load reaches the point of $G = 0.75$. Due to the approximation in the analysis of spatio-temporal cooperation, the conventional scheme can only assign a single degree distribution to all the users. In contrast, frameless ALOHA with our proposed analysis can employ different transmission probabilities for each user group, which means that our proposed scheme outperforms the conventional scheme.

For the area with a smaller load that is $G < 0.5$, frameless ALOHA has worse PLR performance than spatio-temporal cooperation. However, the throughput performance of frameless ALOHA is almost the same as that of spatio-temporal cooperation because the PLR gap in the region is lower than 10^{-2}. In the heavier load area, *i.e.*, $G > 0.8$, the proposed frameless ALOHA performs worse than spatio-temporal cooperation. This is because the saturated channel makes the offered load too heavy to carry out random access schemes. The comparison here, however, has fixed the number of time slots for both frameless ALOHA and conventional schemes, even though frameless ALOHA adaptively determines the number of time slots. In other words, frameless ALOHA always adjusts the channel load to the optimal point where the peak throughput is achieved by its frameless structure. Specifically, frameless ALOHA adaptively determines its frame length so as to retrieve sufficiently large number of users by terminating the frame when the number of retrieved users exceeds the *a priori* given threshold. This means that the protocol finishes when peak throughput is achieved. Moreover, thanks to the exact throughput analysis utilized in the optimization process, our proposed frameless ALOHA has a peak throughput performance which is higher than the average throughput performance of the conventional scheme. Thus, we can say that our frameless ALOHA scheme outperforms a state-of-the-art random access structure for use with multiple BS cooperation.

4.5 Comparison with E-ZDFA

Finally, we compare frameless ALOHA with multiple BS cooperation against Enhanced ZigZag decodable frameless ALOHA (E-ZDFA) proposed in the previous chapter. From the viewpoint of the throughput, recalling that E-ZDFA improves the average throughput by 5%, multiple BS cooperation largely improves the throughput performance, *e.g.*, the throughput is improved by 80% if four BSs are available. Hence, it can be concluded that frameless ALOHA with multiple BS cooperation exhibits much higher throughput than E-ZDFA. However, yet still with the single base station, E-ZDFA is considered to be an efficient protocol. Moreover, E-ZDFA has several advantages than multiple BS cooperation. Thanks to the ZD, the BS can retrieve more packets than the original frameless ALOHA (and frameless ALOHA with multiple BS cooperation) before reaching the waterfall region. This feature is useful to realize low-latency communication, as frameless ALOHA without ZD can only retrieve less users before the waterfall region. Furthermore, E-ZDFA can lower the error floor by increasing the transmission probability, which is accomplished by acknowledging the retrieval of

users. We can conclude that multiple BS cooperation can achieve higher throughput performance than E-ZDFA, while E-ZDFA has several advantages on reliability.

4.6 Chapter Summary

In this chapter, we examined frameless ALOHA with multiple BS cooperation and showed how much performance improvement is achievable by defining the multi-access diversity gain. An exact theoretical analysis of the throughput performance was given, along with a simple lower bound. Theoretical analysis was used to optimize target degrees so that the achievable throughput could be maximized. Numerical examples have shown that the multi-access diversity gain monotonically increases as the number of BSs increases. Specifically, while E-ZDFA can improve the throughput performance by 5% compared with the original frameless ALOHA, multiple BS cooperation can improve the throughput performance by 80%.

This chapter contributes to throughput improvement of multiple access networks with multiple cooperative BSs. As cellular network utilizes multiple BS cooperation, WLANs and WSNs are considered to employ cooperative BSs in near future. Our proposed frameless ALOHA with multiple BS cooperation definitely exhibits better throughput performance than conventional schemes, and the analysis is useful to design transmission probability of users in arbitrary type of networks.

Chapter 5

ZigZag Decodable Frameless ALOHA with Multiple Base Station Cooperation

We have proposed two modifications of frameless ALOHA schemes, namely E-ZDFA and frameless ALOHA with multiple BS cooperation. Both proposals are shown to achieve higher throughput performance than conventional schemes; E-ZDFA outperforms the original frameless ALOHA while lowering the error floor, and the multiple BS cooperation attains positive throughput gain as the number of BSs increases. Moreover, these schemes are not exclusive, but they can be combined together.

In this chapter, these two schemes are jointed so as to further increase the throughput performance, yielding a scheme named ZigZag decodable frameless ALOHA with multiple BS cooperation (*ZDFA-coop*). ZD, which resolves collision of two packets, is also useful to improve the throughput performance in the multiple BS scenario. Supposing a simple network consisting of two BSs, we evaluate the throughput performance of ZDFA-coop via computer simulation, and it is revealed that ZDFA-coop achieves higher throughput performance than frameless ALOHA with multiple BS cooperation.

Finally, we compare ZDFA-coop with conventional coded ALOHA schemes in a practical environment, where the number of users fluctuates so that BSs cannot track the precise number of active (contending) users. Numerical results show that our proposed scheme outperforms competitors in terms of the achieved throughput performance. It is also revealed that the framed scheme with the optimized degree distribution causes an *outage*, where the throughput highly degrades so that only a small fraction of users can be retrieved.

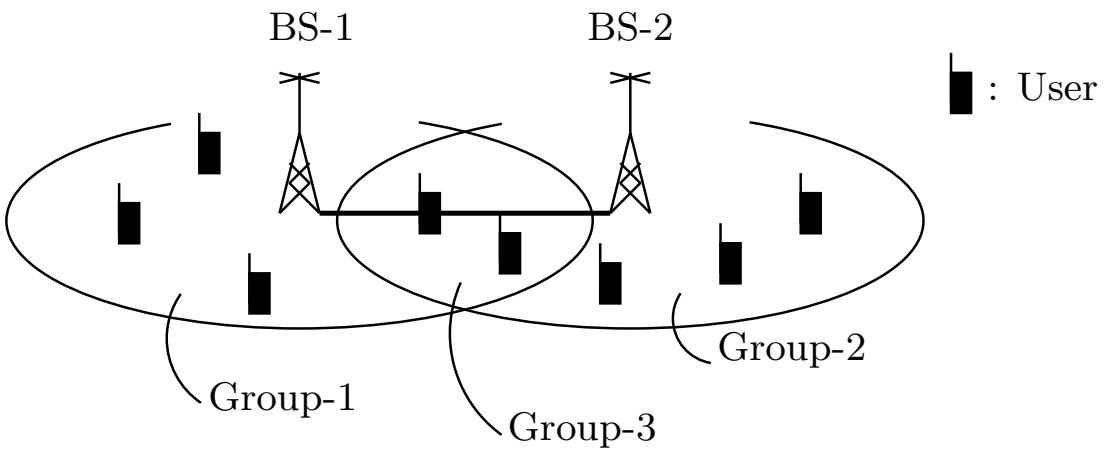

Fig. 5.1 Network model.

5.1 System Model

Let us consider a network with N users and two BSs, where the BSs are connected via a backhaul network, as shown in Fig. 5.1. Users are categorized into three groups depending on which BS(s) they are able to communicate with. Similarly with Chapter 4, u_i denotes the i-th user group, and s_j denotes BS-j, where $i \in \{1, 2, 3\}$ and $j \in \{1, 2\}$. Specifically, in case of a network with two BSs, users in u_1 and u_2 can communicate only with s_1 and s_2, respectively, and users in u_3 can communicate with both BSs. Time slots comprise two kinds of subslots, *i.e.*, uplink subslot (US) and downlink subslot (DS), similarly with the model in Chapter 3. Users transmit their packets in the US, and the BS broadcasts feedback signal to the following DS. Upon transmission, slots are organized into a frame. Users are assumed to have one packet at the start of a frame, and no new packets are generated during the frame.

The BS is assumed to be able to distinguish the following conditions for each time slot:

(a) No users have transmitted.

(b) Only one user has transmitted, *i.e.*, the time slot is a singleton.

(c) Two users have transmitted and collided.

(d) Three or more users have transmitted and packets have collided.

This is realized by supposing that each packet contains a unique word, which identifies the transmitter.

5.2 Transmission Based on Enhanced ZigZag Decodable Frameless ALOHA

In ZDFA-coop, users transmit their packets based on E-ZDFA protocol, which has been introduced in Chapter 3. Let T denote the present time slot. At every slot, each user in $\mathtt{u}_i$ decides whether or not to transmit the packet, based on the following transmission probability

$$p = \frac{G_i}{N_i - N_{\mathrm{ret},i}^{(T)}}, \tag{5.1}$$

where $N_{\mathrm{ret},i}^{(T)}$ is the number of users that have stopped retransmission. In E-ZDFA, users are able to exactly estimate the number of such users by observing the feedback signal from the BS. However, in ZDFA-coop, users cannot exactly track $N_{\mathrm{ret},i}^{(T)}$, as there are multiple user groups; even when users knows that two packets are retrieved at the BS, they cannot know which user group the retrieved packets have been transmitted from. To this end, users in $\mathtt{u}_i$ approximately estimate $N_{\mathrm{ret},i}^{(T)}$ as follows:

- If $\mathtt{s}_j$ has retrieved one packet, $N_{\mathrm{ret},i}^{(T)}$ is increased by $N_i / \sum_{n:\mathtt{u}_n \in \mathcal{U}(\mathtt{s}_j)} N_u$.
- If $\mathtt{s}_j$ has retrieved two packets, $N_{\mathrm{ret},i}^{(T)}$ is increased by $2N_i / \sum_{n:\mathtt{u}_n \in \mathcal{U}(\mathtt{s}_j)} N_u$.

In other words, each user in $\mathtt{u}_i$ increases $N_{\mathrm{ret},i}^{(T)}$ by the probability of the user in $\mathtt{u}_i$ being retrieved. For instance, when a symmetric network, where $N_i = N_j \forall i \neq j$, $N_{\mathrm{ret},i}^{(T)}$ is increased by 0.5 upon single user being retrieved, and $N_{\mathrm{ret},i}^{(T)}$ is increased by 1.0 upon two users being retrieved. If we need to specify the group which the retrieved packet has been transmitted from, additional overhead should be included in the feedback signal, where the size of required feedback increases exponentially with the number of BS. Due to this reason, we do not specify the group which the retrieved packet has been transmitted from.

Upon receiving packets, BSs check whether the number of retrieved packets attains the threshold. Let us suppose that BSs terminate the frame when $\lfloor \alpha N \rfloor$ packets are retrieved in the network, where $\alpha \in (0, 1]$. In ZDFA-coop, similarly with E-ZDFA, each BS broadcasts a feedback signal to inform users about the following four conditions:

1. The transmitted packet(s) is (are) retrieved.
2. Two packets are collided, and the corresponding users are required to retransmit.
3. The frame is ended as the desired PLR has been achieved at the BS.

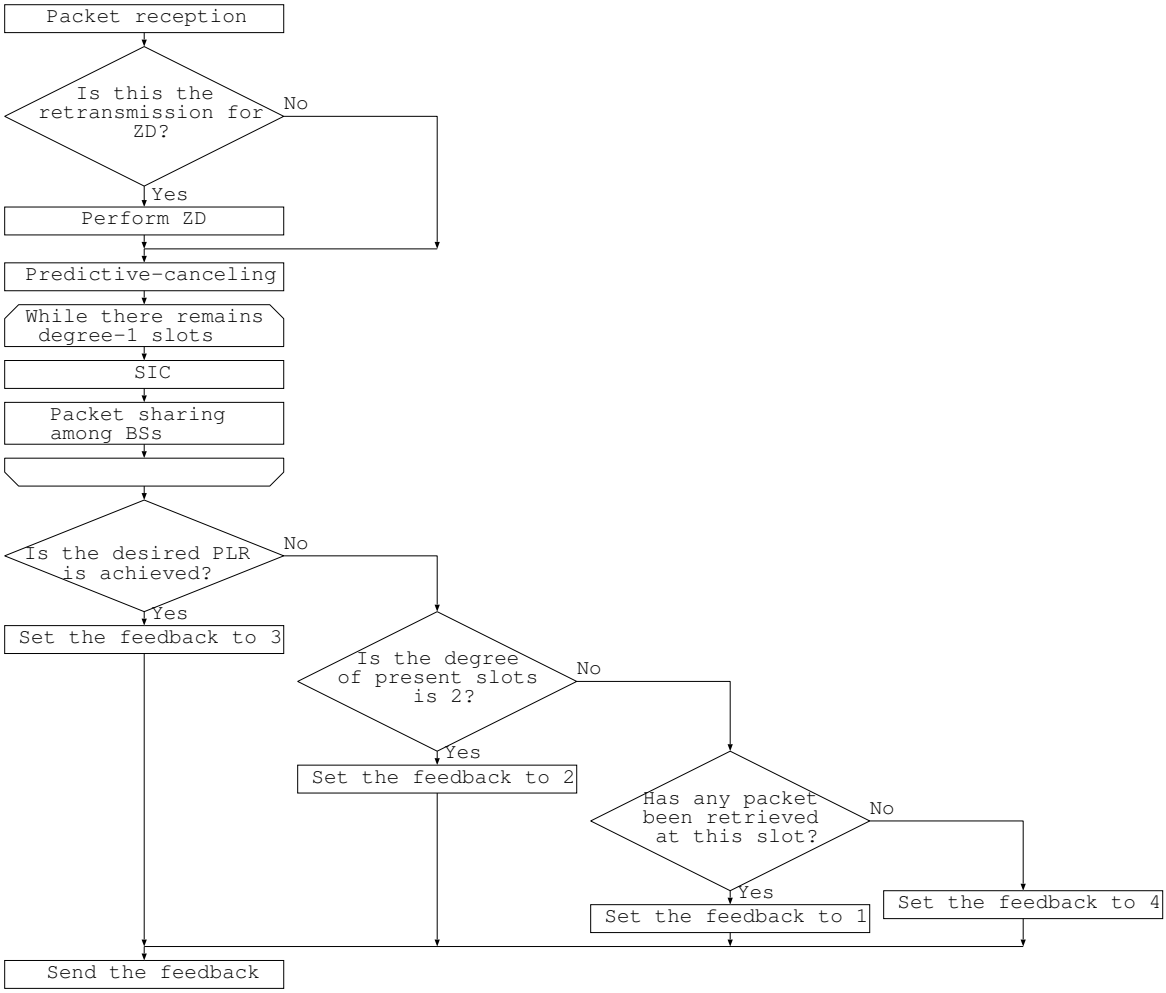

Fig. 5.2 Flowchart for processes at each BS.

4. The frame is continued as the desired PLR has not been achieved.

The BSs would send different feedback signal, except for the third feedback.

5.3 Combination of ZigZag Decoding and Multiple Base Station Cooperation

BSs jointly perform ZD, SIC, and packet sharing. Figure 5.2 depicts the processes at each BS. If the present transmission was required in the previous slot for ZD, the BS performs ZD. Otherwise, each BS firstly performs the predictive-canceling introduced in Chapter 3. Then, BSs cooperatively perform SIC, where retrieved packets are shared among BSs. Upon retrieving packets, the BS decides which feedback to transmit,

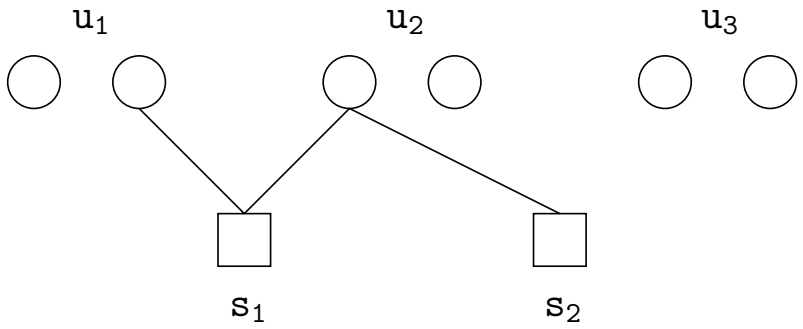

Fig. 5.3 An example of transmission of users. Although two packets are received at $\mathtt{s}_1$, one of them can be canceled so that $\mathtt{s}_1$ does not have to require the retransmission of the packet.

considering the number of retrieved packets, the resulted degree of the present slot, and whether or not the packet(s) transmitted at the current slot has (have) been retrieved.

It is worth noting that the retransmission of packets for ZD occurs only when two packets remain unretrieved after SIC and packet sharing among BSs. Figure 5.3 shows an example of packet reception at two BSs, where two packets are received at $\mathtt{s}_1$, while $\mathtt{s}_2$ receives one packet. Suppose that BSs have not retrieved any packets before receiving these packets. In E-ZDFA, which presumes only single BS, the BS sends the feedback signal which requires immediate retransmission of the users upon receiving collided packet with two transmitters. However, in the case of Fig. 5.3, the packet transmitted from the user of $\mathtt{u}_2$ can be retrieved at $\mathtt{s}_2$, so that $\mathtt{s}_1$ can cancel the packet from the received signal. Hence, the collision of two packets are resolved, and $\mathtt{s}_1$ does not require users to immediately retransmit the packet, which would result in suppression of additional slots and increase of throughput. By combining ZD and multiple BS cooperation, ZDFA-coop has the potential to improve the throughput performance than frameless ALOHA with multiple BS cooperation.

5.4 Numerical Example

5.4.1 Comparison with Frameless ALOHA with Multiple BS Cooperation

In this section, we evaluate the throughput performance of ZDFA-coop via computer simulation. Similarly with Chapter 4, the throughput $S(T)$ is defined as the fraction

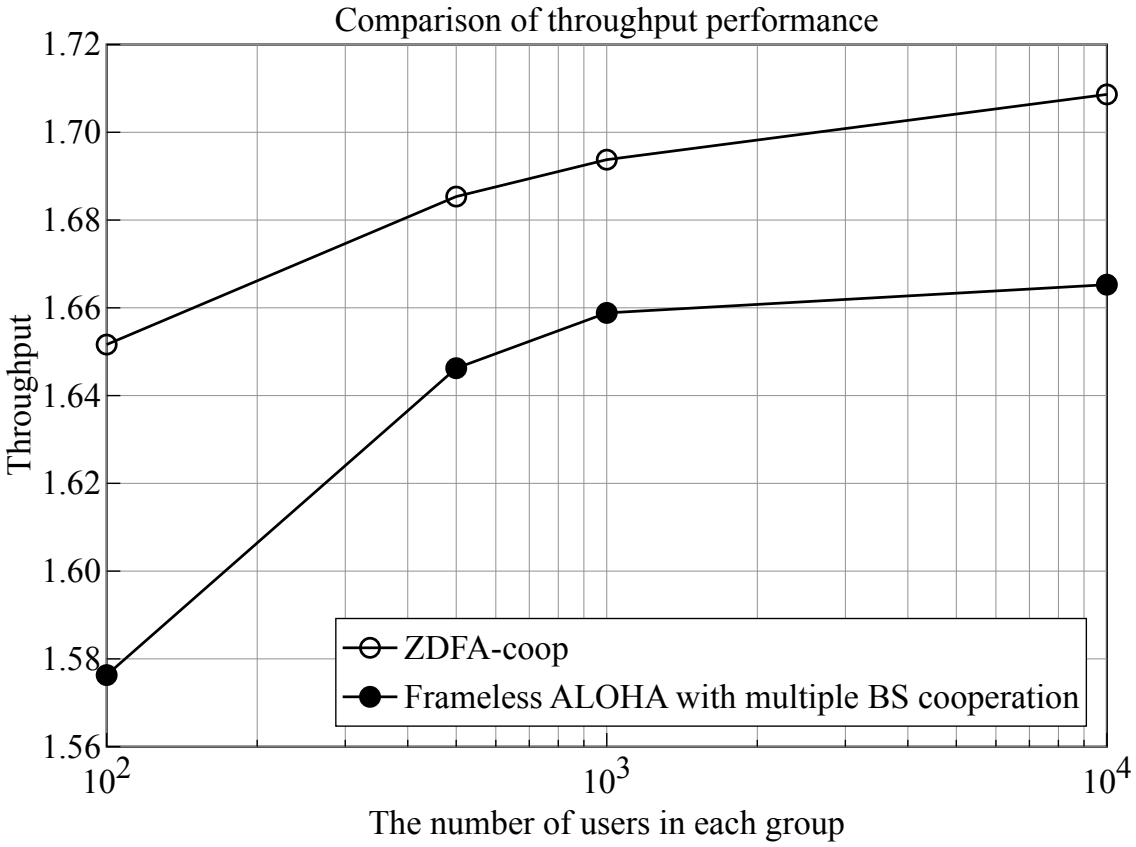

Fig. 5.4 Throughput performance of ZDFA-coop. Both schemes use target degree of $G_1 = 1.83$ and $G = 1.68$.

of successfully retrieved packets and time slots, and is given by

$$S(T) \triangleq \frac{N_{\text{ret}}(T)}{T}, \tag{5.2}$$

where $N_{\text{ret}}(T)$ denotes the number of retrieved packets within T slots.

For the sake of simplicity, a symmetric network is considered, where $N_1 = N_2 = N_3$. The optimized target degrees derived in Chapter 4, namely $G_1 = 1.83$ and $G_3 = 1.68$ are used. Figure 5.4 shows the throughput performance of ZDFA-coop obtained via computer simulation. For comparison, throughput performance of frameless ALOHA with multiple BS cooperation, which has been shown in Chapter 4, is also plotted. Obviously, ZDFA-coop outperforms frameless ALOHA with multiple BS cooperation in terms of the average throughput performance thanks to ZD. However, the throughput performance of ZDFA-coop has not been maximized yet; there is a room for further improvement of throughput performance. Unfortunately, with E-ZDFA, conventional

Table 5.1 Comparison of average throughput and variance.

Scheme	ZDFA-coop	IRSA	spatio-temporal cooperation
Average throughput	1.693	1.514	1.309
Variance of throughput	1.4×10^{-3}	6.3×10^{-2}	2.7×10^{-3}

density evolution cannot be used to calculate the PLR performance of ZDFA-coop, as degree distributions and the transmission probability dynamically vary. The results revealed in this section confirm that ZD can improve the throughput performance than frameless ALOHA with multiple BS cooperation, even if the same target degrees are used.

5.4.2 Evaluation with a Practical Situation

Problem Set-up

Finally, we compare the throughput performance of ZDFA-coop with that of IRSA [57], [63] and spatio-temporal cooperation [87], with a practical situation, where the number of active users fluctuates. A network with two BSs and three user groups, is considered as shown in Fig. 5.1, where the number of users in each group is a random variable following i.i.d. Poisson distribution with mean $\bar{N}$. For the sake of simplicity, the mean for each group is assumed to be identical. BSs assumes that each group always contains $\bar{N}$ users; in case of ZDFA-coop, the transmission probability is calculated using $\bar{N}$, while the frame length of spatio-temporal cooperation and IRSA is determined based on $\bar{N}$. Similarly with Chapter 3, the degree distribution of IRSA is given by

$$\begin{aligned} L(x) =& 0.494155x^2 + 0.159085x^3 + 0.107372x^4 + 0.070336x^5 + 0.045493x^6 \\ &+ 0.019898x^7 + 0.024098x^{11} + 0.008636x^{12} + 0.005940x^{13} + 0.008749x^{15} \\ &+ 0.002225x^{18} + 0.001261x^{20} + 0.002607x^{22} + 0.008092x^{23} + 0.002287x^{24} \\ &+ 0.012274x^{25} + 0.002530x^{26} + 0.003094x^{27} + 0.002558x^{28} + 0.005891x^{29} \\ &+ 0.013419x^{30}, \end{aligned}$$

and the degree distribution of spatio-temporal cooperation is $L(x) = x^2$, similarly with Chapter 4.

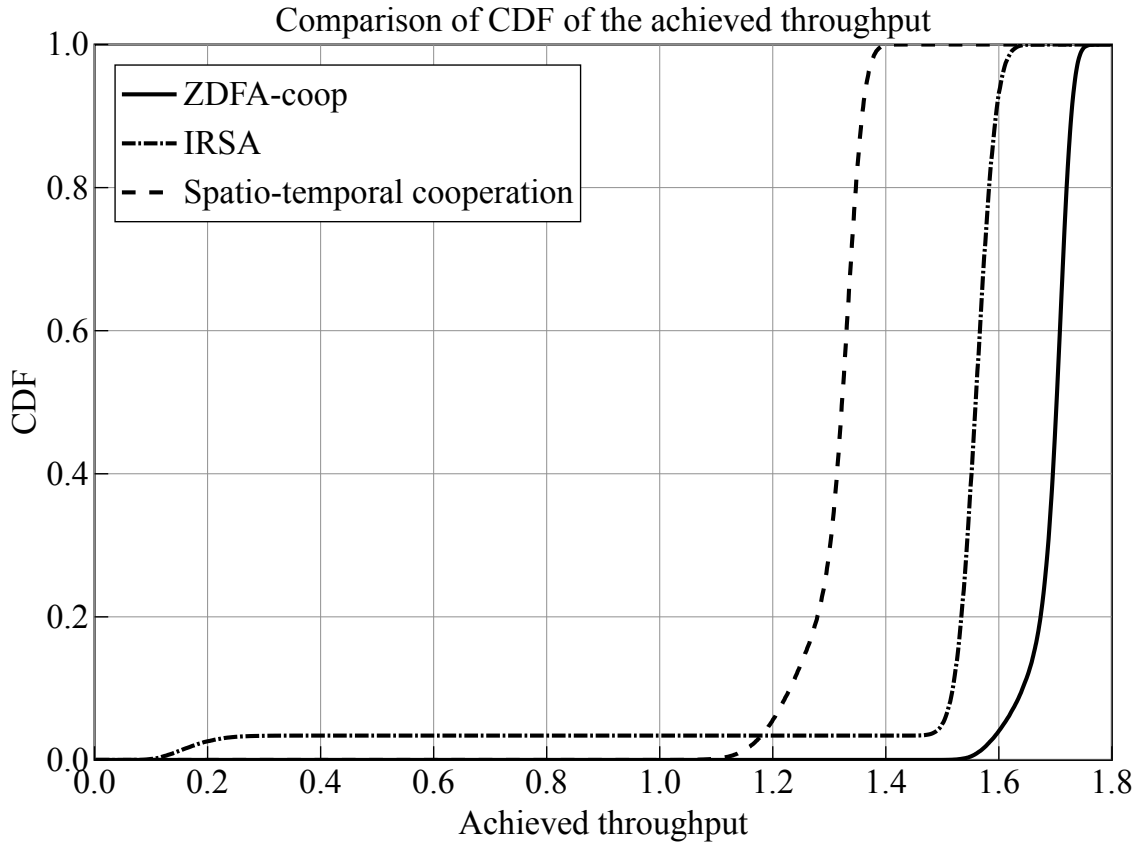

Fig. 5.5 Cumulative histogram of throughput. The average number of users is 1000. ZDFA-coop uses the target degree of $(G_1, G_3) = (1.83, 1.68)$, while IRSA and spatio-temporal cooperation use the optimized degree distributions. IRSA is observed to cause low throughput with non-negligible probability.

Throughput Performance

Supposing that $\bar{N} = 1000$, average throughput performance of each scheme is evaluated via computer simulation. Table 5.1 shows the average throughput and the variance of throughput. Note that, for IRSA and spatio-temporal cooperation, the frame length which yields the highest throughput with fixed number of users is used. Even with the biased frame length, ZDFA-coop is observed to achieve better performance than the other schemes. When it comes to the variance, while ZDFA-coop and spatio-temporal cooperation achieves similar values, IRSA has remarkably high variance.

Figure 5.5 shows the cumulative histogram of the throughput of each scheme. It can be observed that IRSA has long tail, which corresponds to very low throughput, *e.g.*, approximately 0.2. Such event occurs because of channel saturation, where the frame length is too small to retrieve all the users. On the other hand, spatio-temporal

cooperation, which is also a framed scheme, does not have such tail. This is because spatio-temporal cooperation has larger margin for the channel traffic, while IRSA with the sophisticated degree distribution has less margin.

5.5 Chapter Summary

We proposed ZDFA-coop, where E-ZDFA and frameless ALOHA with multiple BS cooperation was jointed together. ZD and multiple BS cooperation were shown to perform together so as to enhance the throughput performance than frameless ALOHA with multiple BS cooperation. Furthermore, numerical examples revealed that ZDFA-coop exhibits higher throughput than conventional schemes even in the presence of fluctuating traffic. Therefore, we conclude that this chapter contributes to the establishment of random access protocol that is suitable for next-generation wireless communications.

Chapter 6

Conclusion and Open Issues

Finally, this chapter concludes this dissertation, while addressing some open issues.

6.1 Conclusion

In Chapter 1, we reviewed the advance in wireless communication systems, especially in physical layer techniques, which motivated us to design MAC protocol. The problem was how can we efficiently accommodate massive number of wireless users, while in practice the demand would be fluctuating. To this end, frameless ALOHA can deal with the fluctuating demand, achieving moderate throughput performance with the aid of SIC. We were then motivated to propose random access protocols suitable for next-generation wireless communication, which involves following requirements:

- Massive number of users should be accommodated.
- High throughput should be achieved even with fluctuating demand.
- Communications should be reliable, *i.e.*, sufficiently high fraction of packets should be retrieved at the receiver.

In advance of the proposals, conventional frameless ALOHA was reviewed in Chapter 2. Based on the theoretical analysis using density evolution, we proposed an optimization scheme for transmission probability to maximize the throughput performance, where the peak throughput was maximized so as to maximize the average throughput. The optimization policy was based on the observation that the theoretical waterfall in the PLR performance can be reproduced in practical situation as the number of users increases, and it was confirmed that the average throughput approached the peak throughput.

In Chapter 3, we considered introducing ZD into frameless ALOHA, leading to the proposal of E-ZDFA. Although ZD can resolve collisions of two packets, it was clarified that the straightforward application of ZD yielded worse throughput and higher error floor, due to additional time slots. We then modified the protocol with additional feedback from the BS, where users retrieved via ZD or received without collision were required to halt following retransmission in order to suppress collisions. Moreover, as the number of contending users decreases, the transmission probability of users was adaptively increased. Numerical examples revealed that E-ZDFA improved the throughput performance by 5% than the conventional frameless ALOHA, while lowering the error floor.

To alleviate additional complexity at the BS, we focused on multiple BS network and proposed frameless ALOHA with multiple BS cooperation in Chapter 4. Users were classified into multiple groups depending on which BSs the user can communicate with, and different transmission probabilities were given for different user groups. We derived the exact PLR expressions, which was used to optimize transmission probabilities. Moreover, as the computational complexity of the exact analysis exponentially increases with the number of BSs, simple upper and lower bound for the throughput performance have been given, revealing that the performance gain monotonically increases as the number of BSs increases. Employing optimized throughput probabilities, we revealed that frameless ALOHA with multiple BS cooperation improved the throughput performance by 80% than the original frameless ALOHA with four BSs.

Finally, two proposals, namely E-ZDFA and frameless ALOHA with multiple BS cooperation, were jointed to propose ZDFA-coop in Chapter 5. It was revealed that ZDFA-coop outperformed frameless ALOHA with multiple BS cooperation in terms of the average throughput. Furthermore, supposing practical environment where the channel traffic fluctuated, ZDFA-coop was compared with conventional IRSA and spatio-temporal cooperation. We confirmed that ZDFA-coop exhibited higher throughput than conventional schemes, while achieving the lowest variance of throughput.

Our proposed schemes are undoubtedly satisfy the requirements mentioned earlier, achieving better throughput than conventional schemes. Moreover, the results shown in this dissertation have wide range of applications. For instance, factory automation would employ large number of wireless devises that control machines or collect a variety of data. High throughput performance of E-ZDFA will realize rapid control of machines or high efficiency of data collection. Smart home would be equipped with multiple access points, where frameless ALOHA with multiple BS cooperation or ZDFA-coop can be used so as to realize high connectivity without any stress of communication

failure. We believe that our proposals can contribute to the design of next-generation multiple access protocols.

6.2 Open Issues

In the dissertation, we have been considering to improve the MAC protocol to enhance the throughput performance. In addition to our discussion, following issues are still opened.

6.2.1 Derivation of Theoretical PLR Expression for E-ZDFA and Generalization

Because of retransmission canceling and transmission probability updating, density evolution analysis cannot be applied to E-ZDFA and ZDFA-coop. In order to exactly track the behavior of PLR, dynamic behavior of degree distribution should be tracked. Another way to analyze the system is to derive some approximation for the PLR, instead of the exact analytical expression. Analytical expressions would be used to theoretically optimize the transmission probability so as to maximize the throughput performance.

Furthermore, the analysis for cases where ZD can retrieve three or more colliding packets would be interesting, where k colliding packets can be retrieved from k received signals including the same colliding packets. Such enhancement may increase the throughput, while the the procedure to retrieve three or more packets via ZD is identical to the case of collision of two packets.

6.2.2 Exploiting Power-Domain Interference Cancellation

While we have assumed equal received power for all the packets, the assumption is the worst case scenario, where collided packets cannot be retrieved unless using ZD. However, in practice, received power of collided signals are different, so that capture effect [69] is available, where the colliding signal with the highest received power is retrievable by regarding the other colliding signals as noise. Moreover, random access protocols with power-control has been studied so as to resolve collision exploiting difference between power of colliding signals.[105]. Recent trend in such topic would be studies on NOMA-aided design of ALOHA [106]. As frameless ALOHA can control the transmission probability, as we demonstrated in E-ZDFA, it would be interesting

to design the probability so as to promote the retrieval of packets via power-domain interference cancellation.

6.2.3 Memory-Constrained Scenario

Inter-slot SIC requires the BS to store all the received signals, where the number of received signals required to retrieve sufficiently large fraction of packets would linearly increase as the number of users. Therefore, the BS should equip large memory to store huge number of received signals. At this point, discussion for memory-constrained scenario, where the number of packets that can be stored at the BS is limited, would be important for practical implementation.

6.2.4 Delay-Constrained Design

As well as the throughput, the delay is an important metric for random access protocols [107]. The PLR performance of SIC has waterfall region; in other words, until reaching the waterfall, only a few packets can be retrieved, which results in large delay for most users. In order to achieve low-latency, we would need to consider the design of random access protocol taking into account the delay. This could be related to the memory-constrained scenario.

6.2.5 Energy-Conscious Design

We have mainly focused on the increase of throughput performance, without considering power consumption of users and BSs. On the other hand, as IoT is expected to accommodate huge number of wireless devises, the power consumption should be suppressed [108, 109]. Another option is to use energy harvesting techniques, which enable users to communicate for longer life time [110]. There should be a tradeoff between total power consumption and throughput performance, and hence, the design of the random access protocol considering both energy consumption (and the amount of harvested energy) and throughput would be an important topic.

6.2.6 Cooperative Transmission of Users

While we have considered the cooperation of BSs, users may perform cooperative transmission with the aid of feedback from the BS [111], [112]. Conventional cooperative transmission has been aimed at obtaining diversity gain by referring channel information of each user. Moreover, most of existing works do not consider SIC, *i.e.*, only slotted

ALOHA or framed ALOHA has been focused on, an exception is the work by Missaoui *et al.* [113], where collided packets are jointly estimated, while inter-slot SIC has not been taken into account. Hence, there is a possibility to achieve higher throughput or lower PLR than non-cooperative transmission, by introducing the cooperation of users with the aid of inter-slot SIC.

References

[1] CISCO systems, "IEEE 802.11ax: The sixth generation of Wi-Fi," *Technical white paper*, June 2018. [Online]. Available: https://www.cisco.com/c/dam/en/us/products/collateral/wireless/white-paper-c11-740788.pdf

[2] A. Goldsmith, *Wireless Communications*. Cambridge University Press, 2005.

[3] R. E. Blahut, *Algebraic Codes for Data Transmission*. Cambridge University Press, 2003.

[4] R. W. Hamming, "Error detecting and error correcting codes," *The Bell Syst. Tech. J.*, vol. 29, no. 2, pp. 147–160, Apr. 1950.

[5] I. Reed and G. Solomon, "Polynomial codes over certain finite fields," *J. Soc. for Ind. and Appl. Math.*, vol. 8, no. 2, pp. 300–304, 1960. [Online]. Available: https://doi.org/10.1137/0108018

[6] S. B. Wicker, *Reed-Solomon Codes and Their Applications*. Piscataway, NJ, USA: IEEE Press, 1994.

[7] P. Elias, "Coding for noisy channels," *IRE Convention Record, Part 4*, pp. 37–46, 1955.

[8] "IEEE standard for information technology–telecommunications and information exchange between systems local and metropolitan area networks–specific requirements - part 11: Wireless LAN medium access control (MAC) and physical layer (PHY) specifications," *IEEE Std 802.11-2016 (Revision of IEEE Std 802.11-2012)*, pp. 1–3534, Dec. 2016.

[9] A. Viterbi, "Error bounds for convolutional codes and an asymptotically optimum decoding algorithm," *IEEE Trans. Inf. Theory*, vol. 13, no. 2, pp. 260–269, Apr. 1967.

[10] G. Ungerboeck, "Channel coding with multilevel/phase signals," *IEEE Trans. Inf. Theory*, vol. 28, no. 1, pp. 55–67, Jan. 1982.

[11] ——, "Trellis-coded modulation with redundant signal sets part I: Introduction," *IEEE Commun. Mag.*, vol. 25, no. 2, pp. 5–11, Feb. 1987.

[12] ——, "Trellis-coded modulation with redundant signal sets part II: State of the art," *IEEE Commun. Mag.*, vol. 25, no. 2, pp. 12–21, Feb. 1987.

[13] G. D. Forney, *Concatenated Codes*, ser. M.I.T. Press research monographs. M.I.T. Press, 1966. [Online]. Available: https://books.google.co.jp/books?id=7ul_QgAACAAJ

[14] Association of Radio Industries and Businesses, "Transmission system for digital television broadcasting," *ARIB STD-B31 Version 1.6*, Nov. 2005.

[15] D. Divsalar and J. H. Yuen, "Performance of concatenated Reed-Solomon/Viterbi channel coding," *Telecommun. and Data Acquisition Progress Rep.*, Sept. 1982.

[16] C. Berrou, A. Glavieux, and P. Thitimajshima, "Near Shannon limit error-correcting coding and decoding: Turbo-codes. 1," in *Proc. IEEE Int. Conf. Commun.*, vol. 2, May 1993, pp. 1064–1070 vol.2.

[17] "3rd generation partnership project; technical specification group radio access network; evolved universal terrestrial radio access (E-UTRA); multiplexing and channel coding (release 8)," Sept. 2008.

[18] R. Gallager, "Low-density parity-check codes," *IRE Trans. on Inf. Theory*, vol. 8, no. 1, pp. 21–28, Jan. 1962.

[19] D. J. C. MacKay and R. M. Neal, "Near Shannon limit performance of low density parity check codes," *Electronics Lett.*, vol. 32, no. 18, pp. 1645–1646, Aug. 1996.

[20] T. J. Richardson and R. L. Urbanke, "The capacity of low-density parity-check codes under message-passing decoding," *IEEE Trans. Inf. Theory*, vol. 47, no. 2, pp. 599–618, Feb. 2001.

[21] R. J. Wilson, *Introduction to Graph Theory*. England: Pearson Education Limited, 1996.

[22] R. Tanner, "A recursive approach to low complexity codes," *IEEE Trans. Inf. Theory*, vol. 27, no. 5, pp. 533–547, Sept. 1981.

[23] T. Richardson and R. Urbanke, *Modern Coding Theory*. NY, USA: Cambridge University Press, 2008.

[24] X.-Y. Hu, E. Eleftheriou, and D. M. Arnold, "Regular and irregular progressive edge-growth tanner graphs," *IEEE Trans. Inf. Theory*, vol. 51, no. 1, pp. 386–398, Jan. 2005.

[25] T. Richardson, M. Shokrollahi, and R. Urbanke, "Design of capacity-approaching irregular low-density parity-check codes," *IEEE Trans. Inf. Theory*, vol. 47, no. 2, pp. 619–637, Feb. 2001.

[26] E. Arikan, "Channel polarization: A method for constructing capacity-achieving codes for symmetric binary-input memoryless channels," vol. 55, no. 7, pp. 3051–3073, July 2009.

[27] K. Niu and K. Chen, "CRC-aided decoding of polar codes," *IEEE Commun. Lett.*, vol. 16, no. 10, pp. 1668–1671, Oct. 2012.

[28] A. Kaye and D. George, "Transmission of multiplexed PAM signals over multiple channel and diversity systems," *IEEE Trans. Commun. Tech.*, vol. 18, no. 5, pp. 520–526, Oct. 1970.

[29] S. M. Alamouti, "A simple transmit diversity technique for wireless communications," *IEEE J. Sel. Areas Commun.*, vol. 16, no. 8, pp. 1451–1458, Oct. 1998.

[30] V. Tarokh, H. Jafarkhani, and A. R. Calderbank, "Space-time block codes from orthogonal designs," *IEEE Trans. Inf. Theory*, vol. 45, no. 5, pp. 1456–1467, July 1999.

[31] G. J. Foschini, "Layered space-time architecture for wireless communication in a fading environment when using multi-element antennas," *Bell Labs Tech. J.*, vol. 1, no. 2, pp. 41–59, Autumn 1996.

[32] E. Telatar, "Capacity of multi-antenna Gaussian channels," *European Trans. Telecommun.*, vol. 10, no. 6, pp. 585–595, 1999. [Online]. Available: https://onlinelibrary.wiley.com/doi/abs/10.1002/ett.4460100604

[33] L. Zheng and D. N. C. Tse, "Diversity and multiplexing: a fundamental tradeoff in multiple-antenna channels," *IEEE Trans. Inf. Theory*, vol. 49, no. 5, pp. 1073–1096, May 2003.

[34] J. G. Andrews, S. Buzzi, W. Choi, S. V. Hanly, A. Lozano, A. C. K. Soong, and J. C. Zhang, "What will 5G be?" *IEEE J. Sel. Areas Commun.*, vol. 32, no. 6, pp. 1065–1082, June 2014.

[35] P. Gupta and P. R. Kumar, "The capacity of wireless networks," *IEEE Trans. Inf. Theory*, vol. 46, no. 2, pp. 388–404, Mar. 2000.

[36] A. F. Molisch, *Wireless Communications*, 2nd ed. Wiley Publishing, 2011.

[37] C. Y. Wong, R. S. Cheng, K. B. Lataief, and R. D. Murch, "Multiuser OFDM with adaptive subcarrier, bit, and power allocation," *IEEE J. Sel. Areas Commun.*, vol. 17, no. 10, pp. 1747–1758, Oct. 1999.

[38] A. Azari, P. Popovski, G. Miao, and Č. Stefanović, "Grant-free radio access for short-packet communications over 5G networks," in *Proc. 2017 IEEE Global Commun. Conf.*, Dec. 2017, pp. 1–7.

[39] G. Bianchi, "Performance analysis of the IEEE 802.11 distributed coordination function," *IEEE J. Sel. Areas Commun.*, vol. 18, no. 3, pp. 535–547, Mar. 2000.

[40] F. Tobagi and L. Kleinrock, "Packet switching in radio channels: Part II - the hidden terminal problem in carrier sense multiple-access and the busy-tone solution," *IEEE Trans. Commun.*, vol. 23, no. 12, pp. 1417–1433, Dec. 1975.

[41] L. Liu, E. G. Larsson, W. Yu, P. Popovski, C. Stefanovic, and E. de Carvalho, "Sparse signal processing for grant-free massive connectivity: A future paradigm for random access protocols in the Internet of Things," *IEEE Signal Process. Mag.*, vol. 35, no. 5, pp. 88–99, Sept. 2018.

[42] N. Abramson, "The ALOHA system: Another alternative for computer communications," in *Proc. Fall Joint Computer Conf.*, New York, NY, Nov. 1970, pp. 281–285.

[43] J. Seo and H. Jin, "Optimally controlled pure ALOHA systems for wireless sensor networks," *IEEE Commun. Lett.*, vol. 21, no. 11, pp. 2460–2463, Nov. 2017.

[44] A. Baiocchi and F. Ricciato, "Analysis of pure and slotted ALOHA with multipacket reception and variable packet size," *IEEE Commun. Lett.*, vol. 22, no. 7, pp. 1482–1485, July 2018.

[45] A. I. B and T. G. Venkatesh, "Order statistics based analysis of pure ALOHA in channels with multipacket reception," *IEEE Commun. Lett.*, vol. 17, no. 10, pp. 2012–2015, Oct. 2013.

[46] L. G. Roberts, "Aloha packet system with and without slots and capture," *SIGCOMM Comput. Commun. Rev.*, vol. 5, no. 2, pp. 28–42, Apr. 1975.

[47] K. Morishita, T. Maeda, and M. Yasui, "Development of wireless communications technology for ETC system," *Mitsubishi Heavy Industries Ltd. Tech. Review*, vol. 38, no. 3, pp. 116–120, Oct. 2001.

[48] S. A. Ahson and M. Ilyas, *RFID Handbook: Applications, Technology, Security, and Privacy.* CRC Press, 2008.

[49] X. Jian, Y. Liu, Y. Wei, X. Zeng, and X. Tan, "Random access delay distribution of multichannel slotted ALOHA with its applications for machine type communications," *IEEE Internet of Things J.*, vol. 4, no. 1, pp. 21–28, Feb. 2017.

[50] K. Sakakibara and K. Takabayashi, "Modeling and analysis of slotted ALOHA systems with energy harvesting nodes and retry limit," *IEEE Access*, vol. 6, pp. 63 527–63 536, 2018.

[51] W. Saad, S. A. El-Feshawy, M. Shokair, and M. I. Dessouky, "Optimised approach based on hybrid MAC protocol for M2M networks," *IET Networks*, vol. 7, no. 6, pp. 393–397, 2018.

[52] N. Sriranga, K. G. Nagananda, and R. S. Blum, "Shared channel ordered transmissions for energy-efficient distributed signal detection," *IEEE Commun. Lett.*, vol. 23, no. 1, pp. 96–99, Jan. 2019.

[53] H. Okada, Y. Igarashi, and Y. Nakanishi, "Analysis and application of framed ALOHA channel in satellite packet switching networks– FADRA method," *Electron. and Commun. in Japan*, vol. 60, pp. 60–72, Aug. 1977.

[54] S. Lam, "Packet broadcast networks– a performance analysis of the R-ALOHA protocol," *IEEE Trans. Comput.*, vol. C-29, no. 7, pp. 596–603, July 1980.

[55] G. L. Choudhury and S. S. Rappaport, "Diversity ALOHA–a random access scheme for satellite communications," *IEEE Trans. Commun.*, vol. 31, no. 3, pp. 450–457, Mar. 1983.

[56] E. Casini, R. De Gaudenzi, and O. Herrero, "Contention resolution diversity slotted ALOHA (CRDSA): An enhanced random access scheme for satellite access packet networks," *IEEE Trans. Wireless Commun.*, vol. 6, no. 4, pp. 1408–1419, Apr. 2007.

[57] G. Liva, "Graph-based analysis and optimization of contention resolution diversity slotted ALOHA," *IEEE Trans. Commun.*, vol. 59, no. 2, pp. 477–487, Feb. 2011.

[58] A. G. i Amat and G. Liva, "Finite-length analysis of irregular repetition slotted ALOHA in the waterfall region," *IEEE Commun. Lett.*, vol. 22, no. 5, pp. 886–889, May 2018.

[59] A. Amraoui, A. Montanari, T. Richardson, and R. Urbanke, "Finite-length scaling for iteratively decoded LDPC ensembles," *IEEE Trans. Inf. Theory*, vol. 55, no. 2, pp. 473–498, Feb. 2009.

[60] G. Abreu, "Very simple tight bounds on the Q-function," *IEEE Trans. Commun.*, vol. 60, no. 9, pp. 2415–2420, Sept. 2012.

[61] M. Wu, Y. Li, M. Gurusamy, and P. Kam, "A tight lower bound on the Gaussian Q-function with a simple inversion algorithm, and an application to coherent optical communications," *IEEE Commun. Lett.*, vol. 22, no. 7, pp. 1358–1361, July 2018.

[62] L. Toni and P. Frossard, "Prioritized random MAC optimization via graph-based analysis," *IEEE Trans. Commun.*, vol. 63, no. 12, pp. 5002–5013, Dec. 2015.

[63] E. Paolini, G. Liva, and M. Chiani, "Coded slotted ALOHA: A graph-based method for uncoordinated multiple access," *IEEE Trans. Inf. Theory*, vol. 61, no. 12, pp. 6815–6832, Dec 2015.

[64] M. Luby, "LT codes," in *Proc. 43rd Annu. IEEE Symp. Found. Comput. Sci.*, Vancouver, BC, Canada, Nov. 2002, pp. 271–280.

[65] A. Shokrollahi, "Raptor codes," *IEEE Trans. Inf. Theory*, vol. 52, no. 6, pp. 2551–2567, June 2006.

[66] J. Perry, P. A. Iannucci, K. E. Fleming, H. Balakrishnan, and D. Shah, "Spinal codes," in *Proc. ACM SIGCOMM 2012 Conf. Applicat., Tech., Architectures, and Protocols for Comput. Commun.*, Helsinki, Finland, 2012, pp. 49–60. [Online]. Available: http://doi.acm.org/10.1145/2342356.2342363

[67] C. Stefanovic, P. Popovski, and D. Vukobratovic, "Frameless ALOHA protocol for wireless networks," *IEEE Commun. Lett.*, vol. 16, no. 12, pp. 2087–2090, Dec. 2012.

[68] Č. Stefanović and P. Popovski, "ALOHA random access that operates as a rateless code," *IEEE Trans. Commun.*, vol. 61, no. 11, pp. 4653–4662, Nov. 2013.

[69] C. Stefanovic, M. Momoda, and P. Popovski, "Exploiting capture effect in frameless ALOHA for massive wireless random access," in *Proc. IEEE Wireless Commun. Networking Conf.*, Istanbul, Turkey, Apr. 2014, pp. 1762–1767.

[70] F. Lázaro and Č. Stefanović, "Finite-length analysis of frameless ALOHA," in *Proc. 11th Int. ITG Conf. on Syst., Commun. and Coding*, Hamburg, Germany, 2017, pp. 1–6.

[71] ——, "Finite-length analysis of frameless ALOHA with multi-user detection," *IEEE Communications Letters*, vol. 21, no. 4, pp. 769–772, Apr. 2017.

[72] Č. Stefanović, F. Lazaro, and P. Popovski, "Frameless ALOHA with reliability-latency guarantees," in *Proc. 2017 IEEE Global Commun. Conf.*, Dec. 2017, pp. 1–6.

[73] S. Rahimian, M. Noori, and M. Ardakani, "Adaptive frameless slotted ALOHA considering energy efficiency," in *Proc. 2016 24th Iranian Conf. Elect. Eng.*, May 2016, pp. 92–96.

[74] I. Hussain, M. Juntti, and T. Matsumoto, "Improved frameless ALOHA for wireless networks," in *European Wireless 2016; 22th European Wireless Conf.*, May 2016, pp. 1–6.

[75] G. Durisi, T. Koch, and P. Popovski, "Toward massive, ultrareliable, and low-latency wireless communication with short packets," *Proc. IEEE*, vol. 104, no. 9, pp. 1711–1726, Sept. 2016.

[76] B. Holfeld, D. Wieruch, T. Wirth, L. Thiele, S. A. Ashraf, J. Huschke, I. Aktas, and J. Ansari, "Wireless communication for factory automation: an opportunity for LTE and 5G systems," *IEEE Commun. Mag.*, vol. 54, no. 6, pp. 36–43, June 2016.

[77] D. Valtchev and I. Frankov, "Service gateway architecture for a smart home," *IEEE Commun. Mag.*, vol. 40, no. 4, pp. 126–132, Apr. 2002.

[78] S. Pandi, F. H. P. Fitzek, C. Lehmann, D. Nophut, D. Kiss, V. Kovacs, A. Nagy, G. Csorvasi, M. Toth, T. Rajacsis, H. Charaf, and R. Liebhart, "Joint design of communication and control for connected cars in 5G communication systems," in *Proc. 2016 IEEE Global Commun. Conf. Workshops*, Dec. 2016, pp. 1–7.

[79] D. L. Donoho, "Compressed sensing," *IEEE Trans. Inf. Theory*, vol. 52, no. 4, pp. 1289–1306, Apr. 2006.

[80] D. L. Donoho, A. Maleki, and A. Montanari, "Message-passing algorithms for compressed sensing," *Proceedings of the National Academy of Sciences*, vol. 106, no. 45, pp. 18 914–18 919, 2009. [Online]. Available: https://www.pnas.org/content/106/45/18914

[81] D. L. Donoho, Y. Tsaig, I. Drori, and J. Starck, "Sparse solution of underdetermined systems of linear equations by stagewise orthogonal matching pursuit," *IEEE Trans. Inf. Theory*, vol. 58, no. 2, pp. 1094–1121, Feb. 2012.

[82] V. Boljanovic, D. Vukobratović, P. Popovski, and Č. Stefanović, "User activity detection in massive random access: Compressed sensing vs. coded slotted ALOHA," in *Proc. 2017 IEEE 18th Int. Workshop on Signal Process. Advances in Wireless Commun.*, July 2017, pp. 77–82.

[83] M. Centenaro, L. Vangelista, S. Saur, A. Weber, and V. Braun, "Comparison of collision-free and contention-based radio access protocols for the Internet of Things," *IEEE Trans. Commun.*, vol. 65, no. 9, pp. 3832–3846, Sept. 2017.

[84] A. Rajandekar and B. Sikdar, "A survey of MAC layer issues and protocols for machine-to-machine communications," *IEEE Internet of Things J.*, vol. 2, no. 2, pp. 175–186, Apr. 2015.

[85] A. Varghese and D. Tandur, "Wireless requirements and challenges in Industry 4.0," in *Proc. 2014 Int. Conf. Contemporary Computing and Informatics*, Nov. 2014, pp. 634–638.

[86] S. Gollakota and D. Katabi, "ZigZag decoding: Combating hidden terminals in wireless networks," in *Proc. the ACM SIGCOMM 2008 Conf. Data Commun.*, Seattle, WA, 2008, pp. 159–170. [Online]. Available: http://doi.acm.org/10.1145/1402958.1402977

[87] D. Jakovetic, D. Bajovic, D. Vukobratović, and V. Crnojevic, "Cooperative slotted aloha for multi-base station systems," *IEEE Trans. Commun.*, vol. 63, no. 4, pp. 1443–1456, Apr. 2015.

[88] F. Ricciato and P. Castiglione, "Pseudo-random ALOHA for enhanced collision-recovery in RFID," *IEEE Commun. Lett.*, vol. 17, no. 3, pp. 608–611, Mar. 2013.

[89] R. Storn and K. Price, "Differential evolution - a simple and efficient heuristic for global optimization over continuous spaces," *J. Global Optimization*, vol. 11, no. 4, pp. 341–359, Dec. 1997.

[90] R. Storn, "On the usage of differential evolution for function optimization," in *Proc. North American Fuzzy Inf. Process.*, June 1996, pp. 519–523.

[91] S. Ogata and K. Ishibashi, "Frameless ALOHA with multiple base stations," in *Proc. 2015 49th Asilomar Conf. Signals, Syst. and Comput.*, Pacific Grove, CA, 2015, pp. 47–51.

[92] P. M. Olmos, J. J. Murillo-Fuentes, and F. Perez-Cruz, "Tree-structure expectation propagation for LDPC decoding over the BEC," *IEEE Trans. Inf. Theory*, vol. 59, no. 6, pp. 3354–3377, June 2013.

[93] M. Oinaga, S. Ogata, and K. Ishibashi, "ZigZag decodable coded slotted ALOHA," in *Proc. IEEE 15th Workshop on Positioning, Navigation and Commun.*, Bremen, Germany, 2018, pp. 1–6.

[94] S. Ogata, K. Ishibashi, and G. T. F. de Abreu, "Optimized frameless ALOHA for cooperative base stations with overlapped coverage areas," *IEEE Trans. Wireless Commun.*, vol. 17, no. 11, pp. 7486–7499, Nov. 2018.

[95] R. Irmer, H. Droste, P. Marsch, M. Grieger, G. Fettweis, S. Brueck, H. Mayer, L. Thiele, and V. Jungnickel, "Coordinated multipoint: Concepts, performance, and field trial results," *IEEE Commun. Mag.*, vol. 49, no. 2, pp. 102–111, Feb. 2011.

[96] H. Burchardt and H. Haas, "Multicell cooperation: evolution of coordination and cooperation in large-scale networks," *IEEE Wireless Commun.*, vol. 20, no. 1, pp. 19–26, Feb. 2013.

[97] T. Wang, Q. Yang, K. Tan, J. Zhang, S. C. Liew, and S. Zhang, "DCAP: Improving the capacity of WiFi networks with distributed cooperative access points," *IEEE Trans. Mobile Comput.*, vol. 17, no. 2, pp. 320–333, Feb. 2018.

[98] X. Lu, W. Cheng, Q. He, and X. Xie, "Cooperative communication based regular topology to achieve coverage and K-connectivity for WSNs," in *Proc. 2018 13th IEEE Conf. Ind. Electronics and Applicat.*, May 2018, pp. 2514–2518.

[99] L. P. Qian, Y. Wu, H. Zhou, and X. Shen, "Joint uplink base station association and power control for small-cell networks with non-orthogonal multiple access," *IEEE Trans. Wireless Commun.*, vol. 16, no. 9, pp. 5567–5582, Sept. 2017.

[100] H. Lin and W. Y. Shin, "Multi-cell aware opportunistic random access," in *Proc. 2017 IEEE Int. Symp. Inf. Theory*, Aachen, Germany, 2017, pp. 2533–2537.

[101] S. Ogata, K. Ishibashi, and G. Abreu, "Multi-access diversity gain via multiple base station cooperation in frameless ALOHA," in *Proc. 2017 IEEE 18th Int. Workshop on Signal Process. Advances in Wireless Commun.*, Sappro, Japan, 2017, pp. 103–107.

[102] E. G. Kounias, "Bounds for the probability of a union, with applications," *Ann. Math. Statist.*, vol. 39, no. 6, pp. 2154–2158, Dec. 1968. [Online]. Available: http://dx.doi.org/10.1214/aoms/1177698049

[103] M. S. Corson and A. Ephremides, "An analysis of multi-receiver, non-adaptive, slotted aloha with capture for wireless communications in factories," in *Proc. Twelfth Annu. Joint Conf. the IEEE Comput. and Commun. Societies. Networking: Found. for the Future*, San Francisco, CA, 1993, pp. 421–428 vol.2.

[104] A. Bar-David and M. Sidi, "Collision resolution algorithms in multistation packet-radio networks," *IEEE Trans. Commun.*, vol. 37, no. 12, pp. 1387–1391, Dec. 1989.

[105] H. Lin, K. Ishibashi, W. Shin, and T. Fujii, "A simple random access scheme with multilevel power allocation," *IEEE Commun. Lett.*, vol. 19, no. 12, pp. 2118–2121, Dec. 2015.

[106] J. Choi, "NOMA-based random access with multichannel ALOHA," *IEEE J. Sel. Areas Commun.*, vol. 35, no. 12, pp. 2736–2743, Dec. 2017.

[107] D. Malak, H. Huang, and J. G. Andrews, "Throughput maximization for delay-sensitive random access communication," *IEEE Trans. Wireless Commun.*, vol. 18, no. 1, pp. 709–723, Jan. 2019.

[108] P. Sathyamoorthy, E. C. . Ngai, X. Hu, and V. C. M. Leung, "Energy efficiency as an orchestration service for mobile Internet of Things," in *Proc. 2015 IEEE 7th Int. Conf. Cloud Computing Technology and Sci.*, Nov. 2015, pp. 155–162.

[109] C. Zhu, V. C. M. Leung, L. Shu, and E. C. . Ngai, "Green Internet of Things for smart world," *IEEE Access*, vol. 3, pp. 2151–2162, 2015.

[110] P. Kamalinejad, C. Mahapatra, Z. Sheng, S. Mirabbasi, V. C. M. Leung, and Y. L. Guan.

[111] D. Wang, C. Comaniciu, H. Minn, and N. Al-Dhahir, "A game-theoretic approach for exploiting multiuser diversity in cooperative slotted Aloha," *IEEE Trans. Wireless Commun.*, vol. 7, no. 11, pp. 4215–4225, Nov. 2008.

[112] M. S. Gokturk, O. Ercetin, and O. Gurbuz, "Throughput analysis of ALOHA with cooperative diversity," *IEEE Commun. Lett.*, vol. 12, no. 6, pp. 468–470, June 2008.

[113] N. Missaoui, I. Kammoun, and M. Siala, "Enhanced slotted ALOHA protocol with collision processing and relay cooperation," in *Proc. 2012 Int. Conf. Commun. and Inf. Technology*, June 2012, pp. 418–422.

Publications

Journal Paper

1. Shun Ogata, Koji Ishibashi, and Giuseppe T. F. de Abreu, "Optimized Frameless ALOHA for Cooperative Base Stations with Overlapped Coverage Areas, " *IEEE Trans. Wireless. Commun.*, vol. 17, no. 11, pp. 7486-7499, Nov. 2018.

International Conference Papers

1. Shun Ogata and Koji Ishibashi, "ZigZag Decodable Frameless ALOHA," the 52nd Asilomar Conf. Signals, Syst., and Comput., Pacific Grove, CA, Oct. 2018.

2. Shun Ogata and Koji Ishibashi, "Coded Frameless ALOHA," in Proc. IEEE 15th Workshop on Positioning, Navigation and Commun., pp. 1-5, Bremen, Germany, Oct. 2018.

3. Masaru Oinaga, Shun Ogata, and Koji Ishibashi, "ZigZag Decoder-Aided Slotted ALOHA with Successive Interference Cancellation," in Proc. IEEE 15th Workshop on Positioning, Navigation and Commun., pp. 1-6, Bremen, Germany, Oct. 2018.

4. Shun Ogata and Koji Ishibashi, "Received-Power-Aware Design of Transmission Probability for Frameless ALOHA," in Proc. SmartCom 2017 (IEICE Tech. Rep.), vol. 117, no. 257, SR2017-93, pp. 73-74, Rome, Italy, Oct. 2017.

5. Shun Ogata, Koji Ishibashi, and Giuseppe Abreu, "Multi-Access Diversity Gain via Multiple Base Station Cooperation in Frameless ALOHA," in Proc. IEEE SPAWC 2017, pp. 103-107, Sapporo, Japan, July 2017.

6. Yuki Goto, Shun Ogata, and Koji Ishibashi, "Energy-Efficient Random Sleep Protocol based on Distributed Coding for Sensor-to-Vehicle Communications,"

in Proc. 50th Asilomar Conf. Signals, Syst., and Comput., pp. 724-728, Pacific Grove, CA, Nov. 2016.

7. Shun Ogata and Koji Ishibashi, "Frameless ALOHA with Multiple Base Stations," in Proc. 49th Asilomar Conf. Signals, Syst., and Comput., pp. 47-51, Pacific Grove, CA, Nov. 2015.

Domestic Conference Papers

1. Shun Ogata and Koji Ishibashi, "On Packet Loss Rate of Frameless ALOHA with ZigZag Decoding, "The 41st Symposium on Information Theory and its Applications (SITA2018), pp. 257-262, Dec. 2018.

2. Masaru Oinaga, Shun Ogata, and Koji Ishiabshi, "ZigZag Decodable Coded Slotted ALOHA, " IEICE Tech. Rep., vol. 118, no. 101, RCS2018-71, pp. 213-218, June 2018.

3. Shun Ogata and Koji Ishiabshi, "Distance-Aware Design of Transmission Probability for Frameless ALOHA, " The 40th Symposium on Information Theory and its Applications (SITA2017), pp. 277–282, Nov. 2017.

4. Shun Ogata, Koji Ishiabshi, and Giuseppe Abreu, "On Generalized Analysis for Packet Loss Rate of Frameless ALOHA with Multiple Base Station Cooperation, "IEICE Tech. Rep., vol. 117, no. 11, RCS2017-17, pp. 83-88, Apr. 2017.

5. Shun Ogata and Koji Ishiabshi, "A Study on Efficient Packet Demodulation of Frameless ALOHA, " IEICE Tech. Rep., vol. 116, no. 396, RCS2016-264, pp. 165-170, Jan. 2017.

6. Shun Ogata and Koji Ishiabshi, "Joint Optimization of Target Degree and Code Degree Distribution for Coded Frameless ALOHA, " The 39th Symposium on Information Theory and its Applications (SITA2016), pp. 544 – 549, Dec. 2016.

7. Yuki Goto, Shun Ogata, Koji Ishiabshi, Yasuhiro Hirayama, and Tsuneo Nakata, "Energy-Efficient Random Sleep Protocol based on Distributed Coding for Sensor-to-Vehicular Communications, " IEICE Tech. Rep., vol. 116, no. 110, RCS2016-75, pp. 167-172, June 2016.

8. Shun Ogata and Koji Ishiabshi, "Optimization of Degree Distribution for Coded Frameless ALOHA, " IEICE Tech. Rep., vol. 116, no. 110, RCS2016-89, pp. 251-256, June 2016.

9. Shun Ogata and Koji Ishiabshi, "On Packet Loss Rate of Coded Frameless ALOHA for Massive Random Access, " IEICE Tech. Rep., vol. 116, no. 11, RCS2016-22, pp. 123-128, Apr. 2016.

10. Shun Ogata and Koji Ishiabshi, "A Study on Road-to-Vehicle Communication based on Frameless ALOHA with Vehicle-to-Vehicle Cooperation, "IEICE General Conoference 2016, Mar. 2016.

11. Shun Ogata and Koji Ishiabshi, "On Road-to-Vehicle Communication based on Coded ALOHA, " IEICE Tech. Rep., vol. 115, no. 411, SR2015-81, pp. 63-68, Jan. 2016.

12. Shun Ogata, Koji Ishiabshi and Giuseppe Abreu, "Analysis of Packet Decoding Probability for Frameless ALOHA with Multiple Base Stations, " The 38th Symposium on Information Theory and its Applications (SITA2015), pp.113-118, Nov. 2015.

13. Shun Ogata, Koji Ishiabshi and Giuseppe Abreu, "Optimization of the Target Degree for Frameless ALOHA with Buffer, " IEICE Society Conference 2015, Sept. 2015.

14. Shun Ogata, Koji Ishiabshi and Giuseppe Abreu, "Optimization of Target Degrees for Frameless ALOHA with Multiple Base Stations, " IEICE Tech. Rep., vol. 115, no. 160, RCS2015-100, pp. 1-6, July 2015.

15. Shun Ogata, Giuseppe Abreu and Koji Ishiabshi, "Optimization of the Target Degree of Frameless ALOHA, " IEICE General Conference 2015, Mar. 2015.

16. Shun Ogata, Giuseppe Abreu and Koji Ishiabshi, "Target Degree Distribution Optimization Using Density Evolution for Frameless ALOHA, "IEICE Tech. Rep., vol. 114, no. 490, RCS2014-314, pp. 77-82, Mar. 2015.